

SUSTAINED RELEASE NANOPARTICLES CONTAINING ACYCLOVIR PRODRUGS
FOR OCULAR HERPES SIMPLEX KERATITIS AND CHARACTERIZATION
OF FOLATE TRANSPORT PROTEINS IN A CORNEAL
EPITHELIAL CELL LINE

A DISSERTATION IN
Pharmaceutical Science
and
Chemistry

Presented to the faculty of the University
of Missouri-Kansas City in partial fulfillment of
the requirements for the degree
DOCTOR OF PHILOSOPHY

by
Jwala Jwala,
B. Pharm., JSS College of Pharmacy, 2005

Kansas City, Missouri
2011

SUSTAINED RELEASE NANOPARTICLES CONTAINING ACYCLOVIR PRODRUGS
FOR OCULAR HERPES SIMPLEX KERATITIS AND CHARACTERIZATION
OF FOLATE TRANSPORT PROTEINS IN A CORNEAL
EPITHELIAL CELL LINE

Jwala Jwala, Candidate for the Doctor of Philosophy Degree

University of Missouri-Kansas City, 2011

ABSTRACT

Ocular herpes is a persistent viral infection caused by the herpes simplex virus-1. It is one of the most common infectious diseases causing corneal blindness in the United States. In this study, polymeric nanoparticles of stereoisomeric di-peptide prodrugs of acyclovir (L-valine-L-valine-ACV, L-valine-D-valine-ACV, D-valine-L-valine-ACV, and D-valine-D-valine-ACV) were developed and characterized for the treatment of ocular herpes keratitis. L-valine-L-valine-ACV and L-valine-D-valine-ACV were determined to be optimum in terms of enzymatic stability, uptake and cytotoxicity. Uptake and docking results indicated that L-valine in the terminal position increases the affinity of prodrug to the peptide transporter protein. Entrapment efficiency values of L-valine-L-valine-ACV and L-valine-D-valine-ACV were optimal with PLGA 75:25 and PLGA 65:35 polymers, respectively. *In vitro* release of prodrugs from nanoparticles exhibited a biphasic release pattern with initial burst phase followed by sustained release. Dispersion of nanoparticles in thermosensitive gels eliminated the burst release phase. Novel nanoparticulate systems of dipeptide prodrugs of ACV suspended in thermosensitive gels may provide sustained delivery following topical

administration. The uptake of nanoparticles into corneal cells can be enhanced by attachment of cell-specific ligands such as folate and biotin. Folate carrier-mediated system is widely used in the targeted delivery of drugs. Thus Staten's Seruminstitut rabbit corneal (SIRC) epithelial cell line was investigated for the expression of folate transport proteins that can be utilized for targeted drug delivery of folate-conjugated nanoparticles and prodrugs to cornea. Linear increase in [³H] Folic acid uptake was observed over 30min. The process followed saturation kinetics with apparent K_m of 14.2 nM, V_{max} of 1.5×10^{-5} micro.moles/min/mg protein and K_d of 2.1×10^{-6} min.⁻¹ Uptake was inhibited in the presence of structural analogs (cold folic acid, MTF and MTX) but structurally unrelated vitamins did not show any effect. RT-PCR and Western blot analysis confirmed the presence of folate receptor- α (FR- α) and proton-coupled folate transporter (PCFT). This work demonstrated the functional and molecular presence of FR- α and PCFT in SIRC cells that can be utilized for enhanced uptake of folate conjugated nanoparticles and prodrugs. In a different study the differential expression of FR- α , sodium dependent multivitamin transporter (SMVT) and amino acid transporter B^(0,+) in retinoblastoma (Y-79) and retinal pigment epithelial (ARPE-19) cells. Higher expression of FR- α , SMVT and B^(0,+) at mRNA level was observed in cancerous Y-79 cells compared to normal ARPE-19 cells.

The faculty listed below, appointed by the Dean of School of Graduate Studies, have examined a dissertation titled, “Sustained release nanoparticles containing acyclovir prodrugs for ocular herpes simplex keratitis and characterization of folate transport proteins in a corneal epithelial cell line” presented by Jwala Jwala, candidate for the Doctor of Philosophy degree, and certify that in their opinion it is worthy of acceptance.

Supervisory Committee

Ashim K. Mitra, Ph.D., Committee Chair
School of Pharmacy

Chi Lee, Ph.D.
School of Pharmacy

Kun Cheng, Ph.D.
School of Pharmacy

David Van Horn, Ph.D.
Department of Chemistry

Andrew J. Holder, Ph.D.
Department of Chemistry

CONTENTS

ABSTRACT	iii
ILLUSTRATIONS	ix
TABLES	xii
ACKNOWLEDGEMENTS	xiii

Chapter

1. INTRODUCTION	1
1.1 Anatomy and Physiology of the Eye:	1
1.2 Constraints to Topical Delivery	3
1.3 Nutrient Transporters and Efflux Pumps in the Eye	6
1.4 Conventional Drug Delivery Systems	12
1.5 Novel Strategies to Enhance Ocular Drug Absorption	18

PART I: Ocular Sustained Release Nanoparticles containing Stereoisomeric Di-Peptide

Prodrugs of Acyclovir

2. RATIONALE FOR INVESTIGATION	32
2.1 Overview	32
2.2 Statement of Problem.....	35
2.3 Objectives	36
3. OCULAR SUSTAINED RELEASE NANOPARTICLES CONTAINING STEREOISOMERIC DI-PEPTIDE PRODRUGS OF ACYCLOVIR	
3.1 Rationale	37
3.2 Materials and Methods.....	40

3.3 Results.....	50
3.4 Discussion.....	64
3.5 Conclusions.....	67

PART II: Functional Characterization of Folate Transport Proteins in Staten’s Seruminstitut Rabbit Corneal Epithelial Cell Line

4. RATIONALE FOR INVESTIGATION	68
4.1 Overview.....	68
4.2 Statement of Problem	69
4.3 Objectives	70

5. FUNCTIONAL CHARACTERIZATION OF FOLATE TRANSPORT PROTEINS IN STATEN’S SERUMINSTITUT RABBIT CORNEAL EPITHELIAL CELL LINE

5.1 Rationale.....	72
5.2 Materials and Methods	74
5.3 Results	84
5.4 Discussion	105
5.5 Conclusion.....	109

PART III: Differential Expressions of Folate receptor-alpha (FR- α), Sodium dependent multivitamin transporter (SMVT), Neutral and Cationic Amino acid transporter B^(0,+) in human retinoblastoma (Y-79) and normal human retinal (ARPE-19) cell lines

6. RATIONALE FOR INVESTIGATION	111
6.1 Overview	111
6.2 Statement of Problem	113
6.3 Objectives	114
7. DIFFERENTIAL EXPRESSIONS OF FOLATE RECEPTOR-ALPHA (FR-A), SODIUM DEPENDENT MULTIVITAMIN TRANSPORTER (SMVT), AND NEUTRAL AND CATIONIC AMINO ACID TRANSPORTER B ^(0,+) IN HUMAN RETINOBLASTOMA (Y-79) AND NORMAL HUMAN RETINAL (ARPE-19) CELL LINES	
7.1 Rationale	115
7.2 Materials and Methods.....	119
7.3 Results.....	125
7.4 Discussion	138
7.5 Conclusions.....	141
8. SUMMARY AND RECOMMENDTIONS	143
8.1 Summary	143
8.2 Recommendations	144
APPENDIX.....	146
REFERENCES	148
VITA.....	161

ILLUSTRATIONS

Figure	Page
1. Structure of the eye	2
2. Fate of a topically administered drug.....	5
3. Histological sections of scleral samples stained by hematoxylin/eosin dye.....	21
4. Uptake of [3H] gly-sar across rabbit primary corneal epithelial culture (rPCEC) cell monolayers	24
5. Evasion of efflux pumps by transporter targeted prodrug approach.....	28
6. Uptake of [3H] ritonavir across rabbit primary corneal epithelial culture (rPCEC) cell monolayers.....	29
7. Uptake of [14C] erythromycin across rabbit primary corneal epithelial culture (rPCEC) cell monolayers	30
8. Bioconversion pathway of LV-LV-ACV in rPCEC cell homogenate	54
9. Binding of stereoisomeric peptide prodrugs of acyclovir near tryptophan 294 amino acid.....	55
10. Percentage uptake of [³ H]-Gly-Sar by rPCEC cells in presence of LV-LV-ACV, LV-DV-ACV DV-LV-ACV, and DV-DV-ACV	56
11. Cytotoxicity of ACV, LV-ACV, LV-LV-ACV, LV-DV-ACV, DV-LV-ACV, and DV-DV-ACV in rPCEC cells.....	58
12. Surface morphology of nanoparticles	61
13. <i>In vitro</i> release profile of LV-LV-ACV from PLGA75:25 nanoparticles and from PLGA75:25 nanoparticles suspended in PLGA-PEG-PLGA thermosensitive gel.....	62
14. <i>In vitro</i> release profile of LV-DV-ACV from PLGA65:35 nanoparticles and from PLGA65:35 nanoparticles suspended in PLGA-PEG-PLGA thermo sensitive gel	63

15. Uptake of [³ H]Folic acid by SIRC cells as a function of time.....	85
16. Uptake of [³ H]Folic acid by SIRC cells as a function of pH.....	86
17. Uptake of [³ H]Folic acid by SIRC cells as a function of temperature.....	87
18. Uptake of [³ H]Folic acid by SIRC cells as a function of ions	88
19. Uptake of [³ H]Folic acid by SIRC cells in presence of various energy inhibitors	91
20. Uptake of [³ H]Folic acid by SIRC in presence of membrane transport inhibitors and endocytosis inhibitor colchicine	92
21. Substrate specificity of uptake of [³ H]Folic acid (10 nM) by SIRC cells in presence of various structurally related and unrelated analogs.....	93
22. Uptake of [³ H]Folic acid (10 nM) in presence of various concentrations of cold folic acid on SIRC cell line	94
23. Effect of Ca ²⁺ /calmodulin-mediated pathways modulators on the uptake of [³ H]Folic acid in SIRC cells.....	95
24. Effect of PKA pathway modulators on uptake of [³ H]Folic acid in SIRC cells.....	97
25. Effect of PTK pathway modulators on uptake of [³ H]Folic acid in SIRC cells	98
26. RT-PCR analysis of FR- α (Folate receptor), RFC (reduce folate carrier), PCFT (Proton coupled folate transporter)	100
27. Western blot analysis of FR- α (Folate receptor) and PCFT (Proton coupled folate transporter).....	101
28. <i>Ex vivo</i> permeability of [³ H] Folic acid in excised rabbit cornea. Each data point represents the mean standard deviation of 4 separate determinations	104
29. Schematic representation of transporter/receptor mediated drug delivery	118
30. Qualitative expression of B ^(0,+) , FR- α , and SMVT in ARPE-19 cells	126
31. Qualitative expression of B ^(0,+) , FR- α , and SMVT in Y-79 cells.....	127

32. Relative fold expression of SMVT, B ^(0,+) , FR- α , in ARPE-19 and Y-79 cells by quantitative real time PCR analysis	130
33. Quantitative uptake of [³ H] Folate, [³ H]Biotin and [³ H]B ⁽⁰⁺⁾ in ARPE-19 and Y-79 cells a comparative study	131
34. Uptake of [3H] Folate by ARPE-19 cells as a function of substrate concentration at 37°C, pH 7.4	133
35. Uptake of [3H] Arginine by ARPE-19 cells as a function of substrate concentration at 37°C, pH 7.4	135
36. Uptake of [3H] Arginine by Y-79 cells as a function of substrate concentration at 37°C, pH 7.4	136

TABLES

Table	Page
1. Stability in cell and ocular tissue homogenates-first-order degradation rate constants of all prodrugs	51
2. Docking scores of stereo isomeric dipeptide prodrugs of ACV	53
3. Entrapment efficiency and drug content using various grades of PLGA.....	60
4. Primers for RT-PCR analysis FR- α in SIRC cells	81
5. <i>Ex vivo</i> permeability of [³ H]Folic acid in excised rabbit cornea.....	103
6. Primers for RT-PCR analysis of B ^(0,+) , FR- α and SMVT in ARPE-19 & Y-79 cells.	121
7. q PCR primers for sodium-dependent multivitamin transporter (SMVT), folate, and B ⁰⁺ . Sequence is given from 5'->3'.....	122
8. Relative fold Expression of SMVT, FR- α , B ^(0,+) in ARPE-19 and Y-79	129
9. K _m and V _{max} values of [³ H]Biotin, [³ H] Folate, and [¹⁴ C] Arginine in ARPE-19 and Y-79 cells	137

ACKNOWLEDGEMENTS

My sincere acknowledgment goes to my advisor Dr. Ashim K. Mitra who has been very influential in ensuring my academic and professional well being ever since I have joined the PhD program. He is a great mentor, whose constructive feedback and unfailing support always motivated me to excel in my research. I am thankful to Drs. Lee, Cheng, Van Horn and Holder for serving on my supervisory committee and for their constant encouragement and timely support. It's a great honor to have such outstanding researchers on my PhD supervisory committee. Their constructive feedback at various levels has significantly helped me in shaping my dissertation up to completion.

I am very thankful to Dr. Dhananjay Pal for his professional and emotional support during various stages of my PhD. I owe a big thanks to Mrs. Ranjana Mitra for her cheerful encouragement and help throughout my stay at UMKC. It is my pleasure to extend my gratitude to Dr. Boddu, Dr. Gunda and Dr. Gaudana for their constant support, time, and scientific input into my research. Thanks are due to Sujay Shah, Aswani Dutt Vadlapudi, Ripal Gaudana, Ramya Vadlapatla and all my other lab mates for their help and constant input in my research and for making my stay at UMKC a memorable one. I thank Dr. Suman Sirimulla for his help with the docking studies. I also sincerely thank Joyce Johnson, Sharon Self, and Rodger Palmer at School of Pharmacy and Connie Mahone, Nancy Hover at School of Graduate Studies for their help at various stages.

I would like to express my profound gratitude to my husband Bharaneeshwar.R, my daughter Haasya.R, my parents Bala Buchaiah.V and Venkata Laxmi.V and brothers Mr. Suman and Mr. Rakesh Gupta for their constant encouragement, love and moral support.

DEDICATED TO MY FAMILY

CHAPTER 1

INTRODUCTION

1.1. Anatomy and Physiology of the Eye

Human eye can be viewed as a globe with two compartments i.e. anterior and posterior segments (Fig.1). The anterior segment includes cornea, conjunctiva, iris, pupil, lens, aqueous humor and ciliary body. Cornea is the outermost multilayered (five layers) transparent membrane of eye. It is devoid of blood capillaries and receives nourishment from the aqueous humor (Civan and Macknight, 2004). The cornea comprises of epithelium, bowman's membrane, stroma, descemet's membrane, and endothelium (arranged in the order of outermost to innermost) (Dingeldein and Klyce, 1988). Iris is composed of pigmented epithelial cells and iridial sphincter muscles. These muscles are driven by cholinergic nerves to constrict the pupil (miosis). Similarly, iris also contains the dilator muscles, which are responsible for dilation of the pupil (Snell and Lemp, 1989). Ciliary body is comprised of highly flexible fibrous bundles and ciliary muscles. Non-pigmented epithelial cells located on the blood-aqueous barrier, restrict the transport of proteins and colloids into aqueous humor (Gray and Carter, 1991). Conjunctiva is a clear mucous membrane, which is composed of non-keratinized stratified columnar epithelial cells. It is divided into palpebral, fornical, and bulbar conjunctiva and is followed by underlying basement membrane, which helps in the lubrication of eye by producing mucus and tears (Snell and Lemp, 1989).

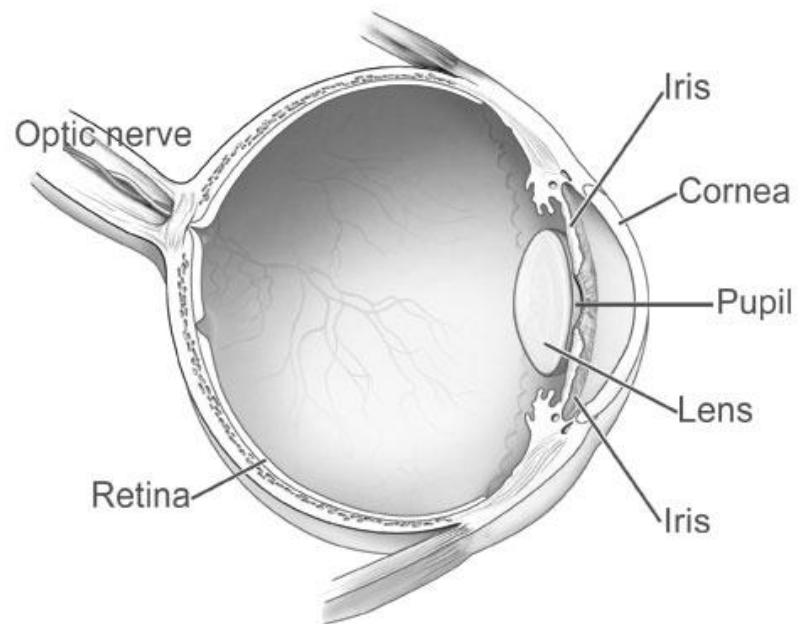


Fig.1. Structure of the eye.
Credit: National Eye Institute, National Institutes of Health

The posterior segment mainly consists of retina, choroid, sclera, vitreous humor and optic nerve. Sclera is a thin spherically shaped connective tissue, which is composed of collagen bundles with dispersed melanocytes and elastic fibers that gives shape to the eye ball and controls its movement (HF. and JL., 2003; Rada et al., 2006). It is internally lined by the choroid, which contains blood vessels, and the retina, contains nerves involved in sight. The choroid is a layer sandwiched between retina and sclera. It contains layers of blood vessels (arteries and veins), choriocapillaries (dense network of capillaries) and Bruch's membrane (composed of basal lamellae of RPE and endothelial cells of choroid) (Sharma and Ehinger, 2003). Retina is divided into retinal pigmented epithelium (RPE) and neurosensory retina. Light sensing neural cells i.e. rods and cones are in direct contact with RPE and nourishes the retina via choroid. Retinal artery provides blood supplies to the inner part of neurosensory retina, whereas choriocapillaries provides nutrition to the outer portion. Vitreous humor is the hydrogel matrix (98 to 99.7% of water, collagen fibrils and hyaluronic acid), localized between retina and lens. This matrix is separated from the anterior chamber by anterior hyaloid membrane (Andersen and Sander, 2003).

1.2. Constraints to Topical Delivery

Topical drug delivery is the most convenient method for drug administration to anterior segment of the eye. This method of administration provides numerous advantages such as ease of administration, non-invasive drug delivery, bypasses first-pass metabolism and provides local drug delivery (Davies, 2000). Though topical administration is the most preferred route, it suffers from several disadvantages such as nasolachrymal drainage, loss in

the conjunctival blood circulation, tear dilution, tear drainage, and blink reflux (Fig. 2). Structural barriers like the cornea and conjunctiva also limit the therapeutic concentrations in anterior segment of the eye (Dey and Mitra, 2005). The corneal epithelium is approximately about 35-50 μm thick and offers a high shunt resistance of 12-16 $\text{kohm}\cdot\text{cm}^2$. The human cornea consists of three layers: the outer lipophilic epithelium, the middle hydrophilic stroma and the inner endothelium. The resistance offered by the cornea to the intraocular drug absorption is sum of the resistance offered by all three layers; $R_{\text{cornea}} = R_{\text{epithelium}} + R_{\text{stroma}} + R_{\text{endothelium}}$. Thus, the cornea contains a formidable barrier for the transcorneal permeation of both hydrophilic and hydrophobic drugs (Prausnitz and Noonan, 1998). It has been reported that drugs which are moderately lipophilic (log octanol-water partition coefficient ~ 2.9) can easily permeate through the corneal epithelium (Schoenwald and Ward, 1978). Drug fraction which is not absorbed by the cornea is either washed off or drained into the blood stream via nasolacrimal duct, leading to undesirable side effects. For example, systemic absorption of ophthalmic drugs such as timolol, cyclopentolate, chloramphenicol, and phenylephrine have shown deleterious effects on the heart and central nervous system (Fraunfelder and Meyer, 1987; Frishman et al., 2001). In addition, the surface area of the conjunctiva is about 17 times larger and 30 times more permeable than cornea. Most of the hydrophilic drugs are absorbed by conjunctiva and diffuse into the systemic circulation via scleral-conjunctival route (Romanelli et al., 1994).

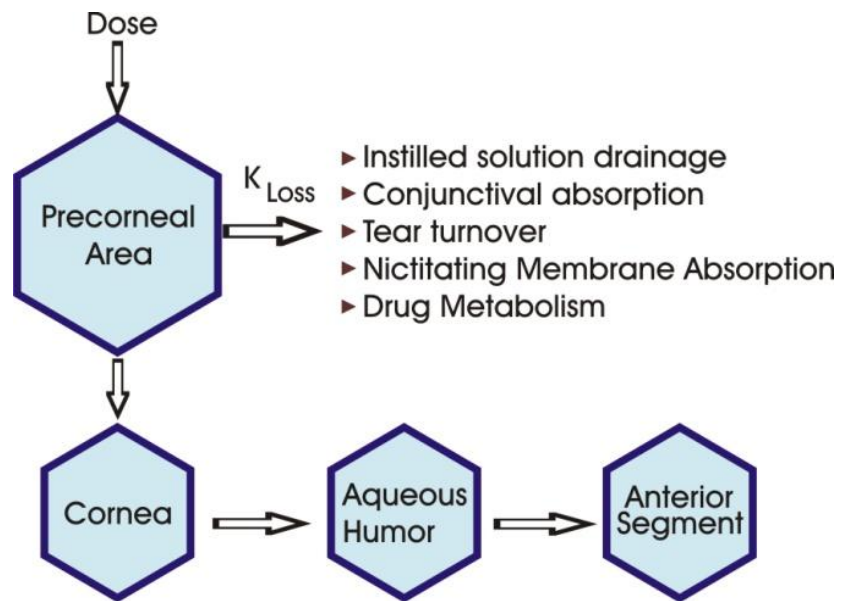


Fig.2. Fate of a topically administered drug

Thus, the conjunctival absorption of drugs can also significantly affect the ocular bioavailability of drugs following topical administration. Various nutrient transporters and efflux proteins are expressed in different parts of the eye. Below is the brief description about various transporters expressed in different parts of eye.

1.3. Nutrient Transporters and Efflux Pumps in the Eye

Epithelial cells express various nutrient transporters and receptors on their membrane surface. These nutrient transporters aid in the movement of various vitamins and amino acids across the cell membrane. Our laboratory has extensively studied various transporters and receptors which are present on ocular structures. We have also shown that attachment of various transporters/receptors targeted ligands can enhance ocular bioavailability significantly. A detailed discussion of all influx transporters is beyond the scope of this review. So, we have summarized a few vital transporters.

1.3.1. Peptide Transporter

It is a robust transporter which has gained considerable attention in the recent years for targeted drug delivery (Ganapathy and Leibach, 1982). These proton coupled transporters help in the translocation of di and tripeptides across the epithelium (Adibi, 1997). These proteins are mainly classified into PepT1, PepT2 and peptide/histidine transporters (PHT 1 and PHT 2). Many drug molecules are known to be substrates for these transporters. Our laboratory has shown the presence of an oligopeptide transporter on rabbit cornea (Anand and Mitra, 2002). Other drugs including β -lactam antibiotics, renin inhibitors and ACE-inhibitors are known to be substrates for PepT1 and PepT2. Ocheltree and his colleagues

have demonstrated the expression of PHT1 in BRPE, HRPE (human RPE cells), ARPE-19 (human RPE cell line), and bovine and human neural retina. However, they could find the expression of PEPT2 and PHT2 only in bovine and human retina; and PEPT1 was not detected. They also concluded that glycylsarcosine uptake studies did not demonstrate any significant functional activity of PHT1 on plasma membranes of RPE (Ocheltree et al., 2003). We have also investigated the mechanism of model dipeptide (glycylsarcosine) transport across the blood-ocular barriers following systemic administration in our laboratory. A time and concentration dependent, carrier mediated uptake of glycylsarcosine across the blood-ocular barrier was reported (Atluri et al., 2004). Prodrugs (valine-ACV and valine-valine-ACV) exhibited higher concentrations of ACV in aqueous humor following systemic administration as compared to parent drug. This study indicates that peptide prodrugs are taken up via carrier mediated transport mechanism (Dias et al., 2002). Hence, drugs with poor ocular bioavailability can be suitably modified so that they can be recognized by peptide transporters.

1.3.2. Glucose Transporter

Glucose is utilized by retina to meet the energy needs for oxidative metabolism. Neural retina is considered to have the highest metabolic rate per unit weight (Winkler, 1981). So, an alteration in the metabolic rate can lead to potential ocular complications. Glucose is transported across the blood-retinal and blood aqueous barriers by a stereo-specific, saturable process of facilitated diffusion. Glucose transporters are expressed in various isoforms GLUT 1, GLUT2, GLUT3, GLUT4, GLUT5, GLUT6 and GLUT7. Out of these GLUT1, GLUT3, and

GLU4 are high-affinity glucose transporters where as GLUT5 is a high-affinity fructose transporter. GLUT2 is considered to be low affinity glucose transporter. GLUT6 is a pseudogene which does not encode for a functional transporter. GLUT7 is similar to GLUT2 but exclusively expressed in endoplasmic reticulum (Merriman-Smith et al., 1999). Mantych and his colleagues have studied the presence of various glucose transporter isoforms (Glut 1, Glut 3, Glut 4, and Glut 5) in human eye using western blot and immunohistochemical techniques. This study reported the presence of Glut 1 in RPE, choroid, pars plana, retinal muller cells, and lens fiber cells (Mantych et al., 1993). Glucose transporters are more efficient and have high capacity than any other nutrient transporter. But high substrate specificity of glucose transporters renders them inefficient for drug delivery purpose.

1.3.3. Vitamin C Transporter

Vitamin C or ascorbic acid (AA) acts as an antioxidant and thereby protects the cornea and other ocular tissues from UV radiations. Aqueous humor is the main source of AA for cornea and lens. AA levels in aqueous humor are partly responsible for preventing cataract (Brubaker et al., 2000). Two specific transporters (SVCT-1 and SVCT-2) of vitamin C were identified in the ocular tissues of human, rabbit and rat. These transporters have identical sequence homology. Transport of AA across the cells is mediated by two different transporter families. One consists of the low affinity and high capacity facilitative hexose transporters (GLUT) which translocate dehydro ascorbic acid (oxidized form of ascorbic acid), and the other consists of high affinity and low capacity sodium dependent vitamin C

transporters (SVCT1 and SVCT2) that ferries L-ascorbic acid (reduced form of ascorbic acid) (Liang et al., 2001).

1.3.4. Amino acid Transporter

Amino acids are responsible for protein synthesis and maintenance of structural and functional integrity of conjunctiva and retina/RPE. These transporters help in transferring amino acids from circulating blood to various organs. The presence of various amino acid transporters (ASCT1, LAT1 and ATB^(0,+)) on the cornea has been confirmed by gene expression. These transporters are actively involved in the transportation of L-alanine, L-arginine and L-phenylalanine across the cornea. Amino acid transporters can be classified on the basis of their sodium dependency and substrate specificity (Kanai and Hediger, 2004). System L (large) and system y⁺ (cationic) amino acid transporters belong to sodium independent transporters while system X⁻ (anionic), system A, B^(0,+), ASC (anionic, cationic, and neutral amino acid transporters) belong to sodium dependent transporter category (Anand and Mitra, 2002). Large neutral amino acid transporter is expressed in two isoforms LAT1 and LAT2. LAT1 is mainly involved in the transport of large neutral amino acids, such as Leu, Phe, Ile, Trp, Val, Tyr, His and Met while LAT2 transports both large neutral amino acids and small neutral amino acids (Fukasawa et al., 2000; Verrey et al., 2000). Transport systems for amino acids have been characterized on corneal epithelium and endothelium. Gandhi and his coworkers have studied the biochemical evidence of sodium independent facilitative transport system, LAT2, with high substrate specificity on ARPE-19 cell line (Gandhi et al., 2004). Blisse et al., reported the presence of sodium-dependent,

B^(0,+) amino acid transporter with broad substrate specificity on rabbit corneal epithelium and human cornea. This transporter belongs to neurotransmitter gene family and found to have comparable affinity towards PEPT1 in the transport of prodrugs, like valine-ACV and valine-GCV (Ganapathy and Ganapathy, 2005; Jain-Vakkalagadda et al., 2004). Such transport systems may be efficiently targeted for enhancing ocular delivery of drugs.

1.3.5. Efflux Transporters

Efflux of various substrates across plasma membrane and cytoplasm into extracellular fluid is mainly governed by ABC (ATP-binding cassette) superfamily of proteins which are encoded by MDR1 gene (Eytan and Kuchel, 1999). ABC transporters are broadly classified into 2 types a) complete transporter, contains four units (two nucleotide-binding domains and two membrane bound domains) and b) half transporter, which possesses only two units (one nucleotide-binding domain and one membrane-bound domain transport). Half transporter must attach with another half transporter to perform its action (Dean et al., 2001). These ABC proteins are actively involved in detoxification process by regulating the transport of various sterols, lipids, endogenous metabolic products and xenobiotics (Sarkadi et al., 2006). Literature search reveals that mainly two multidrug efflux pumps are responsible for the development of chemoresistance a) P-glycoprotein (ABCB1) and b) multidrug resistant protein (MRP) (ABCC1) (Sharom, 2008).

P-gp is a 170 kDa membrane bound efflux protein generally expressed on the apical surface of polarized cells (Bellamy, 1996). P-glycoprotein is actively involved in the efflux of drug molecules thereby reducing drug accumulation inside cells (Gottesman and Pastan, 1993).

The presence of P-gp in the eye has been confirmed on conjunctival epithelial cells (Saha et al., 1998), ciliary non-pigmented epithelium (Wu et al., 1996), human and rabbit cornea (Dey et al., 2003), retinal capillary endothelial cells, iris and ciliary muscle cells (Holash and Stewart, 1993). Constable et al. studied the presence of P-gps on three human RPE cell lines, ARPE19, D407 and h1RPE. They concluded that only D407 cell functionally express P-gp and hence can be used for *in vitro* drug transport studies without any modifications (Constable et al., 2006).

MRP is a 190 kDa membrane bound efflux protein encoded by MRP1 gene. It is generally expressed on basolateral surface of intestine, hepatocytes and kidney cells (Roelofsen et al., 1999; Yang et al., 2007). Till now twelve different members of MRP family have been studied (Kruh et al., 2007). MRP's are actively involved in effluxing glucuronide, sulfate conjugated compounds and organic anions. Aukunuru et al. studied the presence of functionally and biochemically active MRP on human RPE cell line (Aukunuru et al., 2001). Further studies by Steuer et al., confirmed that MRP is present on the choroidal side of outer blood retinal barrier (Steuer et al., 2005). Recent studies from our laboratory revealed the presence of ABCC2 (a MRP homologue) on human corneal epithelium and rabbit cornea (Karla et al., 2007b). Recently Zhang et al., have performed an extensive research on implications of drug transporter and CYP P450 mRNA expression in ocular drug disposition. They concluded that both BCRP and MRP2 have very low expression levels in human cornea while there were moderate MRP1 and low MRP3 expression levels. Moreover, designing

drugs that can efficiently evade MRP1 efflux may play an important role in the enhancement of ocular penetration (Zhang et al., 2008).

Efflux pumps constitute significant barriers to the entry of drug molecules. It is indeed necessary to develop alternative strategies which can improve ocular drug absorption.

1.4. Conventional Drug Delivery Systems

1.4.1. Eye drops

This is the most commonly used dosage form for the treatment of diseases such as glaucoma, dry eye, allergies, inflammation and conjunctivitis. Eye drops are highly patient compliant due to ease of administration and non-invasive nature. Depending on the disease condition, eye drops may contain steroids, prostaglandins, anesthetics, antihistamines, sympathomimetics, parasympatholytics, β -receptor blockers, parasympathomimetics, and non-steroidal anti-inflammatory drugs (NSAID). Eye drops also contain various inactive ingredients such as viscosity enhancers (hydroxypropyl methylcellulose (HPMC), carboxy methylcellulose (CMC), polyvinyl alcohol (PVA), and carbopol), preservatives (benzalkonium chloride and chlorobutanol), demulcents (polyethylene glycol 400 and polypropylene glycol), buffers (disodium phosphate, sodium borate, sodium citrate) and tonicity adjusting agents (sodium chloride) (Christensen et al., 2004). A single dose of timolol/pilocarpine eye drop can control the intraocular pressure for 12 hr (Lofors et al., 1990). Despite of numerous advantages, availability of the drug after topical instillation of ocular drops has always been a major concern. The ocular bioavailability following topical administration is governed by numerous factors. The retention of dosage form in pre-corneal

area greatly influences the volume and amount available for drug absorption. Nearly all marketed eye droppers or dispensers deliver a volume of 30-50 μL to the eye. However, human eye can accommodate a volume of 30 μL (Mishima et al., 1966). File et al., investigated the effect of dose size (0.5% pilocarpine hydrochloride) on the pupillary response in human volunteers. It was found that the miotic response obtained was almost similar for both 20 and 50 μL drops. These findings suggest that commercial eye drops in some cases may deliver higher doses than required for maximal therapeutic response (File and Patton, 1980). Furthermore, rapid tear turnover rate (1 $\mu\text{L}/\text{min}$) also plays an important role in decreasing the availability of drug after topical administration. Under normal physiological conditions, the tear turnover rate in human is approximately 16% per min. The normal tear volume (7 μL) is quickly restored in about 2-3 min; as a result nearly 80% of the administered drug gets drained within the first 15-30 sec. This process reduces the contact time of drug with the membrane which further decreases its absorption (Ahmed and Patton, 1985). Several strategies have been adopted to enhance the bioavailability of drugs following topical administration.

1.4.2. Aqueous Suspensions

These are liquid formulations of fairly hydrophobic drugs where the drug particles are uniformly dispersed in an aqueous vehicle with the help of dispersing agents. This uniform dispersion is important for delivery of an accurate dose by topical drops. A major advantage of aqueous suspension over solution is the retention of drug in the cul-de-sac which in turn improves its contact time with the absorbing membrane (Kaur and Kanwar, 2002). An

increase in the particle size may prolong retention time in cul-de-sac; however, it may also cause severe irritation to the eye. It is very important that the rate of dissolution of drug particles should not be slower than their rate of clearance from the precorneal region (Sieg and Robinson, 1975). Size of the drug particles in aqueous suspensions should be less than 10 μm for an optimal dissolution rate (Kaur and Kanwar, 2002). The effect of 0.1 and 0.5% suspension on the ocular availability of fluorometholone was studied in albino rabbits. Peak levels of fluorometholone in aqueous humor were reached at 30 min with suspension formulations. Furthermore, topical application of suspension formulations substantially sustained the effect of fluorometholone relative to the saturated solution (Zhu and Chauhan, 2008). Aqueous suspension, however suffers from several drawbacks such as physical instability, crystal growth (reduction in drug solubility), aggregation of drug particle, need for shaking prior to administration for accurate dose delivery, difficulty in manufacturing and sterilization. In the recent years, limitations associated with aqueous suspensions have been overcome by using delivery systems such as nanoparticles and microparticles.

1.4.3. Emulsions

Oil in water (o/w) and multiple (o/w/o or w/o/w) emulsions have been utilized in the delivery of poorly soluble drugs. O/W emulsion is an example of a two phase system where, the oil phase evenly dispersed in the water phase. Drugs with poor aqueous solubility are solubilized in the internal oil phase. O/W emulsion prepared with Polawax is well-tolerated. It has enhanced the anti-inflammatory effect of 4-biphenylacetic acid in the rabbit model with ocular inflammation. O/W/O emulsion significantly improved ocular bioavailability of

hydrocortisone in rabbits when compared to O/W emulsion and solution. However, the sensitivity of corneal and conjunctival tissues to surfactants present in the formulation has considerably diminished the interest in utilizing emulsions as drug carriers (Saettone et al., 2001). However, the use of emulsions for topical delivery has been renewed due to the introduction of micro and nanoemulsions.

1.4.4. Ointments

Ointments are highly viscous semisolid preparations containing an active drug, which is homogeneously dispersed in an oleaginous base. Ophthalmic ointments have been extensively studied as a drug carrying vehicle owing to their advantages such as improved drug retention, resistance to nasolacrimal drainage and inhibition of drug dilution with tears (Shell, 1982). In addition to these potential benefits, ointments are also well tolerated, safe and provide sustained release at the site of application. Acyclovir ointment (3%) applied in the cul-de-sac of rabbit's eyes achieved a C_{max} of 3.38 and 45.78 $\mu\text{g/mL}$ in aqueous humor and cornea at 60 and 30 min, respectively (Kitagawa et al., 1989). Miconazole ointment (1%) is highly effective in the treatment of fungal ulcers and associated lesions caused by *Candida*, *Aspergillus* and *Fusarium* organisms in experimental keratomycosis (Gupta et al., 1986). The ointment formulation is well tolerated and it is non toxic to rabbit eye. Moreover, the frequency of administrations is very less compared to eye drops. Ophthalmic ointments are associated with some disadvantages such as inaccurate dose delivery, blurred vision, requirement of preservatives, and manufacturing difficulties. Several ointments have been marketed for night time administrations so as to prevent their interferences with vision during

daytime. Erythromycin (Ilotycin®), gentamicin (Gentak®), tobramycin (Tobrex®) and other ophthalmic ointments are available in the market for ocular infections.

1.4.5. Gels

Gels offer another alternative for improving the residence time of drugs following topical administrations. Gels can also control drug release and thereby reduce its frequency of administrations. Aqueous gels and hydrogels are two different systems developed for prolonging drug contact time on the ocular surface. Aqueous gels are usually prepared with water soluble polymers such as PVA, polyacrylamide, poloxamer, carbomer, CMC, HPMC, polymethylvinylether maleic anhydride and hydropropyl ethylcellulose. CMC and sodium alginate gel containing 1% w/v atenolol was investigated for determining their ability to reduce the IOP in rabbits. Atenolol (1% w/v) solution was administered as control. Results from *in vivo* studies suggested that the gel formulations are more effective in prolonging the effects of atenolol (8 h) relative to atenolol solution (Hassan et al.,2007). Hydrogels are formulated from water insoluble polymers which have the property of absorbing water from the aqueous medium. Such swelling system sustains drug release for a prolonged period of time (Kaur and Kanwar, 2002). Hydrogels prepared using poly (ethylene glycol) (PEG)-based copolymers containing multiple thiol (SH) groups were studied for their efficacy in controlling pilocarpine release (Anumolu et al., 2009). Hydrogel was able to sustain the pupillary constriction for a period of 24 h when compared to pilocarpine solution (3 h). Preformed hydrogels are associated with several deficiencies such as inaccurate dose delivery, lacrimation and crusting of eyelids (Nanjawade et al., 2007). Moreover, blurred

vision, possible bacterial contamination and difficulties in sterilization are other major concerns associated with such gels (Kaur and Kanwar, 2002). Recently, polymer based *in situ* gelling systems has gained significant attention due to their combined advantages of liquid dosage form (solutions or suspensions) and gels. Initially, these systems are in solution or suspension form. Following topical administration, these formulations undergo sol-gel transition in the cul-de-sac. Gelation of these systems can be achieved by shifts in three parameters; temperature, pH and electrolyte composition (Nanjawade et al., 2007). In temperature induced gelation, the initial dosage form is liquid at room temperature (20-25⁰C). Phase transition of the polymer solution occurs in the cul-de-sac (35-37⁰C) of eye following topical instillation. Polymers such as poloxamers (Pluronic®), cellulose derivatives such as methylcellulose (MC), HPMC, ethyl hydroxyethyl cellulose (EHEC), xyloglucan, gelatins and carrageenan are the most commonly used thermal setting polymers. Pluronic F-127 containing formulation showed a temperature dependent sol-gel phase transition and increased retention time of forskolin in rabbit model. IOP reducing effect of forskolin was achieved for 12 h, following topical administration of the formulation (Gupta and Samanta, 2009). Several polymers i.e. pseudolatexes, cellulose acetate phthalate latex, chitosan, and carbopol also form gel when the pH 4.5 of the formulation is raised to 7.4 by the tear fluid, as seen in pH induced in situ gelation. A formulation containing Pluronic F127 and chitosan significantly enhanced transcorneal transport and ocular retention time of timolol maleate. This clear isotonic formulation was liquid at room temperature and converted into gel at 35⁰C and pH of 6.9-7.0. This suggests its usefulness as a potential drug

delivery vehicle for increasing the retention time of drugs following topical administration (Gupta et al., 2007). In ion activated in situ gelation, polymers such as alginates and Gelrite gels by interacting with sodium or calcium ions present in tears. Liu et al. and his coworkers have studied the effect of an ophthalmic formulation containing alginate (gelling agent) and HPMC (viscosity enhancer) on the release and pre-corneal retention of gatifloxacin. This study was based on the concept of ion triggered sol-gel transition of the formulation. They found that alginate along with HPMC significantly retained gatifloxacin as compared to alginate or HPMC solutions alone (Liu et al., 2006).

1.5. Novel Strategies to Improve Ocular Drug Absorption

In spite of the application of various novel drug delivery systems for the topical delivery of drugs across the cornea, this field still remains a potential challenge for drugs such as acyclovir, ganciclovir and cidofovir which are hydrophilic and those drugs that act as substrates for efflux proteins expressed on corneal epithelium. The corneal epithelium is highly lipophilic in nature and this further limits the permeation of these hydrophilic drugs. Furthermore, the efflux proteins also play an important role in limiting the intracellular accumulation of the drugs. Recently, transporter targeted drug delivery and circumvention of efflux proteins via prodrug derivatization has been widely studied for increasing the bioavailability of drugs following topical administration. In addition to these strategies, iontophoresis and phonophoresis are currently investigated for enhancing drug delivery through the cornea.

1.5. 1. Nanoparticles for ocular drug delivery

Nanoparticles are colloidal systems with a size ranging from 10 to 1000 nm. They are classified into two types, nanospheres and nanocapsules. In nanospheres, drugs are either adsorbed or entrapped inside the polymeric matrix (Barratt, 2000). In nanocapsules, the agent is confined to the inner liquid core while the external surface of nanoparticles is covered by the polymeric membrane (Soppimath et al., 2001). Conventional delivery systems often fail to achieve required therapeutic concentrations in the eye due to the presence of ocular barriers. Nanoparticles have been successfully employed to enhance the ocular bioavailability compared to eye drops. Entry of nanoparticles into the ocular tissues require optimal binding, which depends on various properties such as hydrophilic/lipophilic properties of polymer-drug system, optimal retention and biodegradation rate in the precorneal cavity (Ghate and Edelhauser, 2006). Hence it is highly desirable to formulate particles with bioadhesive materials so as to increase their retention time in the cul-de-sac (Li et al., 1986). Poly (D, L-lactide co-glycolide) was employed to prepare flurbiprofen loaded nanospheres and examined for its efficacy in improving corneal permeation. *Ex-vivo* corneal permeation of flurbiprofen loaded nanoparticles exhibited four-fold increase in the corneal penetration (Vega et al., 2008). Nanoparticles have been successfully employed as an alternative for long term drug delivery to posterior segment. Zhang et al. investigated the pharmacokinetics and tolerance of dexamethasone loaded poly (lactic acid-co-glycolic acid) nanoparticles in rabbits following intravitreal injection. The results clearly indicated that dexamethasone when encapsulated in nanoparticles exhibited sustained release for

approximately 50 days and the release pattern was constant until 30 days with a concentration of 3.85 mg/L. These results imply that intravitreal injection of dexamethasone nanoparticles may be utilized for sustained delivery of therapeutics for the treatment of posterior segment eye diseases (Zhang et al., 2009). Boddu et al. have investigated the development and characterization of PLGA nanoparticles of dexamethasone, hydrocortisone acetate, and prednisolone acetate suspended in thermosensitive gels for the treatment of macular edema. When nanoparticles were suspended in thermosensitive gels, the release of dexamethasone, hydrocortisone acetate, and prednisolone acetate was sustained with no initial burst effect. Permeation of dexamethasone from suspension containing 0.5% HPMC occurred for nearly 4 h. A significant increase in the duration of release was observed when nanoparticles were suspended in thermosensitive gels. Histological examination of sclera did not exhibit any noticeable changes after the completion of permeability studies (Fig. 3). This study concluded that steroidal nanoparticles suspended in thermosensitive gels may provide sustained retina/choroid delivery of steroids upon episcleral administration (Boddu et al., 2010). Bourges et al. have studied the migration of PLA nanoparticles to RPE cells following an intravitreal injection. This study concluded that following intravitreal injection, particles were retained in the retina for the duration of approximately 4 months (Bourges et al., 2003). Nanoparticles have been successfully employed for sustaining the drug release and enhancing drug permeation across the cornea. Researchers are now attempting to target drugs to various ocular tissues using surface modified nanoparticles.

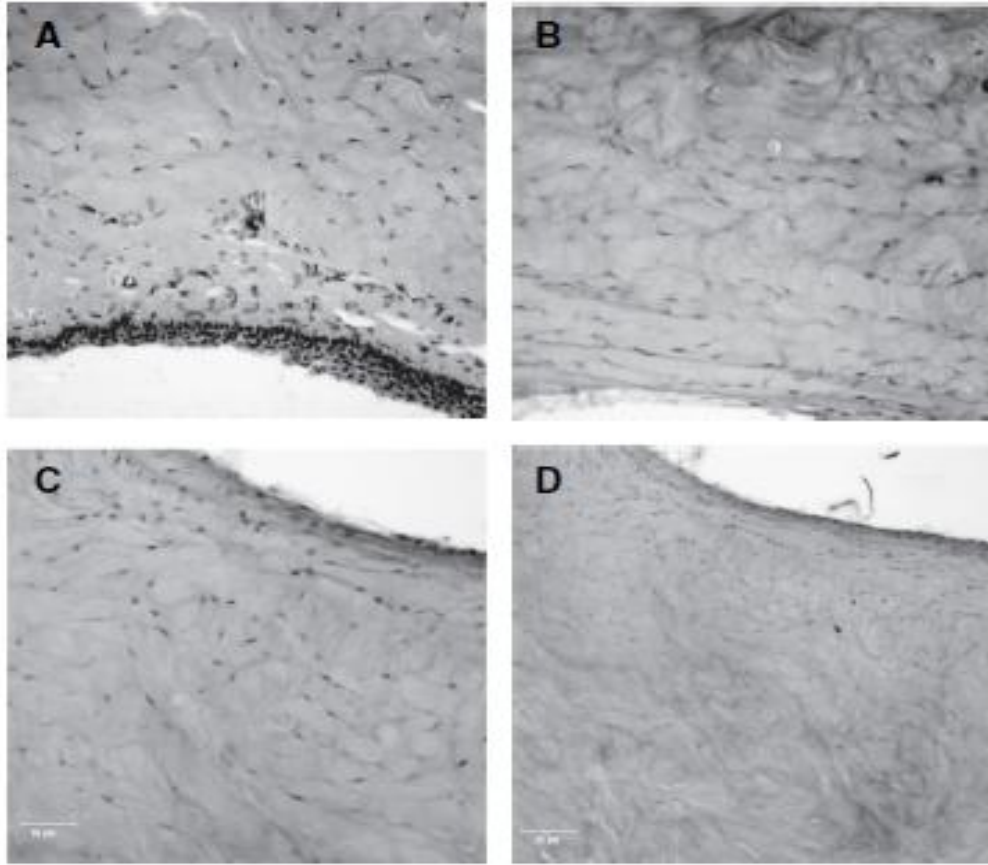


Fig.3. Histological sections of scleral samples stained by hematoxylin/eosin dye. (A) Control, (B) after 1 day, (C) after 2 days, and (D) after 4 days. The black color dots represent the nuclei of the scleral fibroblast cells. (*Boddu SH et.al 2010*)

1.5.2. Transporter Targeted Drug Delivery

This strategy involves the targeting of drug molecules to nutrient transport systems present on the corneal epithelium. Various nutrient transporters are expressed on both apical and basolateral sides of the corneal epithelium. These include peptide transporters, PEPT1 and PEPT2 (Xiang et al., 2009), Na⁺-independent large neutral amino acid transporter, (LAT1) (Jain-Vakkalagadda et al., 2003), Na⁺-dependent cationic and neutral amino acid transporter (B⁰⁺) (Jain-Vakkalagadda et al., 2004), Na⁺-dependent neutral amino acid transporter, (ASCT1) (Katragadda et al., 2005), sodium dependent multivitamin transport system (SMVT) (Janoria et al., 2006), sodium dependent vitamin C transporter 2 (SVCT) (Talluri et al., 2006), and riboflavin transport system (Hariharan et al., 2006). A number of peptides, amino acids and vitamins which are essential for cell maintenance are transferred into the corneal cells via these transporters. Drug molecules can be targeted to these transport systems by conjugating various nutrient moieties or ligands. Such drug-ligand conjugates act as substrate to its respective transporter protein. These chemically modified drugs (also known as prodrugs) often improve the solubility and lipophilic characteristics of drug based on the ligand molecule selected. Once the prodrug reaches into the cytoplasm of cell, it gets cleaved by the enzymes and then regenerates the parent drug and promoeity (Janoria et al., 2007).

The affinity of the val-quinidine and val-val-quinidine prodrugs towards peptide transporter was delineated by performing cellular uptake study in presence of [3H] gly-sar, a well known

substrate of peptide transport system. The uptake of [3H] gly-sar was significantly decreased in presence of val-quinidine and val-val-quinidine, suggesting that the prodrugs may have translocated via peptide transport system present on the apical side of corneal cells (Fig. 4).

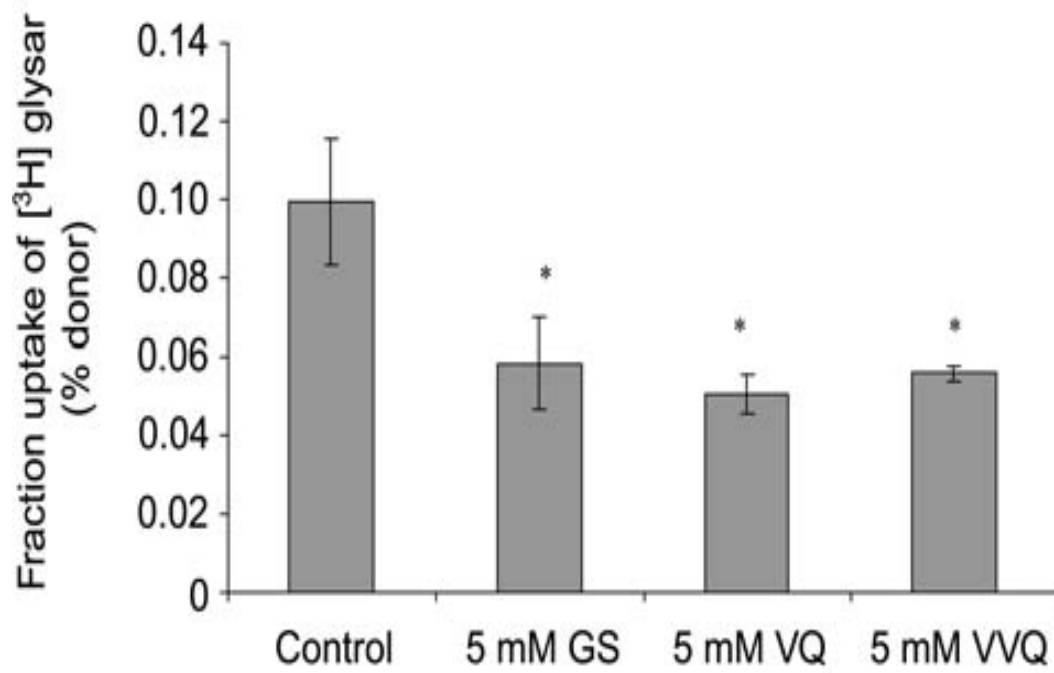


Fig.4. Uptake of [³H] gly-sar across rabbit primary corneal epithelial culture (rPCEC) cell monolayers in the presence of non-radioactive gly-sar, val-quinidine and val-val-quinidine (5 mM each). (Katragadda et al., 2006)

1.5.3. Circumvention of Cellular Efflux by Prodrug Derivatization

Several efflux proteins such as P-glycoprotein (P-gp/MDR1) (Dey et al., 2003), multi-drug resistant associated proteins (MRP 2) (Karla et al., 2007a) and breast cancer resistant proteins (BCRP) (Karla et al., 2009) are expressed on the apical side of the corneal epithelium. These proteins efflux drug molecules from cells thereby, reducing their cellular accumulation following topical delivery. Recently, transporter targeted prodrug derivatization approach has been utilized to circumvent the drug efflux by these proteins. Covalent linkage of drugs to the transporter recognizing ligand may prevent their recognition by efflux proteins and at the same time may result in translocation of prodrugs through the influx transporters (Fig. 5). Katragadda et al. have investigated the circumvention of P-gp mediated efflux of quinidine by using prodrug derivatization approach (Katragadda et al., 2006). In this study, valine (ligand) was conjugated to quinidine and verapamil which are well known P-gp substrates and the cellular uptake was performed in presence of ritonavir .

1.5.4. Prodrug Approach to Enhance Ocular Bioavailability

Prodrug strategy has been attempted for improving therapeutic efficacy of many drug molecules. Significant challenges were met such as improved solubility, stability; permeability and evasion of efflux pump was also noticed. Shirasaki has recently reviewed various molecular approaches to enhance drug permeation across the cornea (Shirasaki, 2007). Our laboratory has also aggressively pursued the exploitation of many of these transporters for ocular drug absorption. Amino acid and peptide prodrugs of acyclovir (ACV) and ganciclovir (GCV), targeting various amino acid and peptide transporters have been

developed and evaluated in our laboratory. Dipeptide (glycine-valine and tyrosine-valine) monoester prodrugs of GCV were found to show superior corneal absorption and bioavailability compared to parent drug (Gunda et al., 2006). These attempts are highly effective in treating herpes simplex virus-1 (HSV-1) induced corneal epithelial and stromal keratitis (Majumdar et al., 2005). Permeability values of valine-GCV, tyrosine-valine-GCV, and glycine-valine-GCV were found to be higher than parent GCV which was attributed to their interaction with oligopeptide transporter present on the retina (Kansara et al., 2007). Sustained release microsphere formulations of GCV and its lipophilic prodrug GCV-monobutyrate, with higher entrapment efficiency, were developed using PLGA in our laboratory (Janoria and Mitra, 2007). By using a similar strategy, L-valyl ester of acyclovir (ACV) was also developed and found to be more permeable across rabbit cornea due to its interaction with the oligopeptide transporter (Dias et al., 2002). Ocular penetration of peptide prodrug of ACV (valine-valine-ACV) was higher than the parent drug following systemic administration in rabbits. The prodrugs appear to be less cytotoxic, highly water-soluble with excellent *in vivo* activity against HSV-1 in rabbit epithelial and stromal keratitis (Anand et al., 2003b). Our laboratory has also demonstrated that prodrug derivatization can effectively circumvent P-gp mediated efflux of quinidine across rabbit cornea (Katragadda et al., 2006). TG100801, which converts to TG100572 by de-esterification, was found to be effective in the treatment of ocular neovascularization and retinal edema following topical administration (Doukas et al., 2008). Due to this prodrug approach, incidence of systemic toxicity was found to be greatly diminished. Role of phase I and phase II ocular metabolic activities was also

reviewed recently to rationalize design of prodrug and co-drug for ocular delivery by Crooks et al., (Al-Ghananeem and Crooks, 2007). UNIL088, a water-soluble prodrug of cyclosporine A was developed via an ester linkage which gets converted into parent drug by chemical or enzymatic hydrolysis of the terminal ester group (Lallemand et al., 2007). Cannabinoids usually lowers IOP by their interaction with the ocular cannabinoid receptors. The solubility related problem of cannabinoids was solved by making arachidonylethanolamide, R-methanandamide, noladin ether and their water-soluble phosphate ester prodrugs (Juntunen et al., 2005). This modification has resulted in higher corneal permeation which could result in more efficient reduction in IOP. In another study, combretastatin A-4-phosphate (CA-4-P), a water soluble prodrug of combretastatin A-4 (CA-4), was found to suppress the development of VEGF-induced neovascularization in the retina and also block development of CNV (Nambu et al., 2003). Topical formulation of nepafenac was found to effectively penetrate into the corneal tissue which also reaches into the posterior segment. In animal models it was found to inhibit CNV and ischemia-induced retinal neovascularization. Nepafenac is converted to amfenac which has significantly higher permeability across the cornea. This property is primarily responsible for the appearance of nepafenac in the posterior segment and causing inhibition of VEGF (Takahashi et al., 2003).

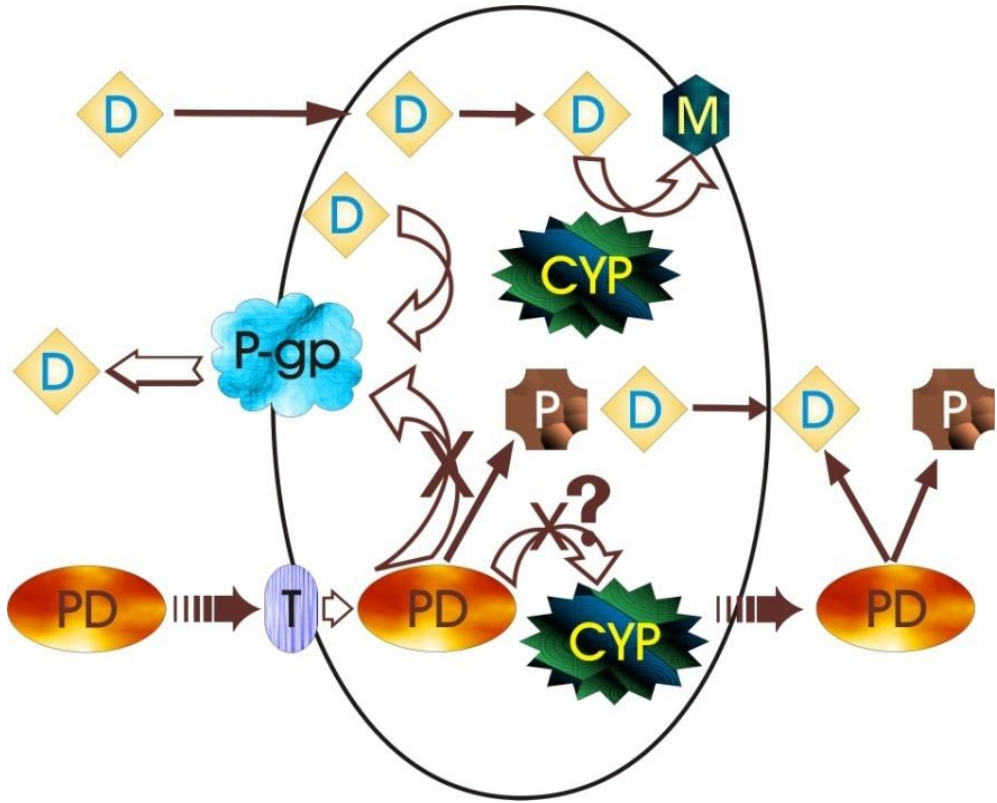


Fig.5. Evasion of efflux pumps by transporter targeted prodrug approach

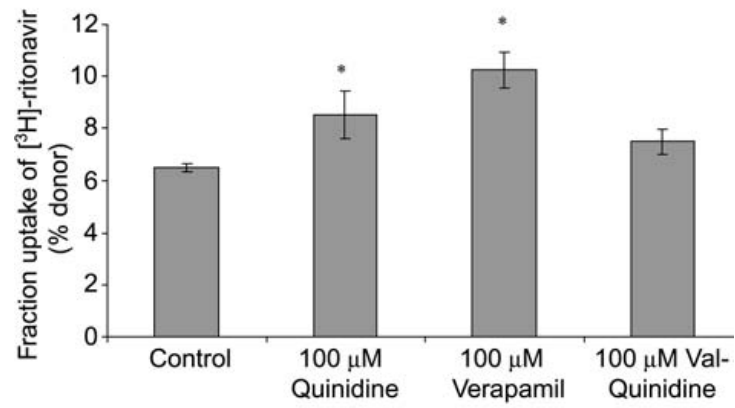


Fig.6. Uptake of [³H] ritonavir across rabbit primary corneal epithelial culture (rPCEC) cell monolayers in the presence of quinidine, verapamil, and val-quinidine (100 μM each). (Katragadda et al., 2006)

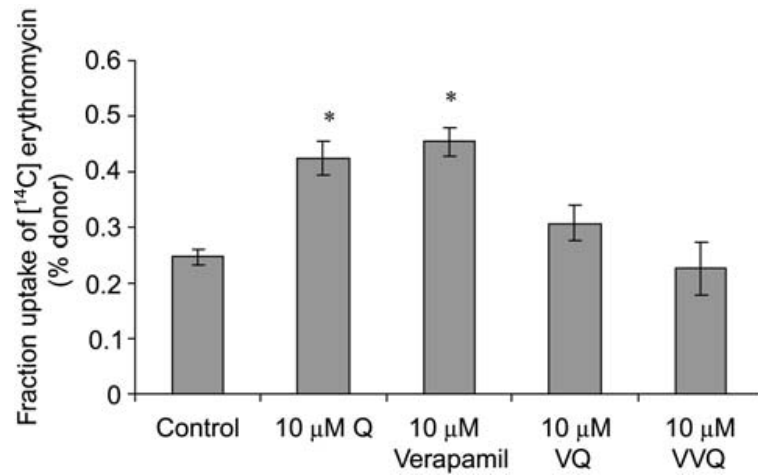


Fig.7. Uptake of [¹⁴C] erythromycin across rabbit primary corneal epithelial culture (rPCEC) cell monolayers in the presence of quinidine, verapamil, and val-quinidine (100 μM each). (Katragadda et. al., 2006)

Fig.6 clearly shows that uptake of ritonavir was increased in presence of quinidine while, uptake remained unaltered in presence of valine-quinidine. A similar study was performed with erythromycin, a model substrate of P-gp to delineate their role in reducing the intracellular accumulation of quinidine. Fig. 7 clearly demonstrates and confirms the evasion of P-gp mediated efflux of quinidine by prodrug derivatization. These studies suggest that the transporter targeted prodrug modification of drugs can evade efflux pumps and increase their ocular bioavailability. Thus, evasion of efflux proteins by prodrug derivatization can be a successful strategy for increasing the intracellular accumulation of drugs following their topical administration.

CHAPTER 2

RATIONALE FOR INVESTIGATION

2.1. Overview

Drug delivery to the anterior segment of eye possesses significant challenge due to its unique anatomical and physiological barriers. Cornea is the outermost multilayered (five layers) transparent membrane of the eye (Civan and Macknight, 2004). The cornea comprises of epithelium, Browman's membrane, stroma, Descemet's membrane, and endothelium (arranged in the order of outermost to innermost) (Dingeldein and Klyce, 1988). Topical drug delivery is the most convenient method of drug administration to the anterior segment of eye. This method of administration provides numerous advantages such as ease of administration, non-invasive drug delivery, bypasses first-pass metabolism and provides local drug delivery (Davies, 2000). Though topical administration is the most preferred route, it suffers from several disadvantages such as nasolachrymal drainage, loss in the conjunctival blood circulation, tear dilution, loss due to normal tear drainage, and reflux blinking. Structural barriers like corneal and conjunctival epithelia also limits the therapeutic concentrations in the anterior segment of the eye (Dey and Mitra, 2005). The corneal epithelium is approximately about 35-50 μm thick and offers a high shunt resistance of 12-16 kohm-cm². The resistance offered by the cornea to intraocular drug absorption is sum of the resistance offered by three layers namely the outer lipophilic epithelium, the middle hydrophilic stroma and the inner endothelium. Thus, the cornea is a formidable barrier for the transcorneal permeation of both hydrophilic and hydrophobic drugs (Prausnitz and Noonan, 1998). It has

been reported that drugs which are moderately lipophilic (log octanol-water partition coefficient ~ 2.9) can easily permeate through the corneal epithelium (Schoenwald and Ward, 1978). Drug fraction which is not absorbed by the cornea is either washed off or drained into the blood stream via nasolacrimal duct, leading to undesirable side effects. For example, systemic absorption of ophthalmic drugs such as timolol, cyclopentolate, chloramphenicol, and phenylephrine has shown to have deleterious effects on the heart and central nervous system (Fraunfelder and Meyer, 1987; Frishman et al., 2001). In addition, the surface area of the conjunctiva is about 17 times larger and 30 times more permeable than cornea. Most of the hydrophilic drugs are absorbed by conjunctiva and diffuse into the systemic circulation via scleral-conjunctival route (Romanelli et al., 1994).

Corneal epithelial cells express various transporters and receptors on their membrane surface. These nutrient transporters aid in the movement of various peptides, vitamins and amino acids across the cell membrane. Our laboratory has extensively studied various transporters and receptors which are present on ocular structures. We have also shown that attachment of various transporters/receptors targeted ligands can enhance ocular bioavailability significantly.

Many drug molecules are known to be substrates for these transporters. Our laboratory has shown the presence of an oligopeptide transporter on rabbit cornea (Anand and Mitra, 2002). We have also investigated the mechanism of model dipeptide (glycylsarcosine) transport across the blood-ocular barriers following systemic administration in our laboratory. A time and concentration dependent, carrier mediated uptake of glycylsarcosine across the blood-

ocular barrier was reported (Atluri et al., 2004). Prodrugs (valine-ACV and valine-valine-ACV) exhibited higher concentrations of ACV in aqueous humor following systemic administration as compared to parent drug. This study indicates that peptide prodrugs are taken up via carrier mediated transport mechanism (Dias et al., 2002). Hence, drugs with poor ocular bioavailability can be suitably modified so that they can be recognized by peptide transporters. An increase in the understanding of drug absorption mechanisms into the cornea from local and systemic administrations has led to the development of various drug delivery systems such as biodegradable and non biodegradable implants, microspheres, nanoparticles and liposomes, gels and transporter targeted prodrugs. Such diversity of approaches is an indication that there is still a need for an optimized noninvasive or minimally invasive drug delivery system to the eye. Entrapment of best stereo isomeric peptide prodrugs in biodegradable nanoparticulate systems may be an alternative strategy for long term drug delivery to anterior segment. Nanoparticles can be further dispersed in PLGA-PEG-PLGA thermosensitive gels which may be conveniently administered as topical eyedrops. Moreover, thermogelling systems also help in preventing drug loss through blink reflux, tear dilution and avoid conjunctival clearance. These systems can form a film above the cornea following topical eye drop administration and then slowly release actives for the treatment of anterior segment diseases.

2.2. Statement of Problem

Research into treatment modalities affecting vision is rapidly progressing due to the high incidence of diseases such as HSV keratitis. ACV owing to its potent anti-viral activity has gained considerable attention as therapeutic candidate for vision threatening viral diseases such as HSV keratitis. Antiviral drug administration by conventional routes fails to achieve required therapeutic concentrations in the eye due to the presence of ocular barriers. Topical eyedrops is the most suitable mode of drug administration but suffers from disadvantages such as drug loss through blink reflux, nasolacrimal drainage, tear dilution etc. Though implants overcome many of the disadvantages associated with eye drops, surgical procedure and risk of drug precipitation due to poor solubility may cause side effects. An ideal sustained drug delivery system for the treatment of HSV keratitis should possess high entrapment efficiency, ability to deliver the drug in zero order fashion, easy to manufacture and a relatively non-invasive delivery route. Entrapment of peptide prodrugs in biodegradable nanoparticulate systems may be an alternative strategy for long term drug delivery to anterior segment of the eye. Polylactide (PLA) and poly lactide-co-glycolide (PLGA) are the most widely used biodegradable polymers that are approved by FDA. These polymers are hydrolyzed to form natural metabolites (lactic and glycolic acids) which are eliminated from the body through Krebs's cycle (Giordano et al., 1995). Nanoparticles can be further dispersed in PLGA-PEG-PLGA thermosensitive gels which may be conveniently administered in the form of eye drops. Moreover, thermogelling systems also help in preventing drug loss through blink reflux, tear dilution, nasolacrimal drainage. These systems

can form a film above the cornea following topical administration and slowly release actives for the treatment of anterior segment diseases.

2.3. Objectives

- I. To examine the stability of stereoisomeric di-peptide prodrugs of acyclovir (L-valine-L-valine-ACV, L-valine-D-valine-ACV, D-valine-L-valine-ACV, and D-valine-D-valine-ACV) prodrugs in rPCEC cells and rabbit ocular tissue homogenates.
- II. To study the affinity of prodrugs towards the peptide transporter protein.
- III. To study the cytotoxicity and uptake of prodrugs in rPCEC cells
- IV. To study the effect of lactide/glycolide ratio on the entrapment efficiency of optimum prodrugs (L-valine-L-valine-ACV and L-valine-D-valine-ACV).
- V. To study the surface morphology, particle size and *in vitro* release of nanoparticles with optimum entrapment efficiency.
- VI. To study the effect of PLGA-PEG-PLGA thermosensitive gel on the *in vitro* release of prodrugs.

CHAPTER 3

OCULAR SUSTAINED RELEASE NANOPARTICLES CONTAINING STEREOISOMERIC DI-PEPTIDE PRODRUGS OF ACYCLOVIR

3.1. Rationale

Ocular herpes is a persistent viral infection caused by the herpes simplex virus-1 (HSV-1). It is one of the most widespread infectious diseases causing corneal blindness in the United States. HSV-1 infections can be mainly classified into HSV neonatal, HSV encephalitis and HSV keratitis. Subsequent to the primary ocular infection, HSV-1 can establish latency in the trigeminal ganglia throughout the lifetime of the host. Intermittent corneal infections can lead to corneal thinning, scarring, stromal opacity and ultimately, blindness.(Shimomura, 2008; Toma et al., 2008) . Previous studies demonstrate that patients infected with HSV-1 have a 50% chance of recurrence (Liesegang, 1988). Herpes simplex keratitis is characterized by rapid spread of virus deep into the cornea and develops into a more severe infection called stromal keratitis, which renders the body's immune system attack and destroy stromal cells. Recurrent episodes of stromal keratitis often results in corneal scarring leading to vision loss (Turner et al., 2003; Wander, 1984). Statistics reveal that every year 50,000 cases are reported in the United States. Acyclovir (ACV) is an antiviral drug with high specificity against herpes viruses and it is the drug of choice for treatment of ocular herpes infections (Jabs, 1998) .Topical treatment of ACV in the form of ointment has been proven to be effective in the treatment of superficial HSV keratitis (Falcon, 1983). However its use in the United States has not been approved by FDA due to side effects associated with this

formulation and the treatment fails especially when deeper ocular tissues are involved such as stromal keratitis. A compound should possess optimum hydrophilicity and lipophilicity for two reasons: a) to allow sufficient permeability across the corneal layers; b) sufficient solubility suitable for eye drops. ACV is a hydrophilic drug with poor aqueous solubility (0.2 mg/mL) and low corneal permeability (Hughes and Mitra, 1993; Turner et al., 2003). Many attempts have been made to increase the corneal penetration of ACV. One of the most widely used approaches is prodrug derivatization. Corneal permeability of ACV has been significantly improved with acyl ester prodrugs. (Hughes and Mitra, 1993) However, enhanced lipophilicity and resulting poor solubility prohibited the formulation of 1-3% eye drops. Later dipeptide prodrugs of ACV such as glycine-valine-ACV (GVACV), valine-valine-ACV (VVACV), and valine-tyrosine-ACV (VYACV) were designed to target the oligopeptide transporter (PEPT) which is widely expressed on the cornea (Anand and Mitra, 2002). These dipeptide prodrugs (GVACV and VVACV) were found to be more permeable due to specific targeting towards PEPT and are considered as the potential candidates for the treatment of ocular HSV infections (Anand et al., 2003a). Talluri et al. synthesized stereo-isomeric dipeptide prodrugs of ACV such as L-valine-L-valine-ACV (LV-LV-ACV), L-valine-D-valine-ACV (LV-DV-ACV), D-valine-L-valine-ACV (DV-LV-ACV), D-valine-D-valine-ACV (DV-DV-ACV) and evaluated permeability across Caco-2 cell monolayer (Anand and Mitra, 2002). However, the effect of stereo-isomerism in the ocular delivery of ACV has not yet been explored.

Successful design of an ocular drug delivery system requires a) optimal physicochemical properties of drugs; and b) drug residence in the precorneal area for an extended period of time. Conventional dosage forms such as solutions and suspensions can produce sub-therapeutic drug levels due to rapid loss through tear turnover and blink reflex in precorneal area (Gulsen and Chauhan, 2004). Moreover conventional dosage forms like eye drops should be administered frequently to achieve the required ocular bioavailability. Alternative drug delivery systems such as ophthalmic inserts are currently indicated to overcome the disadvantages associated with conventional dosage forms. Blurred vision and discomfort can result in some degree of non-compliance with ophthalmic inserts.

An ideal ocular drug delivery system should possess good loading capacity, ability to reside in the precorneal area for a substantial period and capacity to release the drugs in a controlled manner (Boddu et al., 2010b). Colloidal nanocarriers made up of biodegradable polymeric materials have been successfully employed to enhance intraocular drug penetration and controlled release. However, the major limitation with polymeric nanocarriers is short residence in the precorneal area (de Campos et al., 2004).

In this article, we report alternative strategies for increasing the overall therapeutic efficacy of the ACV-prodrugs following topical administration. The stereoisomeric peptide prodrugs of ACV (LV-LV-ACV, LV-DV-ACV, DV-LV-ACV, and DV-DV-ACV) were evaluated for bio-reversion in corneal cell and tissue homogenates. Uptake was conducted in the rPCEC cell line. Docking studies were carried out to examine the affinity of prodrugs to the peptide transporter protein. Prodrugs with optimum stability and affinity towards PEPT

on the cornea were loaded into PLGA nanoparticles. Effect of lactide/glycolide ratio on the prodrug entrapment efficiency was evaluated. Nanoparticles with optimum entrapment efficiency were characterized for size, surface morphology, zeta potential and *in vitro* release properties. We have also investigated the effects of PLGA-PEG-PLGA thermosensitive gel on the release of prodrugs from PLGA nanoparticles.

3.2. Materials and Methods

3.2.1. Materials

Acyclovir, [9-(2-hydroxyethoxymethyl) guanine] was obtained as a gift from Burroughs Wellcome Co. (Research Triangle Park, NC) and Val-Acyclovir was a gift from GlaxoSmithKline (Research Triangle Park, NC). All the stereoisomeric dipeptide prodrugs of ACV were synthesized and purified in our laboratory. [3H]-Glycylsarcosine (Gly-Sar-4 Ci/mMol) was procured from Moravek Biochemicals (Brea, CA). Rabbit primary corneal epithelial cells (rPCEC cells) were cultured in our laboratory. The growth medium i.e. minimal essential medium was procured from Invitrogen. Penicillin, streptomycin, lactalbumin enzymatic dehydrolysate, sodium bicarbonate, and HEPES were purchased from Sigma-Aldrich (St. Louis, MO). Calf-serum (CS) was obtained from Atlanta biologicals. Culture flasks (75-cm² growth area) and 12-well Costar[®] plates, all buffer components and solvents were purchased from Fisher Scientific Co. (Fair Lawn, NJ). PLGA polymers, i.e. PLGA 50:50 (d,l-lactide:glycolide) with molecular weight 45,000-75,000 Da, PLGA 65:35 (d,l-lactide:glycolide), with a molecular weight of 45,000–75,000 Da, PLGA 75:25 (d,l-lactide:glycolide) with a molecular weight of 66,000-107,000 Da, PLA (l-lactide) with a

molecular weight of 85,000-160,000 and polyvinyl alcohol (PVA) were purchased from Sigma Chemicals (St Louis, MO). Thermosensitive gel PLGA-PEG-PLGA (weight average molecular weight [M_{wb}] - 4759 Da) was synthesized and purified in our lab. Cell Titer 96[®] Aqueous Non-Radioactive Cell Proliferation Assay kit was procured from Promega (Madison, WI). Distilled deionized water was used in the preparation of all buffers and mobile phase. Sodium pentobarbital was obtained from the stock maintained by the UMKC school of Pharmacy and used under supervision. All other required chemicals were obtained from Sigma-Aldrich (St. Louis, MO) company.

3.2.2. Synthesis

Stereoisomeric di-peptide prodrugs of ACV (LV-LV-ACV, LV-DV-ACV, DV-LV-ACV and DV-DV-ACV) were synthesized according to a previously published procedure with minor modifications. (Nashed and Mitra, 2003) The products obtained were purified by silica gel column chromatography and were deprotected using trifluoroacetic acid (TFA). These compounds were recrystallized using cold diethyl ether. The progress of the reaction was monitored with TLC and LC-MS/MS. The structures of the intermediate and final compounds were confirmed by ¹H NMR and mass spectrometry. ¹H NMR was carried out using a Varian-400MHz NMR spectrometer. Chemical shifts were expressed in parts per million (ppm) relative to the solvent signal (CD₃OD, 3.31ppm for proton) using tetramethylsilane as an internal standard. Mass spectroscopy was carried out by a hybrid triple quadrupole linear ion trap mass spectrometer (Q trap LC-MS/MS spectrometer,

Applied Biosystems-2000). An enhanced mass (EMS) mode was used for the conformation of intermediates and final compounds (Talluri et al., 2008).

3.2.3. Animals

Rabbits (New Zealand albino adult male) weighing between 2.0 and 2.5 kg were procured from Myrtle's Rabbitry (Thompson Station, TN). All animal studies were conducted according to the ARVO guidelines for the use of animals in vision research.

3.2.4. Cell Culture

rPCEC cell line with a passage number of 10 was utilized. The culture medium containing minimum essential medium supplemented with 10% calf serum (non heat inactivated), 100 units/L of penicillin, 100 units/L of streptomycin, 1.76 g/L lactalbumin enzymatic dehydrolysate and 1.3 g/L HEPES. Cells were grown and maintained in humidified incubator at 37 °C with 5% carbon dioxide in air atmosphere. At 100% confluence, cells were harvested by treating with Tripple Express (Invitrogen) and then 250,000 cells per each well were added to 12-well tissue culture plastic plates. These cells were grown for 10-11 days and utilized for uptake studies. The culture medium was replaced every alternate day during the growth period (Agarwal et al., 2008).

3.2.5. Prodrugs Stability in rPCEC Cell and Rabbit Ocular Tissue Homogenates

Hydrolysis of prodrugs was performed in cell and ocular tissue homogenates. The method is described in the following sections.

3.2.6. Preparation of Cell and Ocular Tissue Homogenates

Rabbits were euthanized by administering sodium pentobarbital (50 mg/kg) through the marginal ear vein. Each eye was instantly enucleated and ocular surface was rinsed with ice-cold, isotonic phosphate buffer saline (IPBS of pH 7.4) to remove any traces of blood.

Aqueous humor was removed with a 27G needle attached to 1 mL tuberculin syringe and then cornea, lens and iris ciliary body were removed sequentially by cutting along the scleral-limbus junction. Aqueous humor and other ocular tissue samples were stored at -80°C prior to any experiment. Tissues were homogenized in 5 mL chilled (4°C) IPBS for about 4 min with a tissue homogenizer (Tissue Tearor, Model 985-370; Dremel Multipro, Racine, WI) in an ice bath. Similarly rPCEC cells were also homogenized in 5 mL chilled (4°C) IPBS for about 4 min. Later, the homogenates and aqueous humor were centrifuged separately at 12,500 rpm for 25 min at 4 °C to remove cellular debris and the supernatant was used for hydrolysis studies. Protein content of each supernatant was estimated with a BioRad assay with bovine serum albumin as the standard (Katragadda et al., 2008)

3.2.7. Bioreversion Studies

The supernatant containing 0.5 mg/mL protein content (1.2 mL) was equilibrated at 34°C for about 30 min prior to an experiment. Hydrolysis was initiated by the addition of 300 µL of 1 mM prodrug solution to the supernatant which is placed in a shaking water bath set at 34°C and 60 rpm. Samples (100 µL) were withdrawn at appropriate time intervals into microcentrifuge tubes prefilled with 100 µL of ice-cold organic mixture containing acetonitrile and methanol (4:5) to precipitate the cellular and tissue proteins as well as to stop

the reaction. The samples were stored at -80°C until further analysis was carried out.

Analysis was performed by HPLC. The samples were thawed and centrifuged to remove any precipitated protein. The supernatant was injected into HPLC. The apparent first-order degradation rate constants were calculated from the slope of log (prodrug concentration) vs. time plots. It is corrected for any chemical hydrolysis observed with the control (Anand et al., 2003a; Tak et al., 2001).

3.2.8. Modeling of rabbit PEPT1 protein

The entire rabbit PEPT1 protein sequence (P36836) was retrieved from the UNIPROT database (<http://www.uniprot.org/uniprot/P36836>) The sequence was submitted to I-Tasser homology model-building server for model calculation (Zhang et al., 2008, 2009). Stereo chemical quality check was performed on the returned model. A few problematic side chain conformations and missing amino acids were identified and rectified using prime (Zhang et al., 2008). The resulting structure was prepared using protein preparation wizard and energy minimized using OPLS 2005 force field (Prime et al.,).

3.2.9. Docking of ACV peptide prodrugs

The structure of ACV peptides was sketched using maestro(Jorgensen and Tirado-Rives, 1988) and prepared using Ligprep (Maestro et al.) Glide (Ligprep et al.) (molecular docking program from Schrodinger, Inc) was engaged to perform the docking studies with standard default settings. Receptor grid generation file was generated by defining the binding site to include all atoms within 20 \AA of TRP 294, as TRP 294 is known to be involved in initial binding of peptides(Glide et al.,). An extra precession docking was performed with the four

ACV peptide prodrugs using the grid file prepared by the above explained process.

GlideScore (GScore) (Friesner et al., 2004; Glide 5.5 et al.; Meredith and Price, 2006) is based on ChemScore, but includes a steric-clash term, adds buried polar terms devised by Schrödinger to penalize electrostatic mismatches, and has modifications to other terms:

$$\text{GScore} = 0.065 * \text{VDW} + 0.130 * \text{Coul} + \text{Lipo} + \text{HBond} + \text{Metal} + \text{BuryP} + \text{RotB} + \text{Site}$$

Binding affinity varies inversely with GScore meaning, lower the GScore stronger is the binding affinity. The components of the GlideScore are described as

Van der Waals energy (VDW): This term is calculated with reduced net ionic charges on groups with formal charges, such as metals, carboxylates, and guanidiniums.

Coulomb energy (Coul): This term is calculated with reduced net ionic charges on groups with formal charges, such as metals, carboxylates, and guanidiniums.

Lipophilic (Lipo): term derived from hydrophobic grid potential. Rewards favorable hydrophobic interactions.

Hydrogen-bonding term (HBond): This term is separated into differently weighted components that depend on whether the donor and acceptor are neutral, one is neutral and the other is charged, or both are charged.

Metal-binding term (Metal): Only the interactions with anionic acceptor atoms are included.

If the net metal charge in the apo protein is positive, the preference for anionic ligands is included; if the net charge is zero, the preference is suppressed.

BuryP: Penalty for buried polar groups

RotB: Penalty for freezing rotatable bonds

Site: Polar interactions in the active site. Polar but non-hydrogen-bonding atoms in a hydrophobic region are rewarded.

3.2.10. Cytotoxicity Studies

Cytotoxicity of all stereo isomeric dipeptide prodrugs was determined with an aqueous non-radioactive cytotoxicity kit based on the MTT assay. The assay examines cell viability based on the principle of mitochondrial conversion of a water-soluble tetrazolium salt [3-(4, 5-dimethylthiazol-2-yl)-2,5-diphenyltetrazolium bromide; MTT] to the water-insoluble blue formazan product. The cytotoxicity kit is supplied as a salt solution of MTT which is composed of MTS and PMS (phenazine methosulfate). PMS has enhanced chemical stability, which allows it to be combined with MTS to form a stable solution eliminating the need to solubilize formazan crystals by an external means. rPCEC cells were grown in 96 well tissue culture plates at 10,000 cells per well density over a period of 24 h prior to drug treatment. Culture medium was then removed and replaced with 100 μ L medium containing serial dilutions of the prodrugs (1-5mM). Cells were then incubated for 24 h at 37 °C under 5% CO₂. At the end of treatment period, medium was aspirated, rinsed with PBS and 20 μ L of MTS containing PMS stock solution was added to each well. After the addition of the MTS dye, cells were incubated for 4 h at 37 °C. Cell viability was then measured by absorbance at 485 nm on an automated plate reader (BioRad, Hercules, and CA). The quantity of formazan product was measured at 485 nm and the absorbance is directly proportional to the number of living cells in the culture (Agarwal et al., 2008).

3.2.11. Uptake studies

Uptake studies were conducted with confluent rPCEC cells. Cells were washed three times with DPBS after aspirating the medium from each well. All the drug and prodrug solutions were added prior to the experiment. ACV and peptide prodrugs (1, 2.5 and 5 mM of LV-LV-ACV, LV-DV-ACV, DV-LV-ACV and DV-DV-ACV) were dissolved in DPBS. Control solutions contained only DPBS. The study was initiated by adding 1 mL of drug or prodrug solution containing 0.5 $\mu\text{Ci/mL}$ of ^3H -Gly-Sar to the wells. Incubation was carried out over a period of 30 min at 37°C. Cells were washed three times with ice-cold stop solution and then lysed overnight with 1 mL 0.1% (w/v) Triton X-100 in 0.3N sodium hydroxide at room temperature. Aliquots (200 μL) were withdrawn from each well and transferred to vials containing 3 mL scintillation cocktail. All samples were analyzed with a Beckman scintillation counter (Model LS-6500, Beckman Instruments, Inc.). Uptake was normalized to the protein content of that specific well. Amount of protein in the cell lysate was estimated by a Bio-Rad protein estimation kit (Bio-Rad) (Katragadda et al., 2006).

3.2.12. Analytical procedure

Drug and prodrug samples were assayed by reversed phase high-performance liquid chromatography (HPLC) as per the previously published procedure.(Talluri et al., 2008) The HPLC system comprised of a Rainin Dynamax Pump SD-200, HP 1100 series fluorescence detector set at excitation wavelength of 285 nm and an emission wavelength 360 nm. Alcott auto sampler Model 718 AL and a C18 Luna column 4.6 \times 250 mm (Phenomenex) were utilized. The mobile phase consisted of 25 mM ammonium phosphate buffer (pH adjusted to

2.5): acetonitrile: (95:5), at a flow rate of 1 mL/min. This method gave rapid and reproducible results. Limits of quantification were found to be: ACV: 50 ng/mL; LV-ACV and DV-ACV: 300 ng/mL; and LV-LV-ACV, LV-DV-ACV, DV-LV-ACV and DV-DV-ACV: 500 ng/mL. Variation among intra and inter day precision (measured by coefficient of variation, CV %) was less than 3%, and 4% respectively.

3.2.13. Preparation of Nanoparticles by W/O/W Method

Nanoparticles were prepared by water in oil in water (W/O/W) emulsion solvent evaporation method. Prodrugs (LV-LV-ACV and LV-DV-ACV) were dissolved in an aqueous solution which forms an internal aqueous phase. This solution was then emulsified in an organic solution containing PLGA polymer to form a primary emulsion. The primary emulsion was sonicated (Fisher 100 Sonic Dismembrator, Fisher Scientific) at a constant power output of 55W for 2 min. Organic phase was slowly mixed with an aqueous solution containing 2.5% w/v PVA under continuous stirring (Vandervoort and Ludwig, 2002). A W/O/W type emulsion was formed upon sonication at a constant power output of 55W for 5 min. The sample was kept in an ice bath during sonication to prevent any overheating of the emulsion. The mixture was stirred gently at room temperature for 3 h. Subsequently, nanoparticle suspension was subjected to vacuum for 1 h to ensure complete removal of organic solvents. Un-entrapped prodrug and PVA residue were removed by washing nanoparticles three times with distilled deionized water. The resultant suspension was centrifuged at 22,000 g for 60 min. Nanoparticles formed were freeze-dried over 48 h (Boddu et al., 2010b).

3.2.14. Entrapment and Loading Efficiencies

For measuring prodrug entrapment in nanoparticles, 1 mg of freeze-dried sample was dissolved in 2 mL of dichloromethane and mixed thoroughly for 24 h. Subsequently these samples were dried under inert atmosphere and dissolved in 200 μ L acetonitrile: water (70:30) and centrifuged at 12,000 g for 10 minutes. The supernatant was analyzed for prodrug content by HPLC. Entrapment efficiency and prodrug loading were calculated by Eq. 1 and 2.

$$\text{Entrapment efficiency (\%)} = \frac{(\text{amount of prodrug remained in nanoparticles})}{(\text{initial prodrug amount})} \times 100 \quad \text{Eq. 1}$$

$$\text{Drug loading (\%)} = \frac{(\text{weight of prodrug in nanoparticles})}{(\text{weight of nanoparticles})} \times 100 \quad \text{Eq. 2}$$

3.2.15. Particle Size Analysis by DLS

Dynamic light scattering (Brookhaven Zeta Plus instrument, Holtsville, NY) technique was applied for the measurement particle size. The polydispersity values were also determined.

3.2.16. Surface Morphology Analysis by SEM

Surface morphology of nanoparticles with optimum entrapment efficiencies were studied using scanning electron microscopy (FEG ESEM XL 30, FEI, Hillsboro, OR). Freeze dried nanoparticles were attached to a double-sided tape and spray-coated with gold–palladium at 0.6 kV and finally examined under the electron microscope and photographed.

3.2.17. Release of Prodrugs from Nanoparticles

Prodrug loaded nanoparticles (40 mg) were dispersed in 1mL isotonic phosphate buffer saline (IPBS), pH 7.4 and subsequently introduced into a dialysis bag (MWCO - 6275 g/mole). PLGA nanoparticles containing LV-LV-ACV were suspended in 1 mL of 23% w/w PLGA-PEG-PLGA polymer solution and then dialysed. The polymer solution inside the dialysis bag formed gel at 37°C within a period of 30-60 seconds. The dialysis bags were introduced into vials containing 10 mL IPBS with 0.025% w/v sodium azide added to avoid microbial growth and 0.02% (w/v) Tween 80 to maintain sink condition. The vials were placed in a shaker bath at 37 ± 0.5 °C and 60 oscillations/minute. At regular time intervals 200 µL of samples were withdrawn and replaced with equal volumes of fresh buffer. Release samples were analyzed using HPLC. Similarly release studies were carried out for PLGA nanoparticles containing LV-DV-ACV alone and when suspended in thermosensitive gels.

3.3. Results

The yield, mass and NMR spectra for LV-LV-ACV, LV-DV-ACV, DV-LV-ACV, and DV-DV-ACV has already been published from our laboratory (Talluri et al., 2008). Bioreversion of all the prodrugs (LV-LV-ACV, LV-DV-ACV, DV-LV-ACV, and DV-DV-ACV) was studied in rPCEC cells and ocular tissue homogenates. Dipeptide prodrugs with D-valine moiety at the terminal position exhibited more stability and were less susceptible to enzymatic degradation. Degradation rate constants of dipeptide prodrugs in rPCEC cell and rabbit ocular tissue homogenates are shown in Table 1.

Table 1. Stability in cell and ocular tissue homogenates-first-order degradation rate constants of all prodrugs

Prodrugs	rPCEC	Cornea	Aqueous Humor	ICB	Lens
L-valine-L-valine-acyclovir	11.36±1.32	17.3±1.12	16.3±2.22	14.8±0.7	14.7±1.1
L-valine-D-valine-acyclovir	0.96±0.15	3.9 ±0.02	3.07±0.03	2.3 ±0.07	1.22±0.26
D-valine-L-valine-acyclovir	0.75±0.04	2.8±0.05	2.1±0.5	0.7±0.20	0.44±0.002
D-valine-D-valine-acyclovir	ND	ND	ND	ND	ND

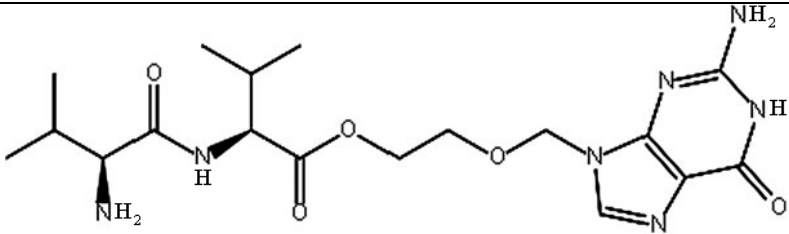
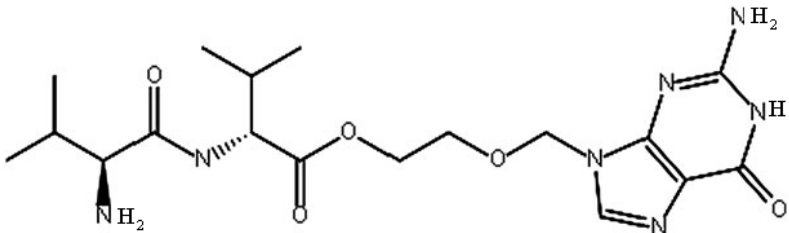
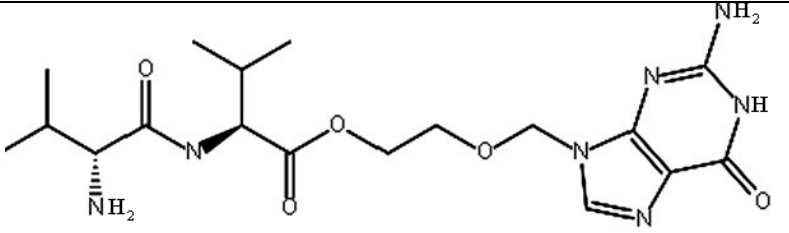
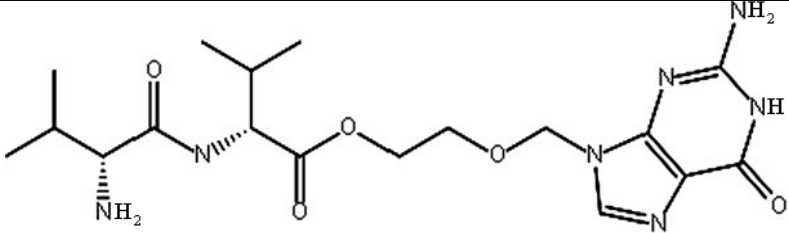
Values are represented as $k \times 10^3 \text{ min}^{-1} \text{ mg}^{-1} \text{ protein}$

Values are mean \pm S.D (n=3)

ND: no degradation in 24 hours

All prodrug except DV-DV-ACV exhibited a first order degradation rate. The descending order of degradation rate constants: LV-LV-ACV > LV-DV-ACV > DV-LV-ACV in rPCEC cell homogenates were found to be $11.36 > 0.96 > 0.75 \text{ k} \times 10^3 \text{ min}^{-1} \text{ mg}^{-1} \text{ protein}$ respectively. The degradation rate constant for the prodrugs in rabbit ocular tissues were found to be in the order of cornea > aqueous humor > ICB > lens. For example the degradation rate of LV-LV-ACV in cornea > aqueous humor > ICB > lens were found to be $17.3 > 16.32 > 14.8 > 14.7 \text{ k} \times 10^3 \text{ min}^{-1} \text{ mg}^{-1} \text{ protein}$ respectively. Similar trend was observed with LV-DV-ACV and DV-LV-ACV. Peptide prodrugs with two D-valine moieties (DV-DV-ACV) was found to be the most stable prodrug and no degradation was evident in cell and ocular tissue homogenate studies for 24 h. Bioreversion pathway of LV-LV-ACV in rPCEC cell homogenates was shown in Fig. 8. LV-LV-ACV bioconversion comprises of two steps: a) hydrolysis of the peptide bond in the presence of peptidases results in the formation of an amino acid derivative LV-ACV and b) esterases cleave the ester bond present in LV-ACV to convert into the parent drug ACV. Traces of ACV can be obtained directly from LV-LV-ACV. The docking results indicate that L-valine in the terminal position increases the affinity of the prodrugs to the peptide transporter protein. The binding affinities (glide docking scores) of prodrugs are summarized in Table 2. Binding of stereo-isomeric peptide prodrugs of ACV near tryptophan 294 amino acid to peptide transporter are shown in Fig. 9. Uptake of LV-LV-ACV, LV-DV-ACV, DV-LV-ACV and DV-DV-ACV prodrugs were carried out in rPCEC cells. All the prodrugs except DV-DV-ACV inhibited the uptake of [³H]-Gly-Sar demonstrating their ability to interact with PEPT (Fig. 10).

Table 2: Docking scores of stereo isomeric dipeptide prodrugs of ACV

Name of the prodrug	Chemical Structure	Glide score
LV-LV-ACV		-4.38
LV-DV-ACV		-4.12
DV-LV-ACV		-3.83
DV-DV-ACV		-3.11

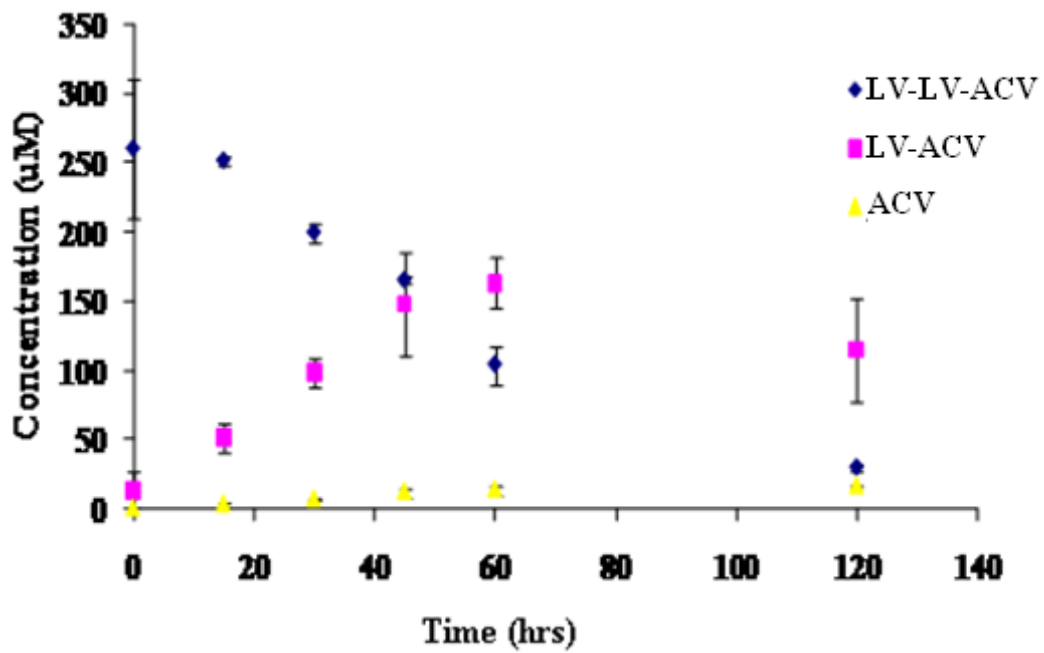


Fig.8. Bioconversion pathway of LV-LV-ACV in rPCEC cell homogenate.

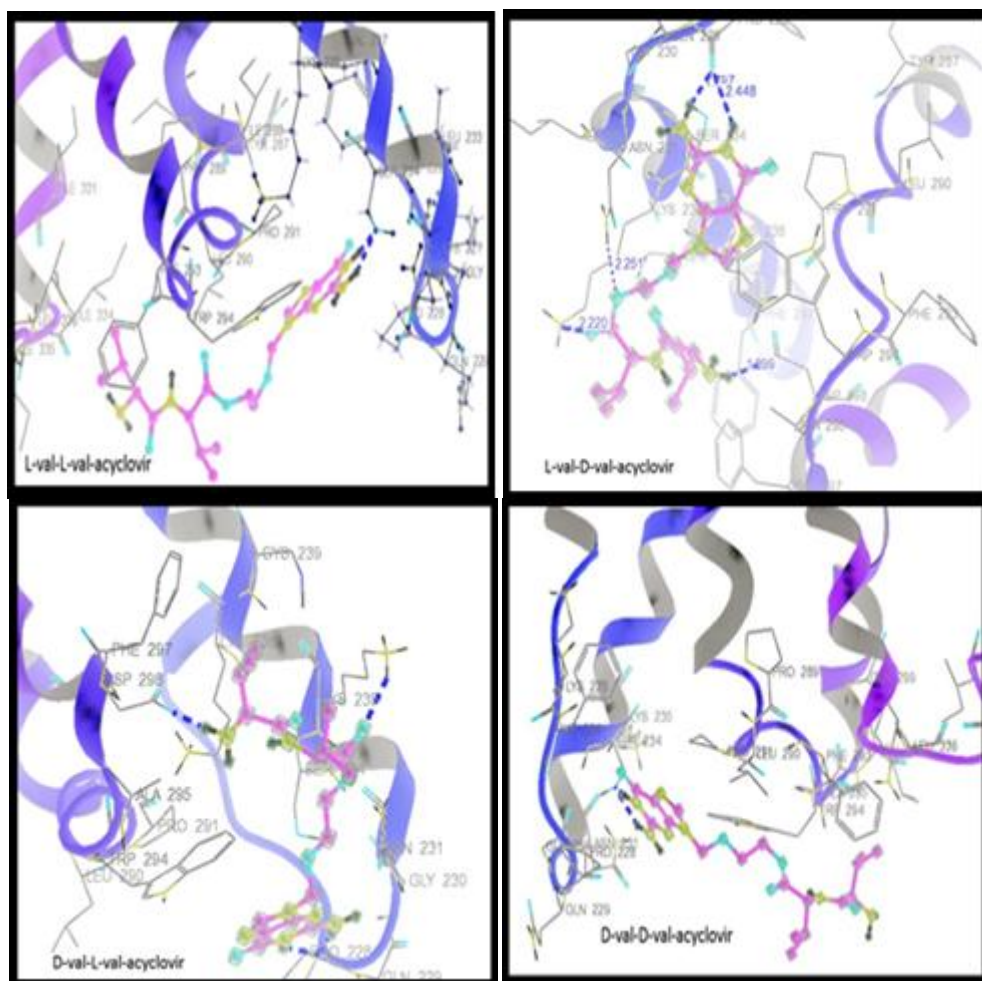


Fig.9: Binding of stereoisomeric peptide prodrugs of acyclovir near tryptophan 294 amino acid.

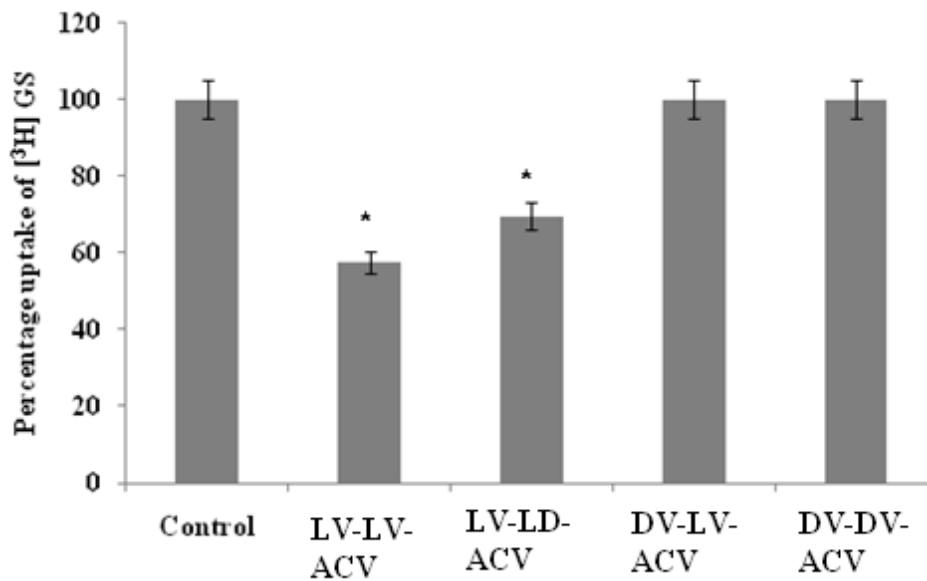


Fig 10: Percentage uptake of [³H]-Gly-Sar by rPCEC cells in presence of LV-LV-ACV, LV-DV-ACV DV-LV-ACV, and DV-DV-ACV. Values are expressed as percent uptake relative to control ([³H] GS alone). * p < 0.05

³H Gly-Sar (GS) is a model substrate for peptide transporter. Uptake of ³H GS (0.5 μCi/mL) was inhibited in the presence of LV-LV-ACV, LV-DV-ACV, and DV-LV-ACV at 1 mM concentration. In this study, it was observed that LV-LV-ACV had significantly inhibited the uptake of [³H]-Gly-Sar across rPCEC cells demonstrating its affinity towards PEPT. Results obtained from cytotoxicity studies on rPCEC cells following exposure for 24 h to ACV, LV-ACV, DV-ACV, LV-LV-ACV, LV-DV-ACV, DV-LV-ACV and DV-DV-ACV are shown in Fig. 11. Blank medium without any drug was selected as the negative control and 10% v/v DMSO was used as a positive control. Stereoisomeric dipeptide prodrugs did not express any significant cytotoxicity at 1.25, 2.5 and 5 mM concentrations, proving that these compounds are safe and nontoxic. Conjugation of various stereo isomeric dipeptides to ACV did not exhibit any sign of toxicity and were equivalent or even better than parent ACV. Based on the bioreversion, interaction with PEPT transporter, and cytotoxicity results, LV-LV-ACV and LV-DV-ACV were considered to be ideal and used in the preparation of PLGA nanoparticles. As LV-LV-ACV and LV-DV-ACV are hydrophilic in nature with fairly high water solubility, water in oil in water (W/O/W) double emulsion solvent evaporation method was used in the preparation of nanoparticles. Entrapment efficiency of LV-LV-ACV and LV-DV-ACV were studied using various grades of PLGA polymers (PLGA 50:50, PLGA 65:35, PLGA 75:25 and PLA). Entrapment efficiencies of LV-LV-ACV with PLGA 50:50, PLGA 65:35, PLGA 75:25 and PLA were found to be 45.7 ± 1.3, 50.5 ± 2.9, 59.7 ± 1.4 and 52.4 ± 2.0% respectively. Entrapment efficiency and drug loading increased with increasing lactide ratios. However, 100% lactide has reduced the entrapment efficiency.

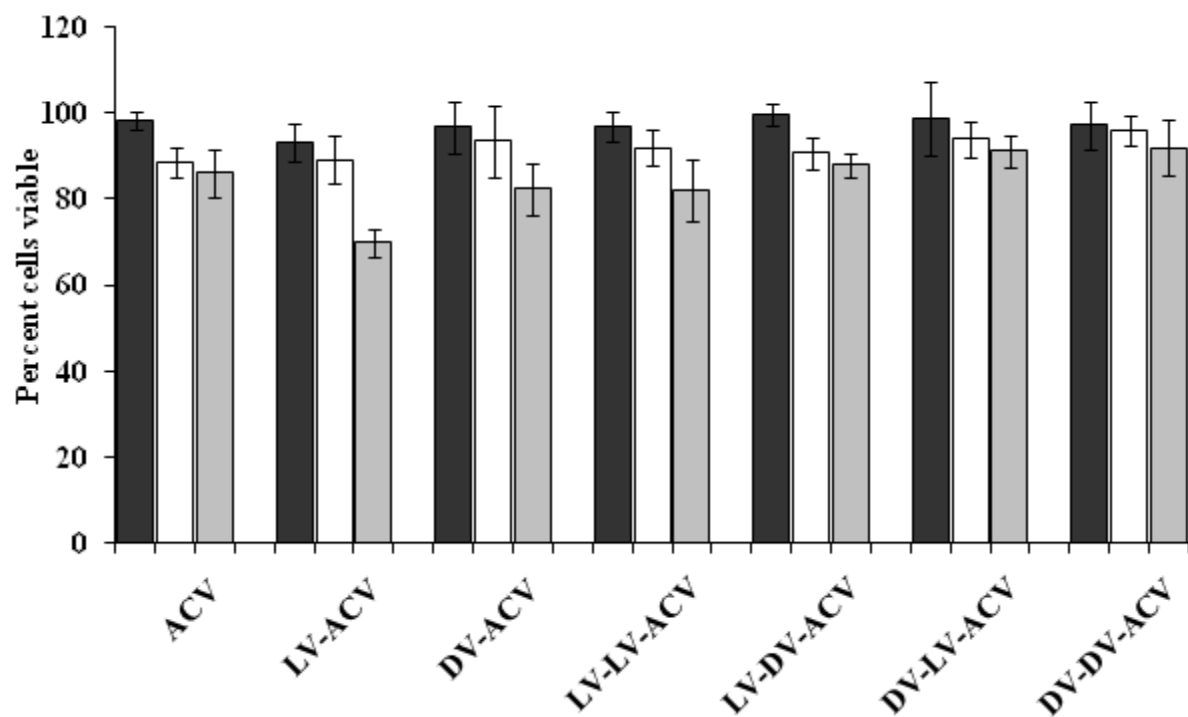


Fig. 11: Cytotoxicity of ACV, LV-ACV, LV-LV-ACV, LV-DV-ACV, DV-LV-ACV, and DV-DV-ACV in rPCEC cells.

Similarly entrapment efficiencies of LV-DV-ACV with PLGA 50:50, PLGA 65:35, PLGA 75:25 and PLA were found to be 38.1 ± 1.5 , 54.4 ± 2.3 , 42.7 ± 1.6 , and $32.7 \pm 1.0\%$ respectively. Entrapment efficiency and drug loading of LV-DV-ACV was highest with PLGA 65:35. Table 3 represents all the experimental values of entrapment efficiencies and drug loading. LV-LV-ACV nanoparticles prepared with PLGA 75:25 and LV-DV-ACV nanoparticles prepared with PLGA 65:35 were further characterized for surface morphology, particle size, zeta potential and *in vitro* release properties. Nanoparticles exhibited unimodal size distribution with polydispersity values very close to zero. The mean particle size and polydispersity values are shown. Scanning electron microscopy substantiates the size uniformity and spherical shape of the particles with a smooth surface (Fig. 12). Sizes of LV-LV-ACV and LV-DV-ACV were found to be 164.9 and 193.3 nm respectively. A biphasic release pattern was observed from the LV-LV-ACV and LV-DV-ACV nanoparticles over duration of 72 h. An initial rapid phase (burst) followed by sustained release was observed in both cases Figs. 13 and 14. Release profiles of LV-LV-ACV and LV-DV-ACV from the formulations prepared by dispersing PLGA 75:25 and PLGA 65:35 nanoparticles in PLGA-PEG-PLGA thermo sensitive gel were also obtained. Synthesis and characterization of triblock copolymer PLGA-PEG-PLGA (weight average molecular weight [M_w] determined by gel permeation chromatography – 4759 Da) has already been published from our laboratory (Wagstaff et al., 1994). Phase transition studies revealed that polymer concentrations ranging between 20-25% w/v form gel at 32-60 °C (Duvvuri et al., 2005).

Table 3: Entrapment efficiency and drug content using various grades of PLGA. Studies were conducted from two batches ($n = 3/\text{batch}$)

Various grades of PLGA	LV-LV-ACV		LV-DV-ACV	
	Entrapment efficiency (%)	Drug content (%)	Entrapment efficiency (%)	Drug content (%)
PLGA50:50	45.7 ± 1.3	4.2 ± 0.2	38.1 ± 1.5	3.9 ± 0.2
PLGA65:35	50.5 ± 2.9	4.7 ± 0.3	54.4 ± 2.3	5.6 ± 0.6
PLGA75:25	59.7 ± 1.4	5.5 ± 0.5	42.7 ± 1.6	4.3 ± 0.3
PLA	52.4 ± 2.0	4.9 ± 0.4	32.7 ± 1.0	3.7 ± 0.1

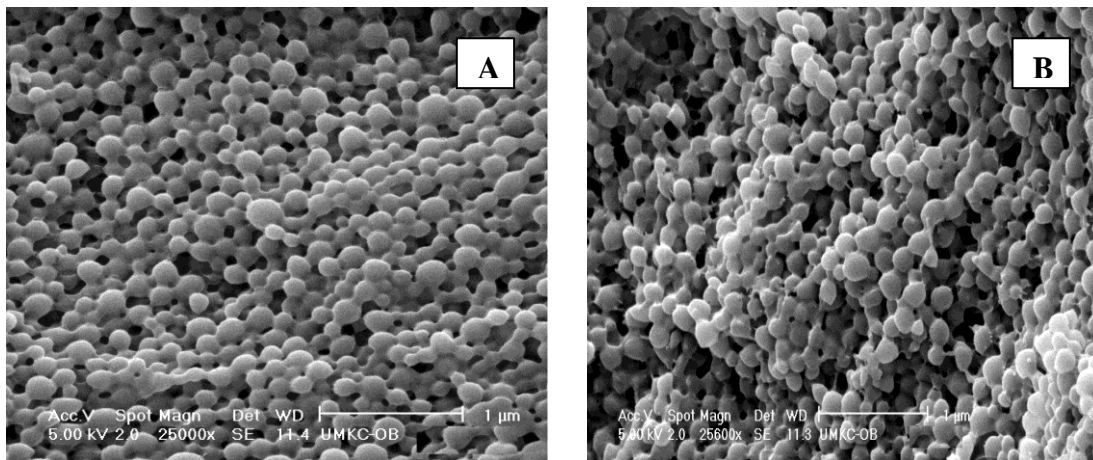


Fig. 12: Surface morphology of nanoparticles. a) PLGA75:25 nanoparticles loaded with LV-LV-ACV, and b) PLGA 65:35 nanoparticles loaded with LV-DV-ACV

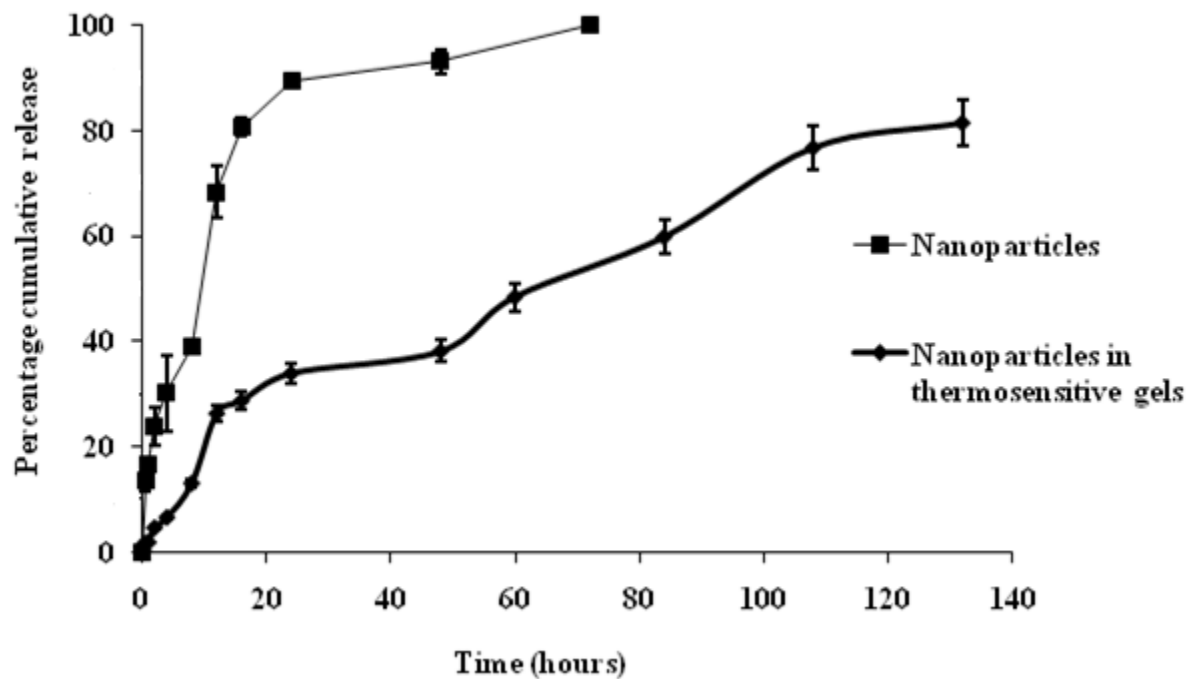


Fig. 13: *In vitro* release profile of LV-LV-ACV from PLGA75:25 nanoparticles and LV-LV-ACV from PLGA75:25 nanoparticles suspended in PLGA-PEG-PLGA thermosensitive gel. Each data point is the average of three samples. Error bars represent the standard error of mean (S.E.M)

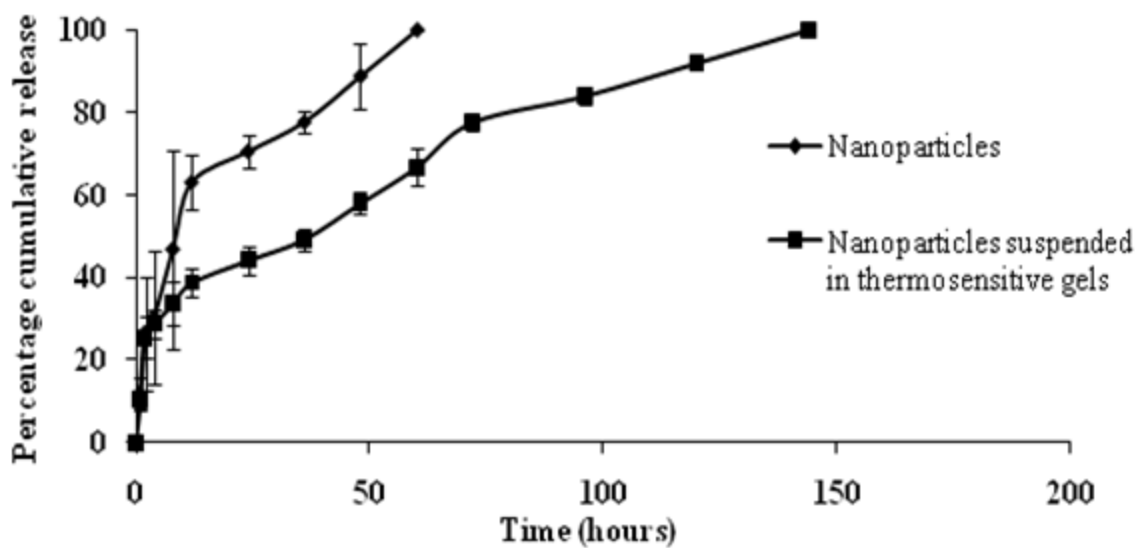


Fig. 14: *In vitro* release profile of LV-DV-ACV from PLGA65:35 nanoparticles and DVACV from PLGA65:35 nanoparticles suspended in PLGA-PEG-PLGA thermo sensitive gel. Each data point represents an average of three samples. Error bars represent the standard error of mean (S.E.M)

As the temperature inside the eye ranges from 34.0-37.0 °C such polymeric gels may be appropriate for delivery. Burst release of active ingredients has been considerably retarded when nanoparticles were dispersed in thermosensitive gels. Moreover, a clear zero order release pattern was observed for the drug from these formulations (Figs. 13 and 14). Burst release of LV-LV-ACV and LV-DV-ACV has been considerably retarded when nanoparticles are dispersed in thermosensitive gels. Dispersion of polymeric nanoparticles in PLGA-PEG-PLGA sustained the release of the prodrug over a period of 1 week.

3.4. Discussion

It's a well known fact that upon topical administration ACV formulations may not achieve optimal therapeutic concentrations in the target sites due to low water solubility and membrane permeability (Cortesi and Esposito, 2008). Novel stereoisomeric dipeptide prodrugs of ACV were developed and the effect of stereoisomerism on enzymatic stability was studied in various rabbit ocular tissues and rPCEC cell homogenates. Results from the hydrolysis study indicated that incorporation of two D-isomers can significantly improve the stability of prodrugs (Talluri et al., 2008). However, D-isomers can also lower affinity towards PEPT. The increase in the stability upon incorporation of D-valine may be attributed to reduced affinity towards hydrolytic enzymes. Previous reports from Anand et al. clearly explained the bioconversion mechanism of dipeptide prodrugs. The dipeptide bond is hydrolyzed by the peptidases resulting in the regeneration of amino acid ester of ACV which is further hydrolyzed by esterases regenerating the parent ACV (Anand et al., 2003a). The regeneration of ACV directly from dipeptide prodrug may occur to a smaller extent. *In vitro*

uptake studies of LV-LV-ACV, LV-DV-ACV, DV-LV-ACV, and DV-DV-ACV were carried out in rabbit primary corneal epithelial cells rPCEC (Anand and Mitra, 2002). LV-LV-ACV and LV-DV-ACV had shown high PEPT affinity where as DV-LV-ACV and DV-DV-ACV did not show any affinity. This result indicates that D-valine moiety in the terminal position is not recognized by peptide transporter. Hence both DV-LV-ACV and DV-DV-ACV did not show any affinity towards peptide transporter on rPCEC cell line. Cell cytotoxicity studies suggest that all the prodrugs are safe and nontoxic (Anand and Mitra, 2002). Ideal prodrugs should enter the cornea via peptide transporter and readily convert to parent drug in the tissue before elimination through aqueous humor. Bioconversion half-life of prodrug should be less than the *in vivo* elimination of half-life. Previous studies from our laboratory by Anand et al. concluded that the half-life of cumulative ACV from the dipeptide prodrugs was calculated as ~180 min. Based on this data we have concluded that LV-LV-ACV and LV-DV-ACV are suitable peptide ACV prodrugs for further formulation studies (Anand et al., 2006). Owing to the appreciable PEPT1 affinity we anticipate that LV-LV-ACV and LV-DV-ACV could be readily absorbed across the corneal epithelium and then get converted to ACV for the treatment of severe HSV infections in deeper corneal tissues like stroma.

LV-LV-ACV and LV-DV-ACV were loaded into PLGA nanoparticles which in turn were dispersed in thermo sensitive gels to overcome the disadvantages associated with conventional eye drops. Dipeptide prodrug loaded nanoparticles dispersed in thermosensitive gels may prevent precorneal degradation of prodrugs and overcome the precorneal drainage

associated with rapid blinking, lachrymation and drainage. A series of PLGA polymers of varying lactide/glycolide ratios were employed in the preparation of nanoparticles.

Entrapment efficiency values of LV-LV-ACV and LV-DV-ACV were observed to be significantly higher with PLGA 75:25 and PLGA 65:35 polymers respectively. This result can be attributed to stronger interactions of LV-LV-ACV and LV-DV-ACV with PLGA 75:25 and PLGA 65:35 polymers respectively. Nanoparticles containing LV-LV-ACV and LV-DV-ACV exhibited uniform size distribution with low polydispersity. *In vitro* prodrug release from nanoparticles exhibited a biphasic pattern with an initial burst phase followed by a sustained release phase. Dispersion of nanoparticles in thermo sensitive gels completely eliminated the burst release. This may be due to the adhesion of thermo gelling polymer to nanoparticle surface (Boddu et al., 2010b). Such nanoparticulate formulations may provide sustained release of LV-LV-ACV and LV-DV-ACV following topical administration.

Moreover this formulation remains in solution form at room temperature and forms a gel at eye temperature following topical administration. Moreover gel also prevents the rapid drainage of nanoparticles, interaction of prodrugs with tear proteins, tear dilution of prodrugs, and prodrug metabolism following topical delivery to the eye (Kaur and Kanwar, 2002). Upon topical administration nanoparticles suspended in thermosensitive gels form of a depot in the cul-de-sac providing a robust concentration gradient for efficient permeation of prodrugs across the cornea in a sustained manner.

For patients suffering from superficial keratitis, LV-LV-ACV loaded nanoparticles may be more appropriate. Superficial keratitis affects the superficial corneal layers. LV-LV-ACV

released from the formulation penetrates the superficial corneal layers and regenerates quickly to ACV for action against HSV-1 infection. Stromal keratitis mainly affects the deeper layers of cornea. LV-DV-ACV loaded nanoparticles may be more effective in the treatment of stromal keratitis. LV-DV-ACV will be metabolically stable enough to penetrate deeper layers of cornea and regenerate the active in the deeper layers of cornea. Hence prodrug entrapped nanoparticles formulations can be selectively applied depending on the severity of infection. Moreover, a cocktail of LV-LV-ACV and LV-DV-ACV nanoparticles can also be indicated in patients with deeper and wide spread HSV-1 ocular infections.

3.5. Conclusion

LV-LV-ACV and LV-DV-ACV appear to be very suitable ACV peptide prodrugs in terms of stability, bioreversion, cytotoxicity, and affinity towards rabbit PEPT1 transporter. Following translocation across the cornea via PEPT transporter, prodrugs are expected to revert rapidly into their parent drug. Entrapment of LV-LV-ACV and LV-DV-ACV in PLGA nanoparticles may retard the degradation of prodrugs in the pre-corneal area and further sustain the release in deep corneal tissues. Dispersion of nanoparticles in the PLGA-PEG-PLGA thermosensitive gel may significantly eliminate the burst release of prodrug and overcome the problems such as drug loss by tear turnover, tears dilution and blink reflex causing rapid extensive loss upon topical administration into the cul-de-sac. *In vivo* pharmacokinetic studies need to be carried out to determine the aqueous humor kinetics of these formulations following topical administration.

CHAPTER 4

RATIONALE FOR INVESTIGATION

4.1. Overview

Folate receptors (FRs) are membrane-bound glycoproteins of 32–36 kDa with a high affinity for folic acid and its structural analogs methyl tetra hydro folate (MTF) and methotrexate (MTX) (Kansara et al., 2008). FRs are clustered on the cell surface and they are associated with uncoated membrane invaginations (caveolae). They are considered as vital components in maintaining the mammalian cellular folate homeostasis. FRs are generally coded by two genes (FR- α and β) with differential tissue expression. FR regulates the uptake of folic acid by a process known as potocytosis (Anderson et al., 1992). They usually move in and out of the cell by means of a new uncoated pit pathway that does not involve with the clathrin-coated pit endocytic machinery. Initially folate binds to the outwardly oriented folate receptor and then internalization of caveolae takes place with the formation of a compartment that is acidified by H⁺ pump (Kamen et al., 1988). Folate conjugated targeted drug delivery systems like nanoparticles, liposomes, micelles promise to expand therapeutic windows of various anticancer drugs by augmenting delivery to the target tissue. Selective targeting reduces the minimum effective dose as well as associated toxicity and also enhances the therapeutic efficacy with equivalent plasma concentrations (Garcia-Bennett et al.; Pan and Lee, 2004). Folate as a targeting moiety offers prospective advantages than macromolecules such as antibodies. These include: (a) miniature size of the targeting moiety, which offers favorable pharmacokinetic properties of the folate conjugates and decreased probability of

immunological reactions which allows repeated administration, (b) very low cost and readily available, (c) high affinity for receptors, (d) the receptor ligand can be internalized into the cell by endocytosis process, which aids in cytosolic delivery of therapeutic agents, (e) High frequency of expression among breast cancer cell lines offers great potential for future therapeutic and diagnostic applications in treating breast cancer patients (Sudimack and Lee, 2000). Expression of folate receptors on the cornea has not been explored and hence we selected SIRC cell line as a model since it can form multilayers and resembles corneal epithelium.

4.2. Statement of Problem

Cornea due to its lipophilic nature does not allow the entry of hydrophilic drugs to enter into corneal epithelium. One such example is acyclovir which is highly hydrophilic and poorly absorbed into cornea. Various nutrient transporters are usually expressed on the cell membranes. Our goal is to establish the presence of folate receptor on cornea and then utilize this for targeted drug delivery. Corneal cells generally express various nutrient transporters but so far the expression of folate receptors on cornea has not been explored. The purpose of this study was to investigate and characterize the expression of folate transport proteins in Staten's Seruminstitut rabbit corneal (SIRC) epithelial *cell line*. The *in vitro* uptake studies were performed in a rabbit corneal cell line, SIRC so as to decrease the use of animal tissues. This cell line has been widely used for the *in vitro* studies to evaluate corneal physiology, immunology, toxicology, and transport. SIRC cell line forms 5-6 layers of epithelium in culture as characterized and reported previously from our laboratory, thus serving as a good

in vitro model for the corneal epithelium (Jain-Vakkalagadda et al., 2003). SIRC has never been investigated for the presence of folate membrane transporters/ receptors. Herein, we report the uptake characteristics of folic acid, in SIRC cells and identify folate transport proteins on the corneal epithelium. These results were confirmed by reverse transcription polymerase chain reaction (RT-PCR) and Western blot studies. Further transport studies were conducted on freshly excised rabbit cornea (Balakrishnan et al., 2002).

4.3. Objectives

- I. To study the uptake of [³H] Folic acid with respect to time, pH, temperature, sodium and chloride ion dependency in Staten's Seruminstitut rabbit corneal (SIRC) epithelial cell line.
- II. To study the inhibition in uptake of [³H]Folic acid in presence of structural analogs methyltetrahydro folate (MTF) and methotrexate (MTX), vitamins and metabolic inhibitors.
- III. To study the uptake of ³[H] Folic acid in presence of varying concentrations of cold folic acid.
- IV. To study the uptake kinetics in the presence of various modulators of intracellular regulatory pathways; protein kinases A and C (PKA and PKC), protein tyrosine kinase (PTK) and calcium-calmodulin modulators.
- V. To substantiate the expression of folate transport proteins using reverse transcription polymerase chain reaction (RT-PCR) and Western blot analysis.

- VI. To carry out the *ex vivo* corneal permeability studies of [³H] Folic acid in presence and absence of 1mM cold folic acid.

CHAPTER 5

FUNCTIONAL CHARACTERIZATION OF FOLATE TRANSPORT PROTEINS IN STATEN'S SERUMINSTITUT RABBIT CORNEAL EPITHELIAL CELL LINE

5.1. Rationale

Folate is a water soluble vitamin B9 that occurs naturally in food, and folic acid (FA) is the synthetic form of this vitamin. It is found in food supplements and this vitamin plays an essential role in a variety of vital cellular processes. The compound aids in growth, differentiation and homeostasis of mammalian cells. It acts as a coenzyme for synthesis and repair of DNA, RNA, and proteins (Bozard et al., 2010). FA also plays a vital role in the interconversion of amino acids such as serine and glycine; and biosynthesis of nucleic acids such as adenine, guanine, thymidine and inosine (Brzezinska et al., 2000). It plays an important role in the development of visual system, and deficiency of FA results in loss of visual function due to optic neuropathy and nutritional amblyopia (Golnik and Schaible, 1994).

Several transport systems have been recognized on the cell membranes that play a critical role in internalization of folates. Every system employs a definite set of membrane proteins that binds to their respective substrates with high affinity and specificity (Brzezinska et al., 2000). These systems are classified into two types: a) membrane channels or carriers that vectorially drive the molecules, and b) endocytotic vesicles that internalize the molecules. These transporters, due to high efficiency, are often secluded from supplementary molecules in the cell membrane to form domains that are enriched with that transporter

species. The transport systems can be distinguished by their preference to a variety of folate compounds as substrates, and more over by differences in temperature and pH dependent uptake (Brzezinska et al., 2000; Matherly and Goldman, 2003; Sierra and Goldman, 1999). Three distinct cellular mechanisms for the transport of folate have been identified: folate receptors (FR), reduced folate carrier (RFC), and the newly identified proton-coupled folate transporter (PCFT). Folate receptors are highly specific forms of folate binding proteins, which are fastened to the cell membrane by glycosylphosphatidylinositol (GPI) residues. FR is coded by two specific genes (FR α and FR β) with differential tissue expression (Spiegelstein et al., 2000). After binding to FR, the folate receptor-complex is internalized into the cell by an endocytotic process. FR contains about 240-260 amino acids and has a molecular mass in the range of ~28-40 kDa, reflecting the extent of glycosylation. The receptor displays much greater affinity for non reduced folates, such as folic acid, over reduced folates like methotrexate (MTX) and methyltetrahydrofolate (MTF). RFC is a 57-65 kDa integral transmembrane protein which has high affinity for N5-methyltetrahydrofolate (MTF). Reduced folate transporter (RFC) belongs to the SLC19 family of solute carriers (*SLC19A1*) (Bozard et al., 2010). RFC functions as an anion exchanger operating optimally at pH 7.4. Its activity and folate-concentrating ability are lower at reduced pH (Bozard et al., 2010). PCFT is a newly described folate transport protein that is encoded by the *SLC46A1* gene. Recently, Goldman's laboratory has discovered the molecular identity of PCFT transporter which is genetically unrelated RFC (Zhao and Goldman, 2007). It is a proton-coupled, electrogenic transporter and works optimally at low pH. PCFT is reported to have a

molecular weight of 50-65 kDa, depending on the extent of glycosylation (Inoue et al., 2008). It is also known as heme carrier protein 1 (PCFT/HCP1) and has been identified as a transporter that mediates the translocation of folates across cellular membrane (Inoue et al., 2008).

The purpose of this study was to investigate and characterize the expression of folate transport proteins in Staten's Seruminstitut rabbit corneal (SIRC) epithelial cell line. *In vitro* uptake studies were performed in a rabbit corneal cell line, SIRC. This cell line has been widely considered as a model corneal membrane for evaluation of corneal physiology, immunology, toxicology, and transport. SIRC cell line forms 5-6 layers of epithelium in culture as characterized and reported previously from our laboratory. Thus it serves as a good *in vitro* model for the corneal epithelium (Jain-Vakkalagadda et al., 2003). SIRC has not been investigated previously for the presence of folate membrane transporters/ receptors. Herein, we determined kinetic parameters of folic acid, in SIRC cells to identify folate transport proteins on the corneal epithelium. These results were further confirmed by reverse transcriptase polymerase chain reaction (RT-PCR) and Western blot studies. Transport studies were also conducted on freshly excised rabbit cornea (Balakrishnan et al., 2002).

5.2. Materials and Methods

5.2.1. Materials

[3H]Folic acid (50 Ci/mmol) was purchased from Perkin-Elmer (Boston, MA). Unlabelled folic acid, methyltetrahydrofolate (MTF), methotrexate (MTX), biotin, ascorbic acid, riboflavin, pantothenic acid, sodium azide, ouabain, 2,4-dinitrophenol, protein tyrosine

kinase (PTK) modulators (genistin and genistein), protein kinase (PKC and PKA) pathway modulators (bisindolylymaleimide-I, phorbol-12-myristate-13-acetate, forskolin, and 3-isobutyl-1-methylxanthine (IBMX), calcium–calmodulin pathway modulators (calmidazolium, KN-62 and trifluoperazine), probenecid, 4,4'-di-isothiocyanatostilbene-2,2'-disulphonic acid (DIDS), 4'-acetamido-4-isothiocyanatostilbene-2,2'-disulfonic acid (SITC), colchicine, choline chloride, Triton X-100, HEPES, d-glucose and all other chemicals were procured from Sigma Chemical Co. (St. Louis, MO). All chemicals were of special reagent grade and used without further purification.

5.2.2. Cell Culture

SIRC cells were obtained from ATCC (passages 410). Cells were grown in culture media consisting of minimum essential medium (MEM) supplemented with 15% non-heat-inactivated calf serum, lactalbumin, HEPES, penicillin (100 µg/mL) and streptomycin (100 µg/mL) (Sigma Chemical Co., St. Louis, MO). Medium was replaced on every alternate day. Cells were maintained at 37°C, in a humidified atmosphere of 5% CO₂ and 90% relative humidity. For uptake studies cells were plated at a density of 500000 cells/well on 12-well culture plates (Costar, Corning, NY) and maintained at 37°C (Lentz et al., 2000).

5.2.3. Uptake Studies

SIRC cells were washed three times with 2 mL of Dulbecco's modified phosphate buffer saline (DPBS) at 37°C for 10 min. Folic acid uptake was initiated by the addition of a fixed amount of [3H]-Folic acid (0.5 µCi/mL) at 37°C and cells were incubated for a definite time period. Following incubation, cells were washed thrice with ice-cold stop solution (200 mM

KCl and 2 mM HEPES) to terminate the folic acid uptake. Cells were lysed overnight with 1 mL of 0.1% (v/v) Triton X-100 in 0.3N sodium hydroxide at room temperature. Aliquots (500 μ L) from each well were then transferred to scintillation vials containing 5 mL scintillation cocktail (Fisher Scientific, Fair Lawn, NJ). Samples were then analyzed by liquid scintillation counter (model LS-6500, Beckman Instruments, Inc., Fullerton, CA). The amount of protein in the cell lysate was measured by BioRad protein estimation kit (BioRad, Hercules, CA). The rate of uptake was normalized to the protein content of each well (Janoria et al., 2006; Kansara et al., 2008; Luo et al., 2006).

5.2.4. Time Dependency

Uptake of [3H] Folic acid was determined at various time points (1, 2, 5, 10, 15, 30 and 45 min) to optimize the time required for carrying out further studies.

5.2.5. Effect of pH and Temperature

In order to carry out pH dependent studies, pH of DPBS was adjusted to 4, 5, 6, 7.4, and 8. To determine the effect of temperature on the uptake buffer temperatures were adjusted to 4, 25, and 37°C. Uptake of [3H] Folic acid (10 nM) in SIRC cells was performed under varying pH and temperature conditions.

5.2.6. Role of Ions

Sodium ion dependency was studied by the addition of equimolar quantities of potassium, ammonium and choline chloride to substitute sodium chloride (NaCl) and sodium phosphate monobasic (Na_2HPO_4), in DPBS, pH 5. Effect of chloride ion was also studied by incorporating equimolar quantities of sodium phosphate dibasic (NaH_2PO_4), potassium

phosphate (KH_2PO_4), and calcium acetate as substitute for NaCl, potassium chloride (KCl) and calcium chloride (CaCl_2), respectively. Uptake was performed in these buffer solutions containing [3H] Folic acid (10 nM).

5.2.7. Effect of Energy Modulators

To examine the energy dependence, SIRC cells were pre-incubated with 1mM metabolic inhibitors such as ouabain (an inhibitor of Na^+/K^+ -ATPase), 2, 4-dinitrophenol (intracellular ATP reducer) and sodium azide (an inhibitor of oxidative phosphorylation) for 1 h. Uptake studies were then initiated as described earlier with buffer solutions containing [3H]Folic acid (10 nM).

5.2.8. Effect of Membrane Transport Inhibitors

To study the effect of anion transport inhibitors on cellular uptake folic acid, cells were first pre-incubated with probenecid, DIDS, SITC at 0.5 mM concentration. To explain the role of folate receptor, cells were incubated with colchicine (100 μM) an endocytotic inhibitor. Uptake studies were then carried out as described earlier with buffer solutions containing [3H]Folic acid (10 nM).

5.2.9. Substrate Specificity

In order to understand the structural requirements for interaction with folate carrier, uptake studies were carried out in the presence of various vitamins and its structural analogs. The unlabeled vitamin or structural analog was incubated with respective radiolabelled folic acid (10 nM). Unlabeled vitamins (biotin, pantothenic acid, riboflavin and niacin) were used at a

concentration of 10 μM . Unlabeled folic acid and its structural analogs (MTF and MTX) at a concentration of 0.1 and 1.0 μM were added to the incubation mixture.

5.2.10. Concentration Dependent Study Data Analysis

Uptake of [3H]Folic acid was carried out in presence of various concentrations of cold folic acid and the data obtained was fitted into a modified Michaelis–Menten equation (Eq. 1).

This equation considers the carrier-mediated active uptake process and a non-saturable passive diffusional uptake process:

$$V = \frac{V_{\max}[C]}{K_m + [C]} + K_d[C] \quad \text{Eq. 1}$$

V represents the total rate of uptake of folic acid, V_{\max} denotes the maximum uptake rate of the carrier-mediated process, K_m (Michaelis–Menten constant) is the substrate concentration at half-maximal saturation process, C is the substrate concentration, K_d represents rate constant for the non-saturable (passive) diffusion component and $K_d[C]$ represents the non-saturable (passive) component, whereas the saturable component of total uptake of folic acid is given by $(V_{\max}[C])/(K_m + [C])$. Data was fitted into Eq.1 with a SCIENTIST[®] program (Micromath, St. Louis, MO, USA). The kinetic parameters which were calculated with SCIENTIST[®] were substituted into above equation to determine the involvement of the saturable and non-saturable components. The excellence of the fit was

examined by evaluating the coefficient of determination (R^2), the standard error of parameter estimates, and by visual inspection of the residuals.

5.2.11. Statistical Analysis

All experiments were conducted at least six times and results were expressed as mean \pm S.D.

Michaelis–Menten parameters such as K_m , K_d and V_{max} are expressed as mean \pm S.E.

Unpaired Student's *t*-test was used to estimate statistical significance. A difference between mean values was considered significant if $p < 0.05$.

5.2.12. Intracellular Regulation

Involvement of intracellular regulatory pathways such as protein kinase C (PKC), protein kinase A (PKA), protein tyrosine kinase (PTK), and Ca^{2+} /calmodulin-mediated pathways in the regulation of [3H]Folic acid uptake into SIRC cells was determined. Cells were first pre-incubated for 30 min separately with PKC pathway activator (phorbol 12 myristate 13-acetate), or with the PKC pathway inhibitor (bisindolylmaleimide I), PTK pathway modulators (genistein and genistin), PKA pathway modulators activators (IBMX and forskolin and specific inhibitor, H-89), calmodulin inhibitors (calmidazolium and trifluoperazine) and Ca^{2+} /calmodulin dependent protein kinase II inhibitor (KN-62). Solutions of these modulating agents were prepared in DMSO or pure ethanol (final concentration of the organic solvent was less than 1%, v/v). Cells were preincubated for 1 h with various modulators and uptake was initiated by the addition of [3H] Folic acid (10 nM). An identical amount of drug-dissolving vehicle (DMSO or ethanol) was incorporated in the bathing medium for control studies to determine the effect of these solvents on untreated SIRC cells.

5.2.13. Molecular Evidence

5.2.13.1. Gene Expression – Qualitative Analysis

Total RNA was isolated from SIRC cells using Trizol® reagent (Invitrogen) by a standard protocol. Briefly, cells were lysed with the addition of 800 µL of Trizol® reagent. The lysate was then transferred to Eppendorf tubes. RNA was extracted by the phenol–CHCl₃–isopropanol method, purified, and dissolved in 50 µL of RNase–DNase-free water. For single strand cDNA synthesis, 2 µg total RNA was reverse transcribed according to a standard protocol using M-MLV Reverse transcriptase (Promega, Madison, WI). The conditions for reverse transcription were denaturation of template RNA for 2 min at 94°C and reverse transcription for 60 min at 40°C. Amplification was performed with 1 µg cDNA and selected primers for the amplification were shown in Table 5. GAPDH served as the internal control. PCR conditions were as follows: denaturation (94°C, 45 s), annealing (55°C, 1 min), and extension (72°C, 45 s) for 35 amplification cycles, followed by a final extension of 72°C for 10 min. The product was separated by 1.5% agarose gel electrophoresis and visualized by chemiluminescence.

5.2.13.2. Computer Analysis

Nucleotide sequence homology matching was carried out with a fundamental local alignment investigating tool (BLAST) via on-line link to the National Center of Biotechnology Information (NCBI).

Table 4: Primers for RT-PCR analysis

Gene	NCBI Accession code	Sequence (5'→3')	Product length
GAPDH	<u>NM_002046.3</u>	Forward : GGGAAGGTGAAGTTCGGAGT Reverse : GCCAGTAGAGGCAGGGATGA	633
GAPDH	<u>NM_002046.3</u>	Forward : GTCCACCACTGACACGTTGG Reverse : GGGAAGGTGAAGGTCGGAGT	729
FRα	<u>NM_016724.2</u>	Forward : GCATTTCATCCAGGACACCT Reverse : TCATGGCTGCAGCATAGAAC	407
RFC	NM_194255.1	Forward : GCTCCTACCAGTTCCTCGTG Reverse : AGACACTGCAAACCCAGCTT	621
PCFT	NM_080669.3	Forward : CTCCACGTCGGCTACTTCGT Reverse : CCATCCCCAGGATGTTGAAG	625
PCFT	NM_080669.3	Forward : CTCCAGGTCGGCTACTTCGT Reverse : CATCCCCAGGATGTTGAAGG	624

5.2.13.3. Western Blot Analysis for Folate Transport Proteins

Protein was extracted from SIRC cells as follows: Cells were washed thrice with DBPS (pH 7.4), centrifuged at 1000 g for 3 min, suspended in protein extraction buffer and incubated on ice for 30 min. The lysate was homogenized for 30 sec followed by centrifugation at 8,000 g for 15 min. Protein samples were subjected to SDS-PAGE and, after transfer to nitrocellulose membranes, were incubated with antibody against FR- α , PCFT, or RFC overnight at 4°C, followed by incubation with horseradish peroxidase-conjugated rabbit-anti goat IgG antibody for FR- α and goat-anti rabbit IgG for PCFT and RFC. After washing, with PBST, protein expression was visualized with the Super Signal West Pico Chemiluminescence detection system (Thermo Scientific, Rockford, IL). β -actin served as the loading control.

5.2.14. Tissue Preparation

Dutch Belted Pigmented rabbits weighing between 2 and 2.5 kg were obtained from Myrtle's Rabbitry (Thompson Station, TN). All procedures were approved by the Institutional Animal Care and Use Committee (IACUC) of University of Missouri- Kansas City (UMKC, Kansas City, MO). Rabbits were anesthetized with intramuscular administration of ketamine HCl (35 mg/kg) and xylazine (5 mg/kg). Then the animals were euthanized by an overdose of sodium pentobarbital (100 mg/kg) administered through marginal ear vein under deep anesthesia. Eyes were removed carefully and a small incision was made on the sclera. The cornea was excised by removing lens and iris-ciliary body. The cornea was placed in a petridish and washed with Dulbecco's phosphate buffered saline.

5.2.15. Permeability Studies

The excised cornea was mounted on a Side-by-Side diffusion apparatus for carrying out permeability studies. The corneal side was placed towards the donor chamber in which 3.0 mL of drug solution ([³H]Folic acid, 10 nM) was placed. The receptor chamber was filled with 3.2 mL of DPBS. Permeability experiment was carried out at 34°C (*in vivo* corneal temperature). The receptor chamber was maintained at a higher volume (3.2 mL) so as to maintain hydrostatic pressure sufficient to maintain corneal curvature. For competitive inhibition studies cold folic acid at a concentration of 1 mM was added. An aliquot (100 µL) was withdrawn at regular time intervals and replaced with equal volume of fresh buffer. All the experiments were carried under sink conditions. Simultaneously, [³H]-mannitol permeability studies were carried out to observe the integrity of corneal tissues. The samples were transferred into scintillation vials, mixed with 5 mL scintillation cocktail and analyzed for radioactivity with the help of a scintillation counter (Model LS-9000; Beckman Instruments, Inc.). All the permeability studies were carried out in triplicate.

Permeability (P_{app}) of folic acid was calculated using Eq. 2.

$$\text{Permeability (P}_{app}\text{)} = \text{Flux}/C_d \quad \text{Eq. 2}$$

Flux (J) is calculated by dividing the slope obtained by plotting cumulative amount of folic acid permeated (M) through the cornea vs time (t) with cross sectional area of the membrane (A) exposed to the drug. C_d represents the initial folic acid concentration in the donor chamber.

5.3. Results

Time-dependent uptake of [³H] Folic acid (10 nM) was carried out in SIRC cells. As shown in Fig.15, the uptake increased linearly up to 30 min and reached equilibrium at 45 min.

Hence all uptake experiments were carried out over 30min unless otherwise mentioned.

Role of hydrogen ions on uptake of [³H] Folic acid was examined by regulating the buffer pH over a range of 4–8. Uptake of folic acid was highest at acidic pH of 4 and 5 suggesting that the uptake process is probably driven by a proton gradient. There was a considerable decrease in the uptake of folic acid at pH 6, 7 and 8 (Fig. 16). The process could be mediated by PCFT transporter which requires proton coupling for the transport of folic acid. Since the folic acid uptake was significantly higher at acidic pH all further uptake experiments were carried out at pH 5. The uptake experiments were carried out at three different temperatures (4, 25 and 37°C). As indicated in Fig. 17, the rate of uptake significantly reduced at 4 and 25°C relative to 37°C. This is due to the arrest of cellular energetics at lower temperatures. At 4°C the uptake of folic acid is very low. This may be due to the arrest of receptor mediated endocytosis. This study clearly indicates that folic acid uptake is temperature dependent and the uptake is optimum at a physiological temperature, 37°C.

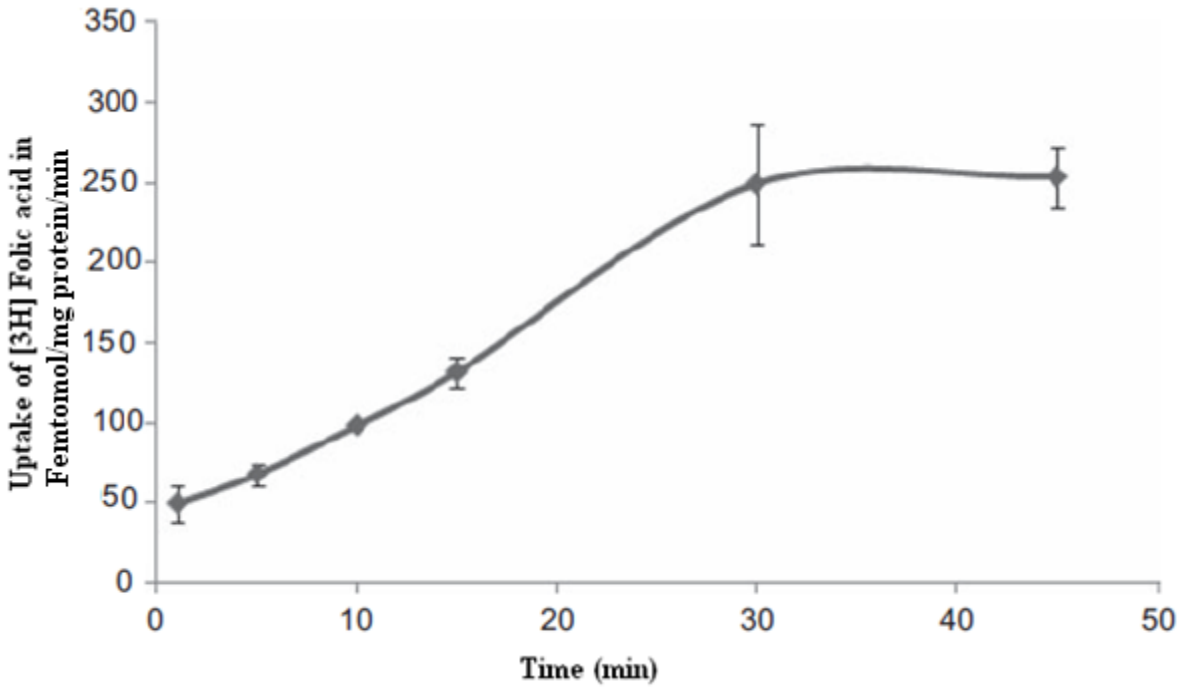


Fig. 15: Uptake of [³H] Folic acid by SIRC cells as a function of time. Each data point represents the mean ± standard deviation of 5 separate uptake determinations.

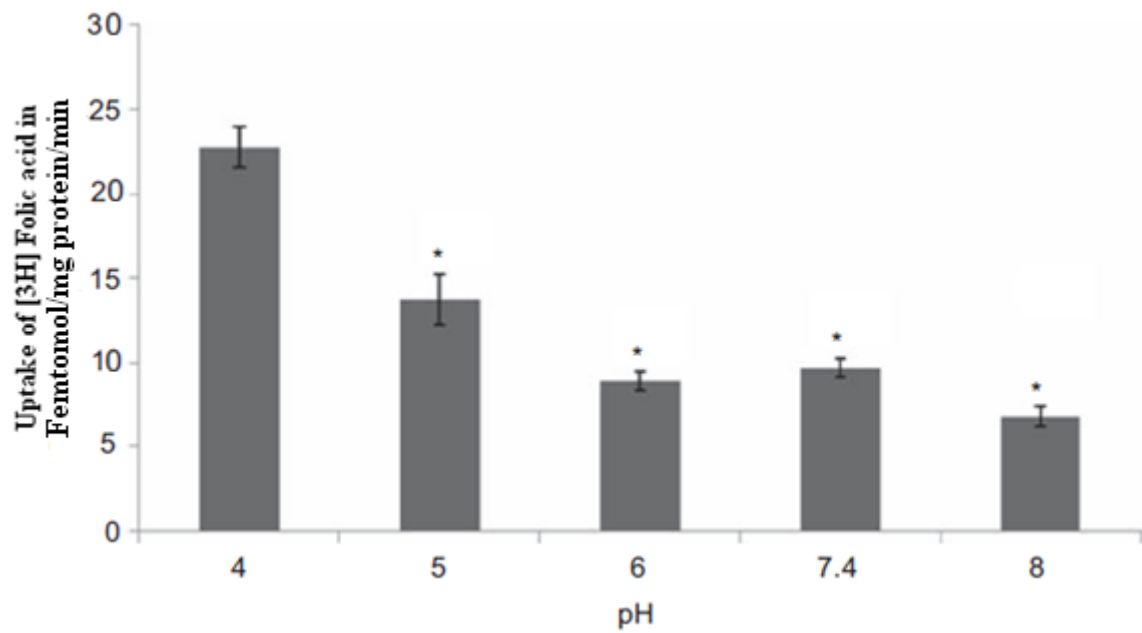


Fig. 16: Uptake of [³H] Folic acid by SIRC cells as a function of pH. Each data point represents the mean ± standard deviation of 5 separate uptake determinations. Asterisk (*) represents significant difference from control ($p < 0.05$).

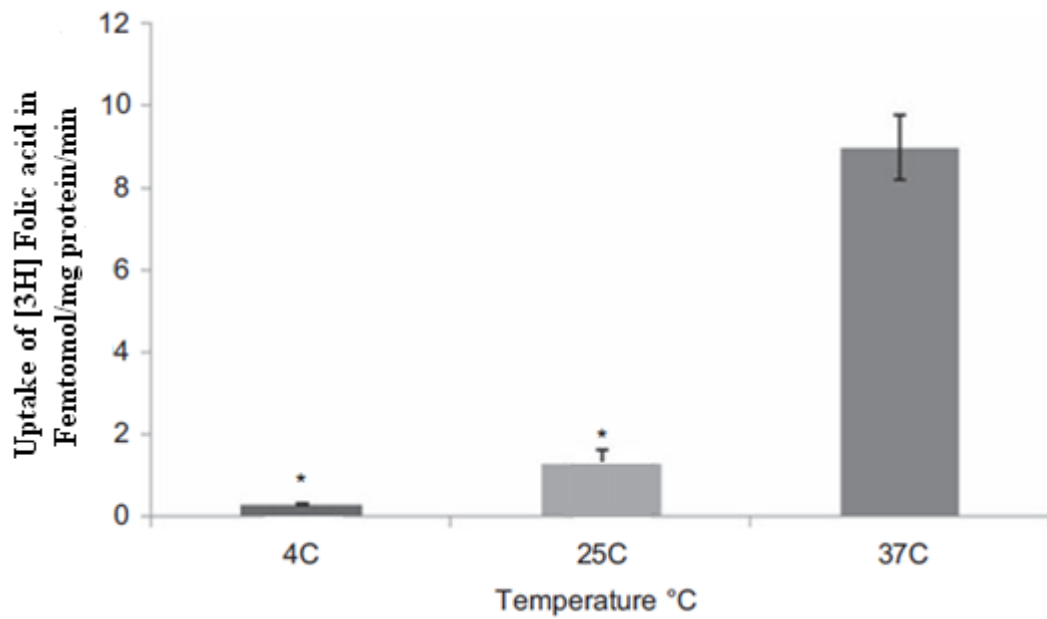


Fig. 17: Uptake of [³H] Folic acid by SIRC cells as a function of temperature. Each data point represents the mean \pm standard deviation of 5 separate uptake determinations. Asterisk (*) represents significant difference from control ($p < 0.05$).

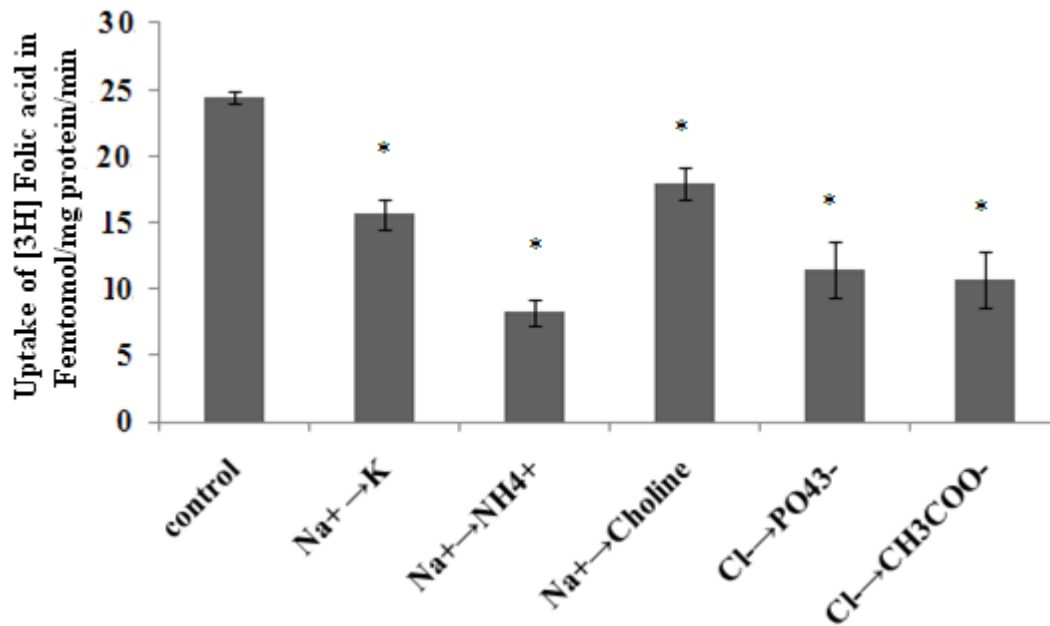


Fig. 18: Uptake of [³H] Folic acid by SIRC cells as a function of ions. Each data point represents the mean ± standard deviation of 5 separate uptake determinations. Asterisk (*) represents significant difference from control ($p < 0.05$).

In order to delineate ion dependency on folic acid uptake mechanism, Na^+ ions in the medium were replaced with equimolar quantity of K^+ , NH_4^+ and choline chloride; while Cl^- ions were replaced with salts of alternative organic and inorganic monovalent anions (phosphate and acetate). There was a significant difference in the uptake of folic acid in the absence of Na^+ and Cl^- ions. Figure 18 clearly illustrates Na^+ and Cl^- ion dependency of the uptake process. The effect of metabolic inhibitors on the uptake of $[3\text{H}]$ Folic acid was examined. A Na^+/K^+ -ATPase inhibitor (ouabain), intracellular ATP reducer (2, 4-dinitrophenol; DNP) and oxidative phosphorylation inhibitor (sodium azide) were used as metabolic inhibitors. Fig.19 shows that the uptake process was significantly inhibited in the presence of all energy inhibitors indicating that the process is highly energy dependent. Role of membrane transporter inhibitors was investigated by incubating the cells with Probenecid, DIDS and SITC and endocytosis process inhibitor colchicine at 0.5 mM concentration. As indicated in Fig. 20, there was a significant lowering in folate uptake in the presence of membrane transport inhibitors indicating the involvement of anion exchanger. Moreover, significant inhibition in uptake of folic acid in presence of 1 μM colchicine suggests the involvement of receptor mediated endocytosis. This result suggests the existence of both folate transporter and receptor on SIRC cell line. Substrate specificity of the saturable uptake process was investigated in presence of various structural analogs on folic acid. The effect of these compounds on the uptake of $[3\text{H}]$ Folic acid was significant. Uptake rate of folic acid is shown in Fig.21 and was found to be 26.96 ± 0.12 , 4.88 ± 0.02 , 3.36 ± 0.25 , 9.22 ± 0.26 , 5.02 ± 1.54 , 12.46 ± 0.15 , 9.20 ± 0.96 , 26.39 ± 0.9 , 25.52 ± 3.05 , 24.90 ± 3.84 ,

27.97±1.53 and 25.73±3.84 fmol/(min mg) protein for control and in the presence of folic acid (0.1 µM), folic acid (1 µM), MTF (0.1µM), MTF (1 µM), MTX (0.1 µM), MTX (1 µM), biotin (10 µM), pantothenic acid (10 µM), riboflavin (10 µM) and niacin (10 µM), respectively. As shown in Fig.21, [3H] Folic acid uptake was significantly reduced in the presence of 0.1 and 1µM of unlabeled folic acid. Significant inhibition was also observed with MTF and MTX at a concentration of 0.1 and 1 µM. Unlabeled vitamins (biotin, pantothenic acid, riboflavin and niacin) did not show any effect on the uptake process. The existence of a carrier-mediated system for folic acid in the SIRC cell line was determined by evaluating the uptake kinetics of folic acid in the presence of unlabeled folic acid. Total [3H] Folic acid uptake was analyzed and the data illustrates that the uptake mechanism consists of two pathways: a saturable pathway (carrier mediated) at lower concentrations and an apparently a non-saturable (passive) pathway that dominates over carrier mediated process at higher concentrations above 0.1 µM for folate (Fig. 22).

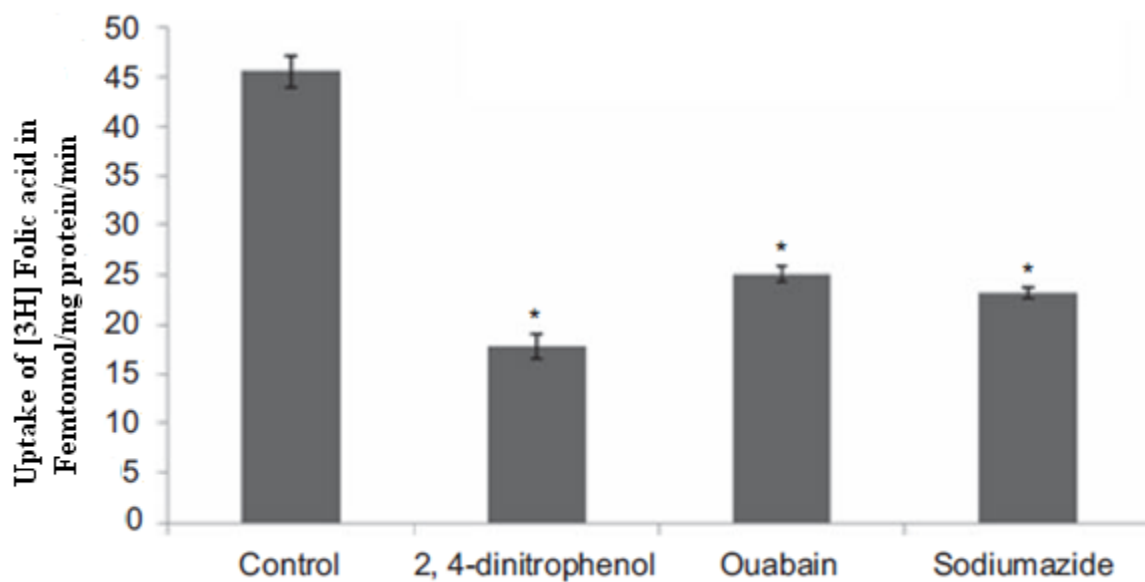


Fig. 19: Uptake of [³H] Folic acid by SIRC cells in presence of various energy inhibitors. Each data point represents the mean ± standard deviation of 5 separate uptake determinations. Asterisk (*) represents significant difference from control ($p < 0.05$).

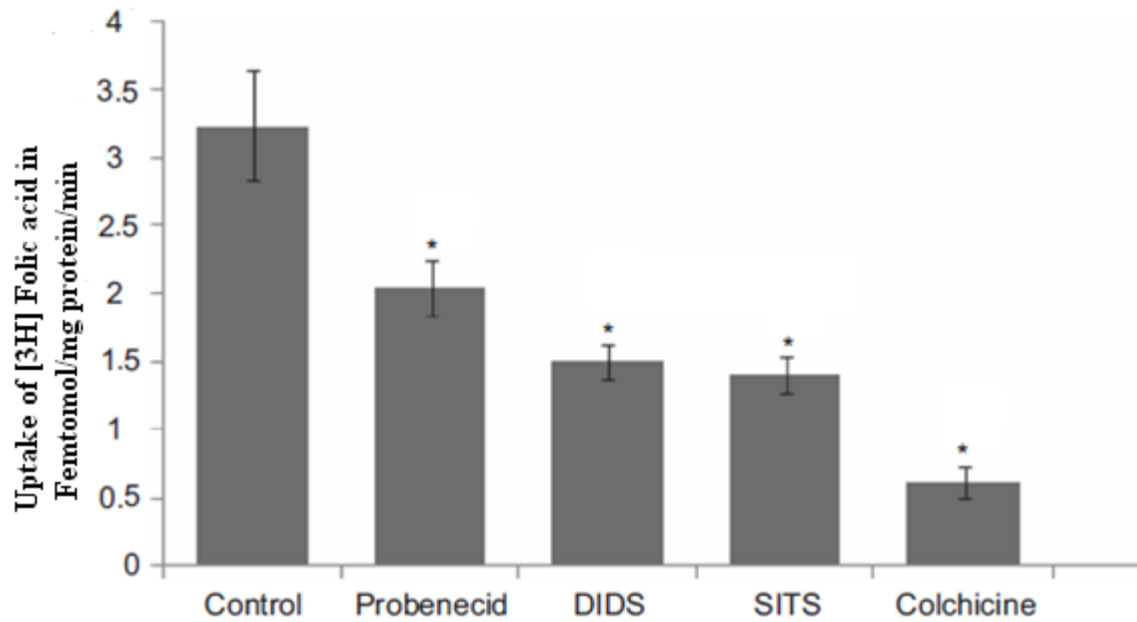


Fig. 20: Uptake of [³H] Folic acid by SIRC in presence of membrane transport inhibitors and endocytosis inhibitor colchicine. Each data point represents the mean ± standard deviation of 5 separate uptake determinations. Asterisk (*) represents significant difference from control ($p < 0.05$).

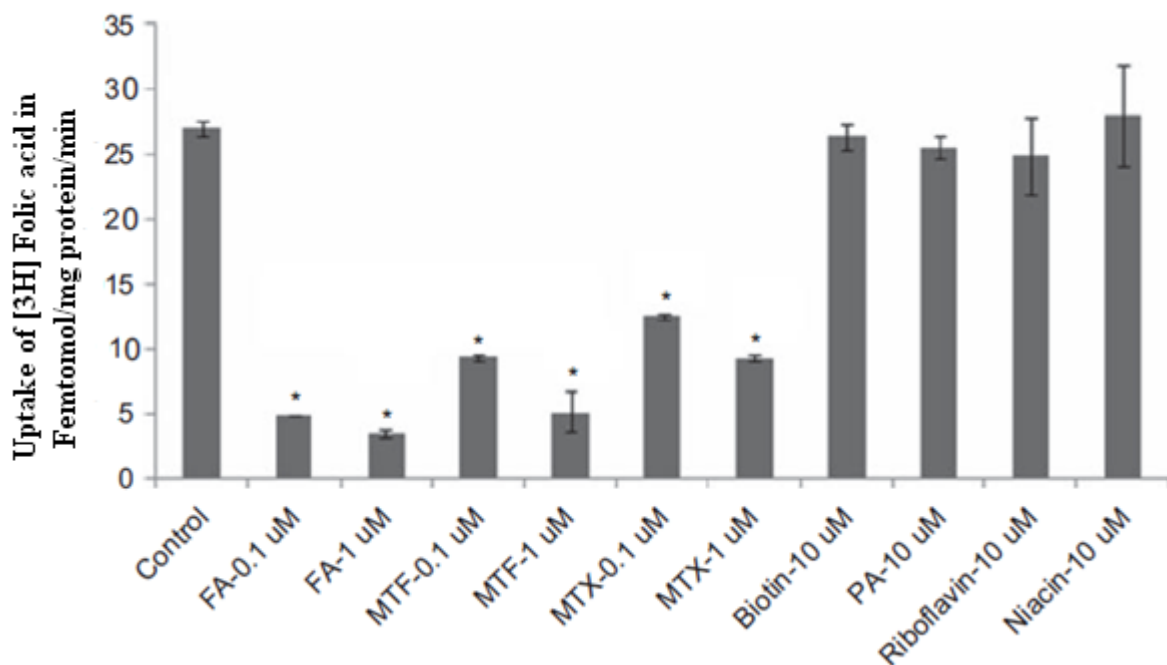


Fig. 21: Substrate specificity of uptake of [³H] Folic acid (10 nM) by SIRC cells in presence of various structurally related and unrelated analogs. Each data point represents the mean ± standard deviation of 5 separate uptake determinations. Asterisk (*) represents significant difference from control ($p < 0.05$).

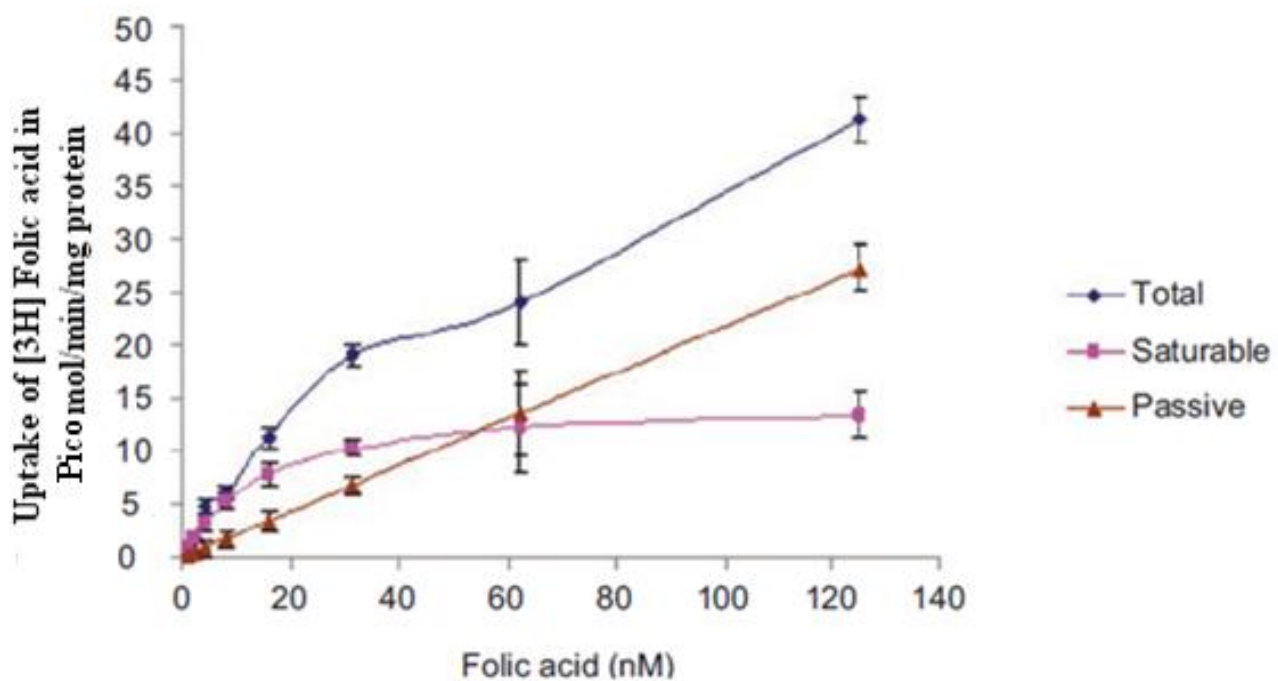


Fig. 22: Uptake of [³H] Folic acid (10 nM) in presence of various concentrations of cold folic acid on SIRC cell line. Saturation kinetic parameters are as follows : V_{max} : $(1.5 \pm 0.1) \cdot 10^{-5}$, K_m : $14.2 \pm 0.2 \cdot 10^3$ Pico mol and K_d : $(2.1 \pm 0.2) \cdot 10^{-6} \text{ min}^{-1}$ Each data point represents the mean \pm standard deviation of 5 separate uptake determinations.

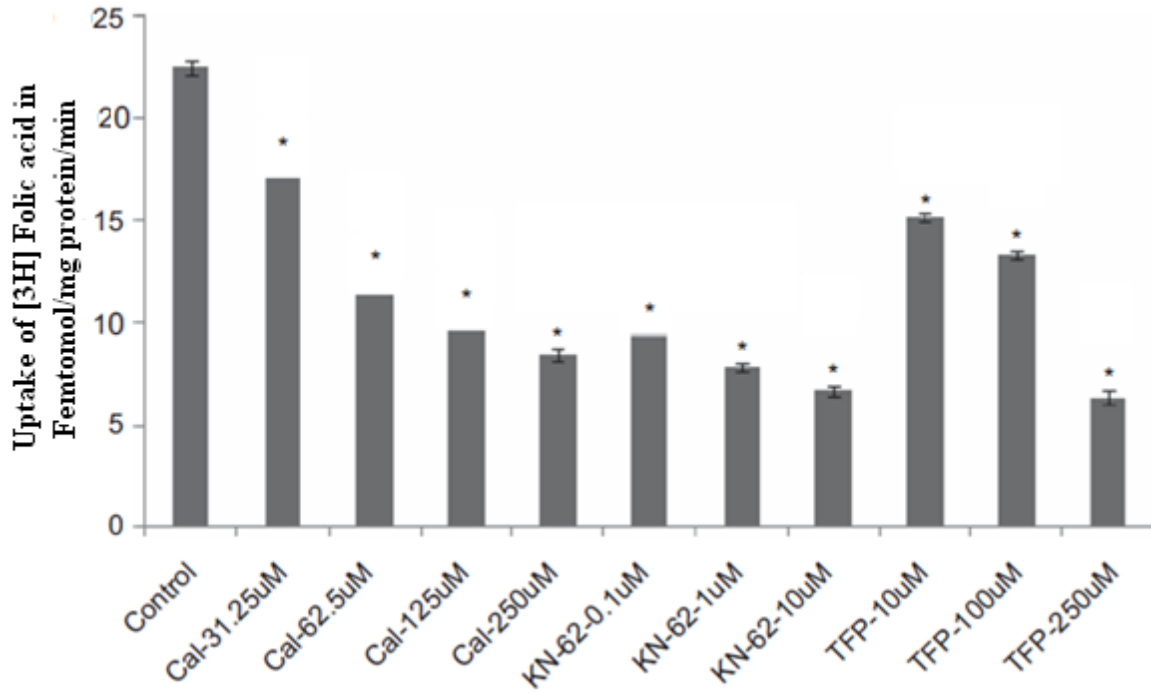


Fig. 23: Effect of Ca^{2+} /calmodulin-mediated pathways modulators on the uptake of $[^3\text{H}]$ Folic acid in SIRC cells. Each data point represents the mean \pm standard deviation of 5 separate uptake determinations. Asterisk (*) represents significant difference from control ($p < 0.05$).

Saturable as well as non-saturable components were determined by substituting the values of the kinetic constants into Michaelis–Menten equation. Uptake process by the saturable components was determined by subtracting the diffusional component from the total uptake at each concentration. After fitting the data to modified Michaelis–Menten equation, an uptake process with apparent K_m of 14.2 ± 0.2 nM, V_{max} of $(1.5 \pm 0.1) \times 10^{-5}$ micromoles/min/mg protein and K_d of $(2.1 \pm 0.2) \times 10^{-6}$ min⁻¹ were obtained. The role of Ca^{+2} /calmodulin-mediated pathways in the regulation of [3H]Folic acid uptake was examined in SIRC cells by pre-treating them with calmodulin inhibitors (calmidazolium and trifluoperazine) and with Ca^{+2} /calmodulin dependent protein kinase II inhibitor (KN-62). These compounds significantly ($p < 0.05$) reduced the folic acid uptake in a concentration dependent manner as shown in Fig.23. Role of PKA-mediated pathway in the regulation of folic acid uptake was also studied by pre-treating SIRC cells for 1 h with compounds that are known to increase intracellular cAMP levels (3-isobutyl-1-methylxanthine and forskolin) thus activating PKA. This study clearly indicated that 3-isobutyl-1-methylxanthine and forskolin significantly ($p < 0.05$) inhibited uptake of folic acid in a concentration dependent manner. The effect of specific PKA inhibitor H-89 on the folic acid uptake was also examined. Forskolin and IBMX induced PKA activity was abolished by H-89 as shown in Fig. 24. Reduction in folic acid uptake by cAMP modulators suggested the involvement of cAMP-dependent protein kinase A (PKA) in the regulation of folic acid transport.

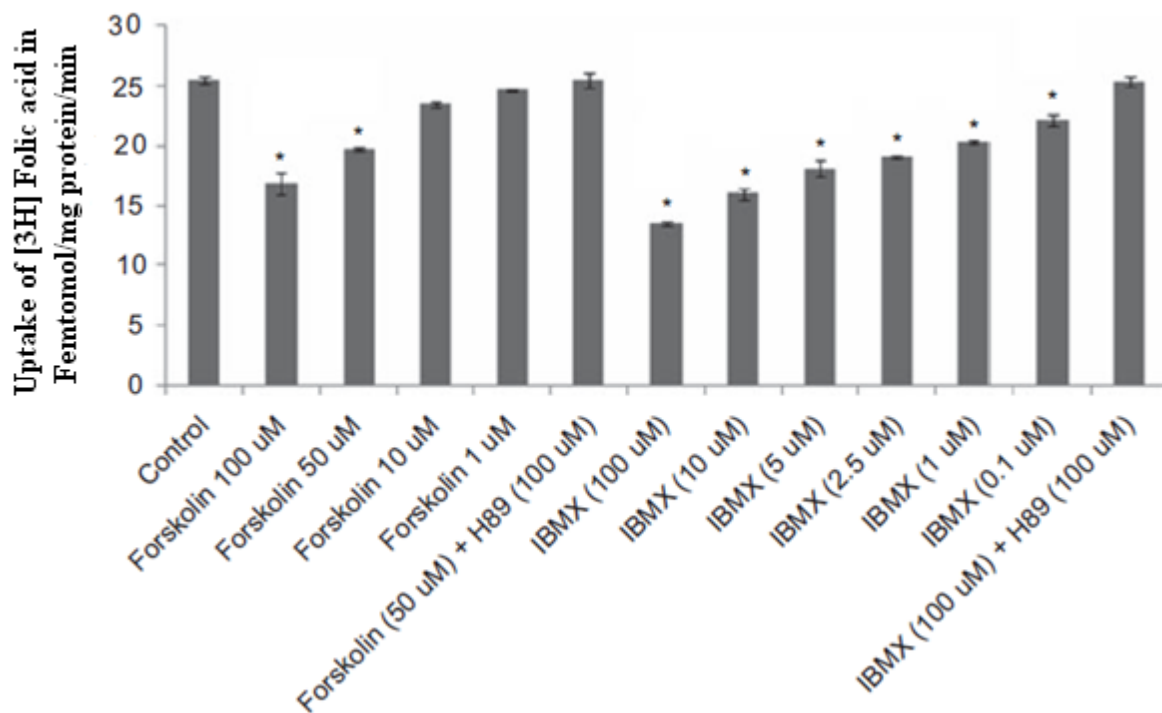


Fig. 24: Effect of PKA pathway modulators on the uptake of [³H] Folic acid in SIRC cells. Each data point represents the mean \pm standard deviation of 5 separate uptake determinations. Asterisk (*) represents significant difference from control ($p < 0.05$).

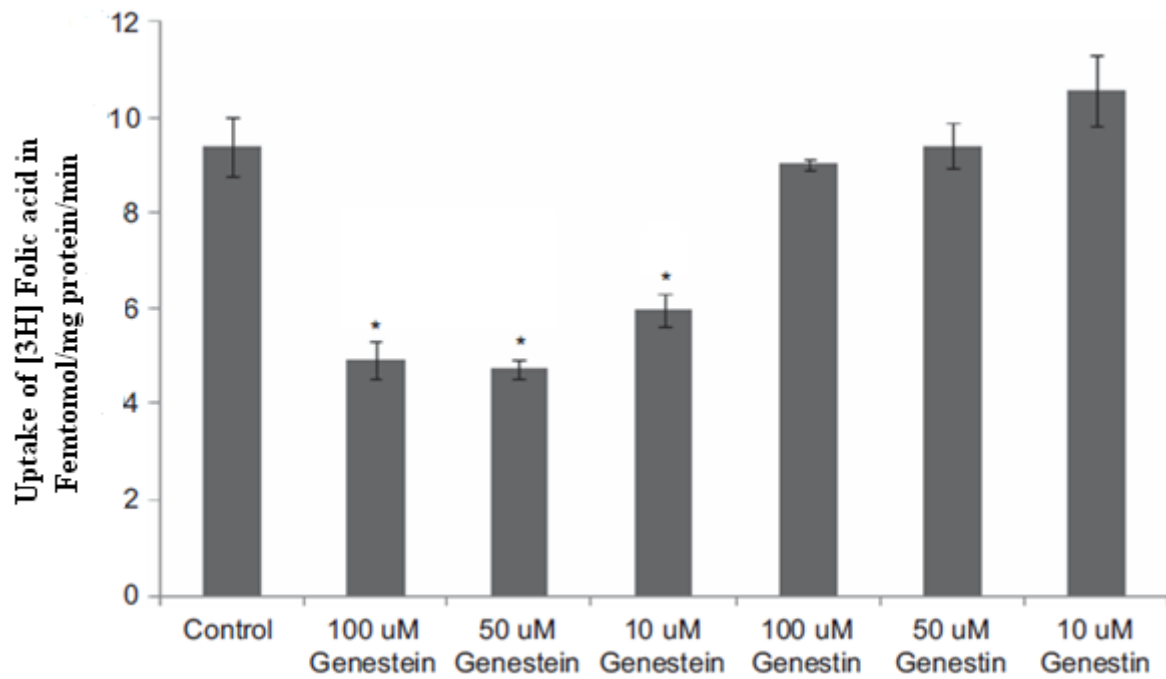
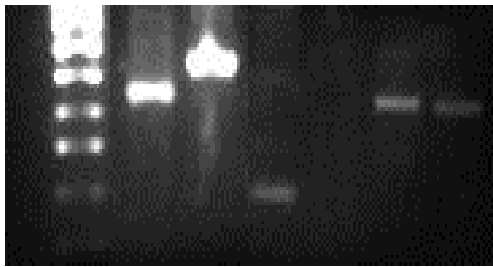


Fig. 25: Effect of PTK pathway modulators on the uptake of [³H] Folic acid in SIRC cells. Each data point represents the mean ± standard deviation of 5 separate uptake determinations. Asterisk (*) represents significant difference from control ($p < 0.05$).

In another study, we examined the involvement of PTK pathway in the regulation of folic acid uptake in SIRC cells which were pretreated for 1 h with the PTK inhibitor, genistein. Genistein is considered as a negative control for this inhibitor. There was significant difference in the uptake of [³H] Folic acid in the presence of genistein (10–100 μM) as shown in Fig. 25. These results suggest that Ca²⁺/calmodulin, PKA and PTK pathways play a significant role in the translocation of folic acid into SIRC cells. Expression of the folate carrier systems in SIRC cells at the mRNA level was determined by RT-PCR analysis (Fig. 26). Gel electrophoresis had shown a major band (407bp) corresponding to the amplified folate receptor alpha (FR α: lane 4). No product was observed for reduced folate carrier (RFC: lane5). Similarly two major bands (625bp, 624bp) were obtained for proton coupled folate transporter (PCFT: lane 6, 7). BLAST analysis showed that the primers used in this study can result in a PCR product size as specified. Western blot analysis (Fig. 27) indicated the expression of folate receptor-alpha protein at 40 kDa molecular weight and a clear distinct band was observed for PCFT at 50 kDa. Hence this result confirms the existence of FR-α and PCFT proteins in SIRC cells. Transport of [³H] Folic acid across rabbit cornea in the presence and absence of 1mM concentration of cold folic acid is shown in Fig. 28.



- (1) 100 bp ladder
- (2,3) GAPDH (633, 729 bp)
- (4) FR- α (407 bp)
- (5) RFC (621 bp)
- (6,7) PCFT (625, 624 bp)

Fig. 26: RT-PCR analysis of FR- α (Folate receptor), RFC (reduce folate carrier), PCFT (Proton coupled folate transporter). GAPDH (Glyceraldehyde 3-phosphate dehydrogenase)

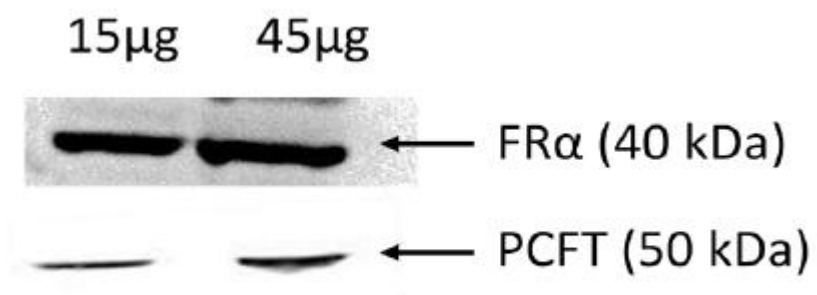


Fig. 27: Western blot analysis of FR- α (Folate receptor) and PCFT (Proton coupled folate transporter).

Permeability of [3H] Folic acid across rabbit cornea was found to be 1.48×10^{-5} cm/sec and in the presence of cold folic acid it was 1.08×10^{-5} cm/sec (Table 5). This study further corroborates the existence of folate carrier mediated system on the rabbit cornea.

Table 5: *Ex vivo* permeability of [³H] Folic acid in excised rabbit cornea

Sample	Permeability (cm/sec)* 10⁵ (mean ±SEM)
Control ([³ H]Folic acid)	1.48± 0.13
In presence of folic acid	1.08± 0.10

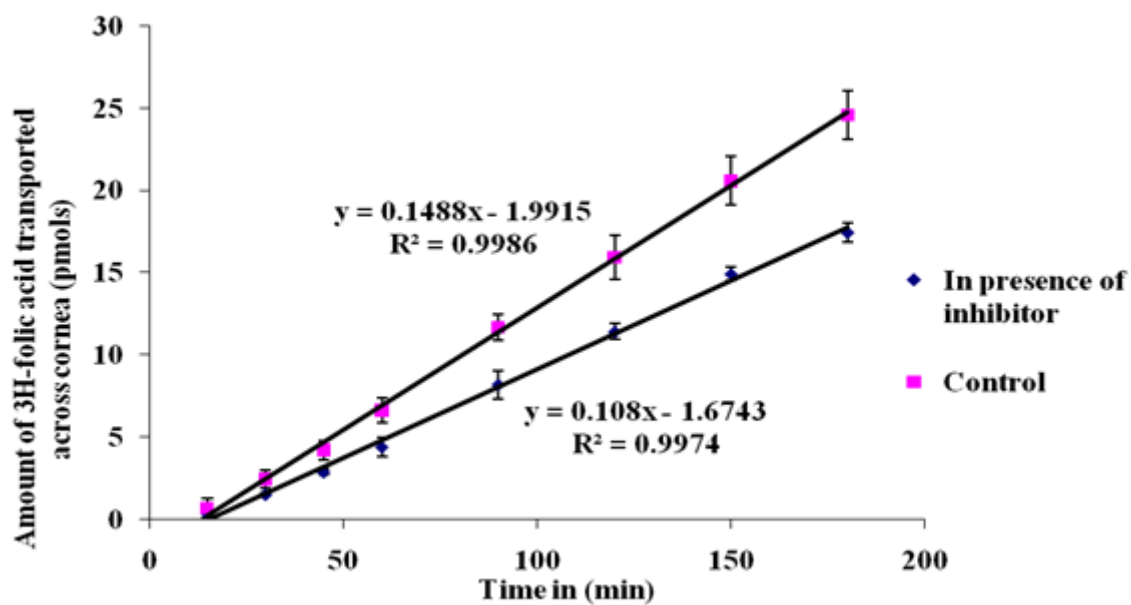


Fig. 28: *Ex vivo* permeability of [^3H] Folic acid in excised rabbit cornea. Each data point represents the mean \pm standard deviation of 4 separate determinations.

5.4. Discussion

The aim of this study was to identify a folate carrier mediated system in the Staten's Seruminstitut rabbit corneal (SIRC) epithelial cell line and to evaluate it as an *in vitro* screening tool for regulating the mechanism and intracellular regulation of folic acid uptake. Previous reports suggest that the use of SIRC cell layers can reasonably predict the uptake of biotin and riboflavin across corneal epithelial membranes (Hariharan et al., 2006; Janoria et al., 2006). SIRC cell line was selected for characterization studies as it exhibits physiological and biochemical properties of rabbit corneal epithelium. Hence it could serve as a better *in vitro* model to study the folate uptake in rabbit cornea (Goskonda et al., 2000). SIRC cell line has been widely utilized as a model for investigating transport of drugs across rabbit cornea. In our study, [³H]Folic acid (10 nM) uptake was found to be saturable with an apparent K_m of 14.22 nM, V_{max} of 1.5×10^{-5} micromoles/min/mg protein and K_d of $2.10 \times 10^{-6} \text{ min}^{-1}$ for folic acid. Existence of different folic acid uptake mechanisms at varying levels of expression depends on cell lines and/or inherent gene sequence of that specific cell line. A common trend observed with folic acid uptake mechanism appears to be specific and saturable process in the range of nanomolar concentration (10–50 nM) suggesting the involvement of FR in the uptake of folic acid in SIRC cells.

Uptake process of folic acid was found to be time dependent and saturation in the uptake was observed after 30 min. The process is pH dependent with maximum rate observed at a low pH 4 and 5. There was a significant decrease in the uptake with increase in the pH at 6, 7 and 8. This result clearly suggests proton coupled uptake of folic acid into SIRC cells. The

process appears to be temperature dependent with optimal uptake at a physiological temperature of 37°C. At room temperature there was a significant decrease in the uptake. The process drastically reduced at 4°C, which clearly suggests the existence of a receptor. These observations were consistent with the previously published results from our laboratory with retinoblastoma (Y-79) cells (Kansara et al., 2008). Presence of chloride and sodium-free buffers caused considerable inhibition of [³H] Folic acid uptake. This implies that chloride and sodium ions are involved in folic acid translocation. Additional support for Na⁺ dependence has been shown through uptake studies performed in the presence of ouabain, a well-known Na⁺/K⁺-ATPase inhibitor. Significant decrease in folic acid uptake was observed in the presence of ouabain, suggesting that carrier-mediated transport is energy dependent. To determine whether the uptake is dependent on a motive energy force, known metabolic inhibitors (sodium azide and 2, 4-dinitrophenol) were added to the incubation media. Significant inhibition of [³H] Folic acid uptake was observed when cells were treated with sodium azide (1 mM) and 2, 4-dinitrophenol (1 mM), which is known to reduce intracellular ATP. Thus, process of folic acid uptake in SIRC cells is found to be energy dependent and appears to be directly coupled to ATP energy sources. These results clearly indicate the involvement of a specialized, energy, sodium and chloride dependent and high-affinity carrier-mediated system which saturates at nanomolar concentrations. Possible involvement of a high affinity FR in the folic acid uptake was further supported by data showing a significant inhibition in the presence of unlabelled folic acid, MTF and MTX.

No significant inhibition in folic acid uptake was observed in the presence of various unlabelled vitamins (biotin, pantothenic acid, riboflavin, niacin and ascorbic acid). Taken together; these results provide an additional support for the presence of a carrier system that specifically mediates the uptake of folic acid into SIRC cells at nanomolar concentrations. Significant inhibition by these anion exchange inhibitors suggests the possible involvement of an anion-exchange transport mechanism probably through proton coupled folate transporter. However colchicine significantly reduced the folic acid uptake, suggesting the involvement of receptor mediated endocytosis process. Further studies are required to corroborate these findings. RT-PCR analysis provided evidence on the molecular expression of folate receptor and PCFT transporter. Therefore this data further supports the existence of a specific transport system for folic acid in SIRC cells. Clear distinct bands in Western blot confirmed the presence of FR- α (40 kDa) and PCFT (50 kDa) protein expressions in SIRC. FR- α and PCFT proteins are involved in the influx of folic acid into corneal cells (SIRC). The possible regulation of the folic acid uptake process by intracellular regulatory pathways was also investigated. The primary goal was to focus on the pathways that involve protein kinase A (PKA) and other pathways that play a critical role in the regulation of uptake of nutrients by other epithelial cells [protein tyrosine kinase (PTK) and Ca^{2+} /calmodulin] (Brandsch et al., 1993; Muller et al., 1996). The role of cAMP (or PKA)-mediated pathway in the regulation of folic acid uptake by SIRC cells was investigated by pre-treating the cells for 1 h with compounds that are known to increase intracellular cAMP level such as IBMX and Forskolin and they resulted in inhibition of folic acid uptake from 25.5 fM to 16.8

fM, 19.7fM and 23.4 fM in the presence of 100uM, 50uM and 10uM Forskolin in a concentration dependent manner and with 100uM, 10uM, 5uM, 2.5uM, 1uM, 0.1 uM IBMX it has decreased from 25.5fM to 13.5fM, 15.9fM, 18fM, 19fM, 20fM and 22.1fM and it was evident that the uptake has decreased in a concentration-dependent manner. This process was inhibited in the presence of H-89 (specific PKA inhibitor) i.e there was no change in the uptake of folic acid it was similar to that of control which was 25.5 fM. Significant decrease in folic acid uptake in the presence of cAMP inhibitors implied the involvement of protein kinases for efficient folate transport process. Since the best defined target of cAMP is PKA, which, in turn, mediates most of the physiological effects of cAMP in eukaryotes (Hamid and Kaur, 2009). The results showed that modulators of cAMP/PKA-mediated pathway cause significant inhibition in folate uptake. These findings clearly indicate that intracellular cAMP affects folic acid uptake through a PKA dependent mechanism. Literature evidences also show that cAMP/PKA-mediated pathway affects the folate uptake mechanism in other epithelial cell types also. (Kumar et al., 1997; Muller et al., 1996). Pretreatment of SIRC cells with specific PTK inhibitors genistein caused a significant inhibition in folic acid uptake from 9.3fM in the control to 4.9fM, 4.7fM and 5.9fM in presence of 100uM, 50uM and 10uM genistein. On the other hand, their negative control, genistin did not show any effect at 10, 50 and 100 uM concentrations. The inhibitory effect of genistein was mediated through inhibition of the folate uptake process. Previous findings suggest the possibility of PTK acting on a supplementary protein, which in turn effects the folic acid uptake process. (Kumar et al., 1997). Role of the Ca²⁺-calmodulin-mediated pathway was apparent in the uptake of

folic acid in SIRC cells. Modulators of this pathway were found to cause a significant inhibition in folate uptake. In the presence of 250 uM, 125uM, 62.5um, 31.25uM concentrations of calmidazolium the uptake of folic acid has decreased from 22.5 fM to 8.48 fM, 10.4fM, 12.2fM, 17.7fM, and in presence of 10uM, 1uM, 0.1uM of concentrations of KN-62 it has decreased from 22.5fM to 6.7fM, 7.9fM, 9.7fM and in presence of 250uM,100uM,10uM TFP the uptake process has decreased 6.39 fM,13.3fM,15.1fM respectively. These experimental observations have clearly indicated that inhibition of folic acid uptake process was inhibited in a concentration dependent manner by all calmodulin pathway inhibitors in SIRC cells. These findings were similar to those seen for the vitamin uptake in intestinal and hepatic epithelial cells. Said et al., suggest that the effect of calmidazolium is facilitated through a decrease in the activity and the affinity of the folic acid uptake process. The exact cellular mechanism through which the Ca^{2+} -calmodulin-mediated pathway regulates its effect on folate uptake is not well known. However, different mechanisms for the action of this pathway may include the activation of specific protein kinase(s) and/or potential direct effect on the folate uptake system. (Said et al., 2005) Therefore, calmodulin mediated reduction of folic acid uptake in SIRC cells might be a manifestation of intertwined regulation of these processes. Uptake of folic acid in SIRC cells is mediated by PKA, PTK and Calmodulin pathways.

5.5. Conclusion

This research article suggests that SIRC cells may serve as a practical *in vitro* experimental model for rabbit cornea for delineating corneal uptake mechanisms. Folate carrier-mediated

system can be utilized for targeted drug delivery to cornea using folate-conjugated nanoparticles and prodrugs to attain enhanced permeability which can result in significant improvement in therapeutic outcome of several corneal diseases.

CHAPTER 6

RATIONALE FOR INVESTIGATION

6.1. Overview

Retinoblastoma is a major vision threatening intraocular malignancy affecting 1 in 18,000 to 30,000 live births worldwide (Aerts et al., 2006; Albert, 1987; Bishop and Madson, 1975). It is common in children between the age of 3 to 7 (Pesin and Shields, 1989). Marginal tumor regression is usually evident following a combination therapy with cyclophosphamide, vincristine, doxorubicin, melphalan, thiotepa, nimustine and cisplatin (Chan et al., 2005; Ragab et al., 1975; White, 1991). In retinoblastoma cells nucleus is the site of DNA intercalation and/or binding for anticancer agents including carboplatin, etoposide and topotecan. However, cellular uptake of these agents is significantly reduced by the efflux pumps on plasma membrane. Upon exposure to anticancer agents, expression levels of efflux pumps appear to be elevated causing lower drug accumulation inside cell cytoplasm as well as nucleus. Generally it is hypothesized that cancer cells express more nutrient transporters than normal cells. Hence we are trying to explore the expression of various nutrient transporters in retinoblastoma cells compared to normal retinal cells. If the relative expression of influx transporters is higher then targeted drug delivery to specific cancer cells is possible. However, for chemotherapy to be successful, the anticancer agents must generate intracellular therapeutic concentrations. Efflux pumps which are highly expressed on the cancer cell membrane are responsible for sub-therapeutic levels of chemotherapeutic agents,

leading to drug resistance. With MDR gene overexpression, tumor cells may develop resistance to a wide range of structurally and functionally diverse chemical agents. MDR genes encode for three main types of efflux proteins: P-glycoprotein (P-gp), multidrug resistance associated proteins (MRP) and breast cancer resistance protein (BCRP) (Amaral et al., 2007; Yamamoto et al., 1998). Of these P-gp and MRPs are known to be expressed on retinoblastoma cells. Most of the chemotherapeutic agents are good substrates for these efflux pumps which may reduce drug concentrations in tumor cells (Kartner et al., 1985; Li et al., 2009). Cell membranes express a definite set of membrane proteins that bind to their respective substrates with high affinity and specificity (Brzezinska et al., 2000). Therefore novel approaches that enhance the selectivity of the anticancer agents to nutrients and vitamin transporters seem to be promising.

Transporter/receptor mediated drug delivery is one of the promising approaches that has been utilized for enhancing the uptake across membranes (Dey and Mitra, 2005). By coupling to a promoeity (ligand) that is a substrate for the transporter/receptor, the parent drug can be transported (Yang et al., 2001). Numerous transporter/receptor systems such as folate receptor (FR- α), sodium-dependent multivitamin transporter (SMVT) and amino acid transporter (B⁽⁰⁺⁾) play a significant role in the internalization of vitamins and amino acids. However, thorough understanding of the transporters/receptors overexpressed on cancer cells can aid in the design of an effective transporter/receptor mediated drug delivery system. It was our objective to determine quantitative expression of FR- α , SMVT and amino acid transporter (B⁽⁰⁺⁾) carrier mediated systems on RB cells and compared to normal retinal cells.

Y-79 and ARPE-19 cell lines were selected as models for RB and healthy retinal cells respectively.

6.2. Statement of Problem

Several strategies are available for the treatment of retinoblastoma and the choice depends on the disease progression. Groups IV and V (according to Reese-Ellsworth classification system) are considered as very advanced and difficult stage and do not respond well to chemotherapy (De Potter, 2002). In such cases, external beam radiotherapy (EBR) and enucleation are employed as the last recourse. Both treatments leave the survivors with complete or nearly complete vision loss. EBR is an option for children who develop bilateral disease and show recurrence after chemotherapeutic treatment (Chintagumpala et al., 2007). In EBR, radiation is applied to the entire retina, lens, lacrimal gland and optic nerve; whereas exposure to the normal tissue is avoided. Currently, EBR is no longer a viable option due to long term side effects like optic neuropathy, cataract, retinopathy and chronic dry eye (Eng et al., 1993). Development of secondary tumors in the area exposed to the radiation after a long time period is the major reason that discourages the application of EBR (Eng et al., 1993). Enucleation is the only treatment option for group V tumors. These tumors also display one or more of side effects i.e., neovascular glaucoma, retinal detachment, involvement of optic nerve, sclera, orbit, anterior chamber or choroid, pars plana tumor seeding apart from tumor. Enucleation involves surgical removal of the eye ball sparing the eye lids and extraocular muscles. In the last decade, chemotherapy has played a vital role in treating the disease and sparing the globe. Several reports suggest that chemotherapy is successful in treating the

group I to III tumors whereas not very effective in group IV and V (De Potter, 2002). This is due to the presence of vitreal seeds responsible for disease recurrence (Chintagumpala et al., 2007). Chemotherapy helps in the reduction of tumor size so that focal therapy can be applied to a relatively small area and tumor can be shrunk without loss of vision. However, cellular uptake of these agents is significantly reduced by the efflux pumps on plasma membrane. Detailed understanding of the transporters/receptors overexpressed on cancer cells can aid in the design of an effective transporter/receptor mediated drug delivery system. Hence this project involves the study of expression of folate, SMVT and B0+ in retinoblastoma cells and further comparing with the expression levels in normal retinal cells.

6.3. Objectives

- I. To study the molecular evidence of folate, SMVT and B0+ expression by qualitative RT-PCR analysis in ARPE-19 cells and Y-79 cells.
- II. To study the relative fold expression of folate, SMVT and B0+ in ARPE-19 and Y-79 by quantitative real time PCR analysis.
- III. To study the quantitative uptake of [3H] Folic acid, [3H] Biotin and [¹⁴C] L-arginine in ARPE-19 and Y-79 cells.
- IV. To study the concentration dependency of [3H] Folic acid in ARPE-19 and Y-79 cells.
- V. To study the concentration dependency of [3H] Biotin in ARPE-19 and Y-79 cells.
- VI. To study the concentration dependency of [¹⁴C] L-arginine in ARPE-19 and Y-79 cells.

CHAPTER 7

DIFFERENTIAL EXPRESSIONS OF FOLATE RECEPTOR-ALPHA (FR-A), SODIUM DEPENDENT MULTIVITAMIN TRANSPORTER (SMVT), AND AMINO ACID TRANSPORTER B^(0,+) IN HUMAN RETINOBLASTOMA (Y-79) AND NORMAL HUMAN RETINAL (ARPE-19) CELL LINES

7.1. Rationale

Retinoblastoma (RB) represents intraocular neoplasm particularly in children, with around 200 new cases being reported every year in the United States (Kyritsis et al., 1984; Parkin et al., 1988). Approximately, 87% of children diagnosed with RB do not survive very long due to metastasis and hematogenous spread. RB is common in children between the age of 3 and 7 (Boddu et al., 2010a). Enucleation coupled with external beam radiotherapy (EBR) remains as the mainstay treatment for intraocular malignancies. Of late, there has been a resurgence of interest in implementing chemotherapy as a major treatment option in RB so as to avoid enucleation and/or EBR to save vision (Boddu et al., 2010a). Moreover, chemotherapy also lowers the risk of secondary malignancies associated with EBR. Tumor regression is evident following a combination therapy with cyclophosphamide, doxorubicin, vincristine, thiotepa, nimustine, melphalan, and cisplatin (Chan et al., 2005). However, for chemotherapy to be successful, the anticancer agents must generate intracellular therapeutic concentrations. Efflux pumps which are highly expressed on the cancer cell membrane are responsible for sub-therapeutic levels of chemotherapeutic agents, leading to drug resistance. With multidrug resistance (MDR) gene over expression, tumor cells may develop resistance to a wide range of structurally and functionally diverse chemical agents. MDR genes encode for three main

types of efflux proteins: P-glycoprotein (P-gp), multidrug resistance associated proteins (MRP) and breast cancer resistance protein (BCRP) (Amaral et al., 2007; Yamamoto et al., 1998). Of these P-gp and MRPs are known to be expressed on retinoblastoma cells. Most chemotherapeutic agents are good substrates for these efflux pumps which may reduce drug concentrations in tumor cells (Kartner et al., 1985; Li et al., 2009).

Moreover, anticancer agents fail to differentiate between normal and tumor cells resulting in adverse effects and systemic toxicity. Over the past few years there has been a growing interest in the development of novel strategies for actively targeting drugs to cancer cells (Dean et al., 2005). Nutrient transporters/receptors including amino acids, glucose, peptide, folate, biotin, riboflavin, monocarboxylic acid, nucleoside/nucleobase, organic anion/cation transporters, present on the retina, play an important role in nutrition and regulation of endogenous/exogenous substances (Kansara et al., 2005). Uncontrolled proliferation of cancer cells require high intake of vitamins and nutrients as compared to normal cells. This requirement is often met by acquiring genetic mutations which functionally alter receptor-initiated signaling pathways in cancer cells. Such pathways in turn help in activating the uptake and metabolism of vitamins and nutrients necessary for promotion of cell survival and growth (Hsu and Sabatini, 2008; Vander Heiden et al., 2009). Cell membranes express a definite set of membrane transport proteins that bind to their respective substrates with high affinity and specificity (Brzezinska et al., 2000). Therefore novel approaches which can enhance the selectivity of anticancer agents to nutrient and vitamin transporters seem to be promising.

Transporter/receptor mediated drug delivery is one such approach that has been successfully utilized for enhancing uptake across membranes (Dey and Mitra, 2005). By chemical modification or coupling to a promoeity (ligand) which is a substrate for the transporter/receptor, the parent drug can be transported (Yang et al., 2001) (Fig. 29). Several transporter/receptor systems such as folate receptor (FR- α) (Jwala et al., 2011), sodium-dependent multivitamin transporter (SMVT) and neutral and cationic amino acid transporter (B^(0,+)) play a critical role in the internalization of vitamins and amino acids. However, detailed understanding of the transporters/receptors over expression in cancer cells can aid in designing an effective transporter/receptor mediated drug delivery system. Therefore, our objective to determine quantitative expression of FR- α , SMVT and B^(0,+) carrier mediated systems on RB cells and compare to normal retinal cells. Y-79 and ARPE-19 cell lines were selected as models for RB and retinal pigment epithelial cells respectively. Various reports suggest that RB originates from a primordial bipotential neuroectodermal cell containing neuronal and glial characteristics. Hence Y-79 cell line may be considered as a model of human retinal neoplasm (Kyritsis et al., 1984). Though several nutrient and vitamin transporters (peptide, amino acids, glucose, folate, monocarboxylic acid, nucleoside and nucleobase, organic anion and organic cation transporters) are expressed on plasma membranes, this work investigates the differential expression of FR- α , SMVT and B^(0,+) carrier systems due to their importance in drug delivery (Gaudana et al., 2009; Kansara et al., 2006). Based on our studies and some published results from our laboratory we made an

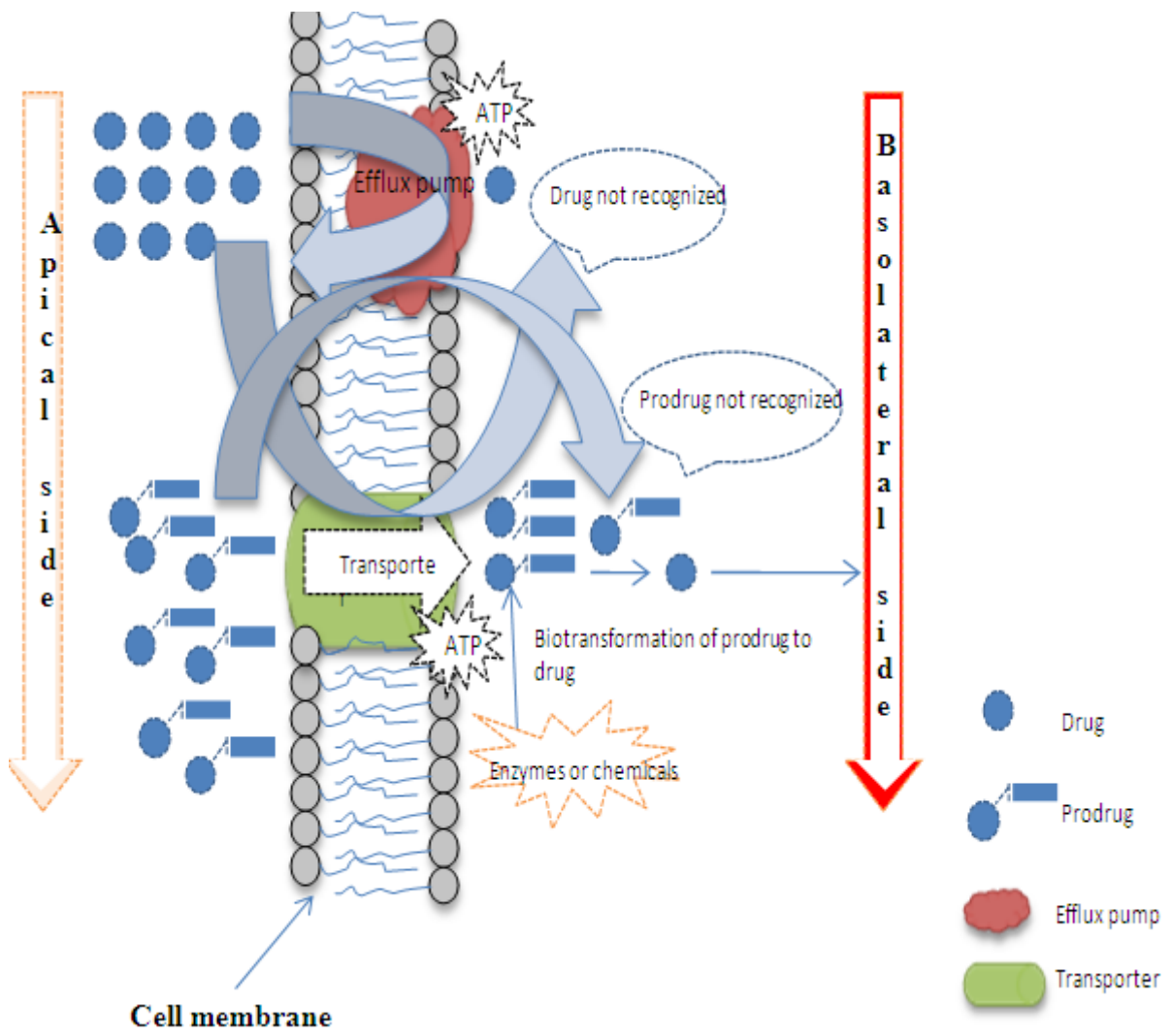


Fig. 29: Schematic representation of transporter/receptor mediated drug delivery.

attempt to compile the differential expression of FR- α , SMVT and B^(0,+) carrier mediated systems on RB cells and compare to ARPE-19 cells.

7.2. Materials and Methods

7.2.1 Materials

[³H]Folic acid (50 Ci/mmol), [³H] Biotin (50 Ci/mmol), [¹⁴C] Arginine (8.5 mCi/mmol) were procured from Perkin-Elmer (Boston, MA). ARPE-19 and Y-79 cells were obtained from ATCC (Manassas, VA). The growth medium and nonessential amino acids (NEAA) were obtained from Gibco (Invitrogen, GrandIsland, NY). Penicillin, streptomycin, sodium bicarbonate, and HEPES were purchased from Sigma-Aldrich (St. Louis, MO). Culture flasks (75 cm² growth area) and 12-well tissue culture plates were purchased from Costar (Cambridge, MA). The buffer chemicals were of analytical grade and obtained from Sigma-Aldrich.

7.2.2. Cell culture

ARPE-19 cells (passages 18–25) were cultured in DMEM/F-12 containing 10% heat-inactivated fetal bovine serum, 15 mM HEPES, 29 mM sodium bicarbonate, penicillin (100 units/mL) and streptomycin (100 μ g/mL). Y-79 cells were cultured as a suspension in RPMI 1640 medium supplemented with 15% non-heat-inactivated fetal bovine serum, 1 mM glutamine, penicillin (100 units/mL) and streptomycin (100 μ g/mL). Cells were maintained in 75 cm² tissue culture flasks at 37°C, in a humidified atmosphere of 5% CO₂ and 90% relative humidity. The medium was replaced every other day.

7.2.3. RT-PCR analysis

RNA was extracted from cells using TRIzol® reagent (Invitrogen, GrandIsland, NY) according to the manufacturer's protocol. Briefly, cells were lysed using phenol-chloroform and isopropanol method. RNA was suspended in DNase-RNase free water and concentration was determined using Nanodrop (Thermo Scientific, Wilmington, DE, USA). cDNA was generated for specific amount of mRNA using oligodT and M-MLV RT polymerase. Three micro liter of cDNA was then introduced into PCR. Primers used for the amplification of specific genes were summarized in Table 6. The PCR conditions were as follows: denaturation (94 °C, 45 s), annealing (56 °C, 1 min), and extension (72 °C, 45 s) for 45 amplification cycles, followed by a final extension of 72 °C for 10 min. The product was then subjected to gel electrophoresis with 1.5% agarose gel and visualized under UV.

7.2.4. Quantitative real time PCR

Quantitative real time PCR was performed to compare the FR- α , SMVT and B^(0, +) transporter expression levels in ARPE-19 and Y-79 cells. Quantitative real-time PCR was performed with Light cycler SYBR-green technology (Roche) using cDNA equivalent to 80 ng of total RNA with specific primers for each gene. PCR products were subjected to a melting-curve analysis to confirm the PCR specificity. The comparative threshold method was used to calculate the relative amount of mRNA in ARPE-19 with Y-79. The real time primers used for the study were summarized in the Table 7. GAPDH was used as an internal control in both the cells.

Table 6: PCR primers for neutral and cationic amino acid transporter ($B^{0,+}$), folate receptor (FR- α), and sodium-dependent vitamin transporter (SMVT)

Gene		Sequence 5'→3'	Product length
$B^{0,+}$	Forward	CCAGCCGAGGGAGTGAACCATG	698
	Reverse	TTGACCGTTGGAGCGCCACTT	
FR- α	Forward	AGGACAGACATGGCTCAGCGGA	396
	Reverse	TACCCGCTCTTTGCGCCAGC	
SMVT	Forward	AGGGCTGCAGCGGTTCTATT	774
	Reverse	GCAGCTTCCAGTTTTATGGTGGAG	

Table 7: qPCR primers for sodium-dependent vitamin transporter (SMVT), folate receptor (FR- α), and neutral and cationic amino acid transporter ($B^{0,+}$) sequence is given from 5'→3'

Gene		Sequence 5'→3'
SMVT	Forward	TACCAGTTCTGCCAGCCACAGTG
	Reverse	CAGGGACACCAAAACCTCCCTCT
FR-α	Forward	AGGACAGACATGGCTCAGCG
	Reverse	TGTGGTGCTTGGCGTTCATG
$B^{0,+}$	Forward	AGCCGAGGGAGTGAACCATG
	Reverse	GGACCAGTTACCACGGTCCT

7.2.5. Uptake experiments

Y-79 cells were collected following centrifugation and then washed three times with Dulbecco's phosphate-buffered saline (DPBS), pH 7.4, containing 130 mM NaCl, 0.03 mM KCl, 7.5 mM Na₂HPO₄, 1.5 mM KH₂PO₄, 1 mM CaCl₂, 0.5 mM Mg SO₄, and 5 mM glucose. Aliquots of approximately 5×10^6 cells were then pre-incubated in 1 ml DPBS for 10 min at 37 °C. Uptake was initiated by the addition of a fixed amount of [³H] Folic acid, [³H] Biotin and [¹⁴C] Arginine. Cells were incubated for 30 min at 37 °C. At the end of each experiment, tubes were immediately centrifuged, the solution was aspirated and cells were washed with 3×1 ml of ice-cold stop solution (210 mM KCl, 2 mM HEPES), pH 7.4, to arrest the reaction. Cells were then solubilized in 1 ml of 0.1% Triton-X solution in 1% NaOH and an aliquot was then transferred to vials containing 5 ml of scintillation cocktail. Radioactivity associated with the cells was quantified with a scintillation counter (Beckman Instruments Inc., Model LS-9000, Fullerton, CA) and protein content of each sample was measured by the methods of Bradford with bovine serum albumin as the standard (Bio-Rad protein estimation kit, Hercules, CA, USA). Cell viability under all treatment regimens was monitored by the Trypan blue exclusion test and was routinely observed to be between 90 and 95%. Similarly, uptake studies were carried out with 21-day old ARPE-19 cells. Following aspiration of the culture medium, cells were washed with DPBS thrice and uptake was performed as mentioned previously (Jwala et al., 2011). Following the above method, saturation kinetics of all the substrates was studied by performing the uptake in presence of various concentrations of unlabeled cold substrates.

7.2.6. Data analysis

Uptake data was fitted to a modified Michaelis–Menten equation. This equation takes into account the carrier-mediated process (as described by the classical Michaelis–Menten equation) and a linear non-saturable diffusion process.

$$V = \frac{V_{max} * [C]}{K_m + [C]}$$

V is the total rate of uptake, V_{max} represents the maximum uptake rate for the carrier-mediated process, K_m (Michaelis–Menten constant) is the concentration at half-saturation, C denotes substrate concentration. Data was fitted to above equation with a nonlinear least square regression analysis program (Kaleida Graph Version 3.09, Synergy Software, PA) and the kinetic parameters were calculated. Quality of the fit was determined by evaluating the coefficient of determination (R^2), the standard error of parameter estimates, and by visual inspection of the residuals.

7.2.7. Statistical analysis

All experiments were conducted at least six times and results were expressed as mean \pm S.D. Michaelis–Menten parameters such as K_m and V_{max} are expressed as mean \pm S.E. Unpaired Student's t-test was used to estimate statistical significance. A difference between mean values was considered significant if $p < 0.05$.

7.3. Results

7.3.1. RT-PCR analysis

The expression of the B^(0,+) in ARPE-19 and Y-79 cells at the mRNA level was determined by RT-PCR analysis. A major band (698 bp) corresponding to the amplified B^(0,+) precursor mRNA in ARPE-19 (Fig. 30) and Y-79 cells (Fig. 31) was observed in gel electrophoresis.

BLAST analysis showed that the primers used in this study can result in a PCR product size 698 bp by binding to the B^(0,+) precursor mRNA. Expression of FR- α in ARPE-19 and Y-79

cells at the mRNA level was determined by RT-PCR analysis. A major band (396 bp) corresponding to the amplified FR- α precursor mRNA in ARPE-19 (Fig. 36) and Y-79 cells (Fig. 37) were noted by gel electrophoresis. BLAST analysis indicated that the primers used in this study could result in a PCR product of 396 bp by binding to the FR- α precursor

mRNA. Similarly, the expression of SMVT in ARPE-19 and Y-79 cells at the mRNA level was also determined. A major band (774 bp) corresponding to the amplified SMVT precursor mRNA in ARPE-19 (Fig. 30) and Y-79 cells (Fig.31) was observed in gel electrophoresis.

BLAST analysis showed that the primers used in this study can result in a PCR product size 774 bp by binding to the SMVT precursor mRNA.

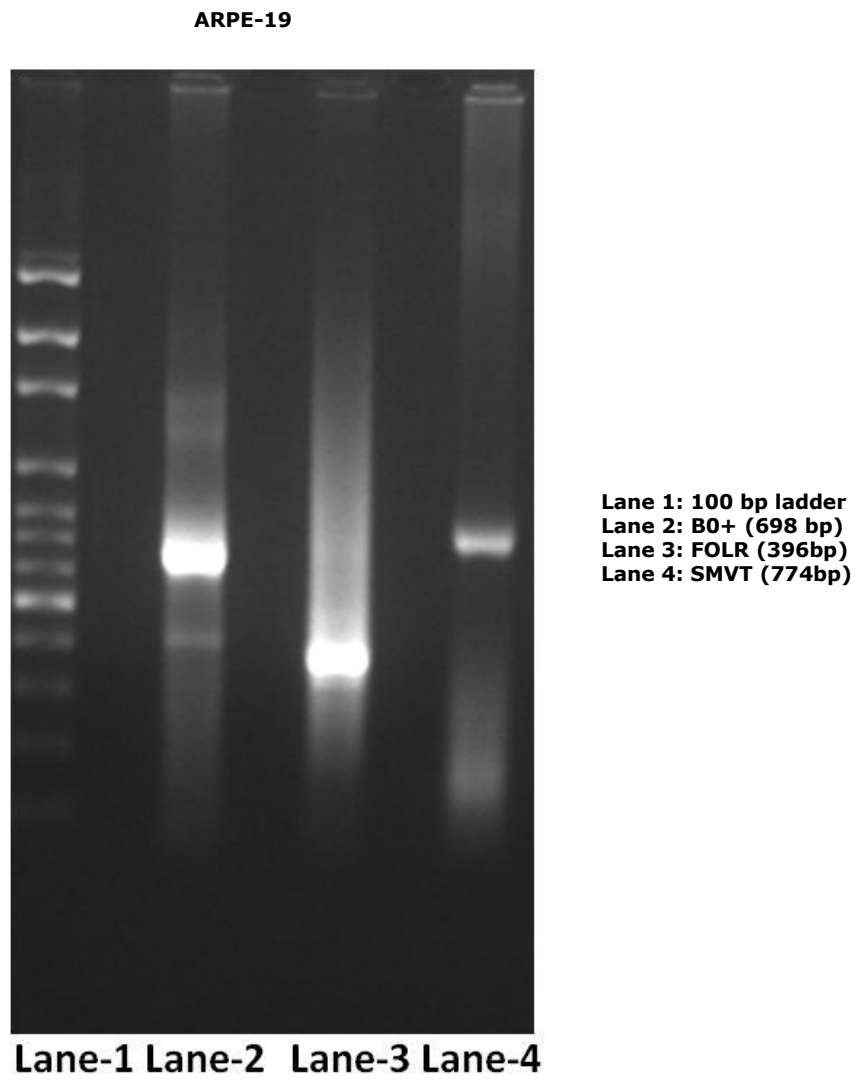
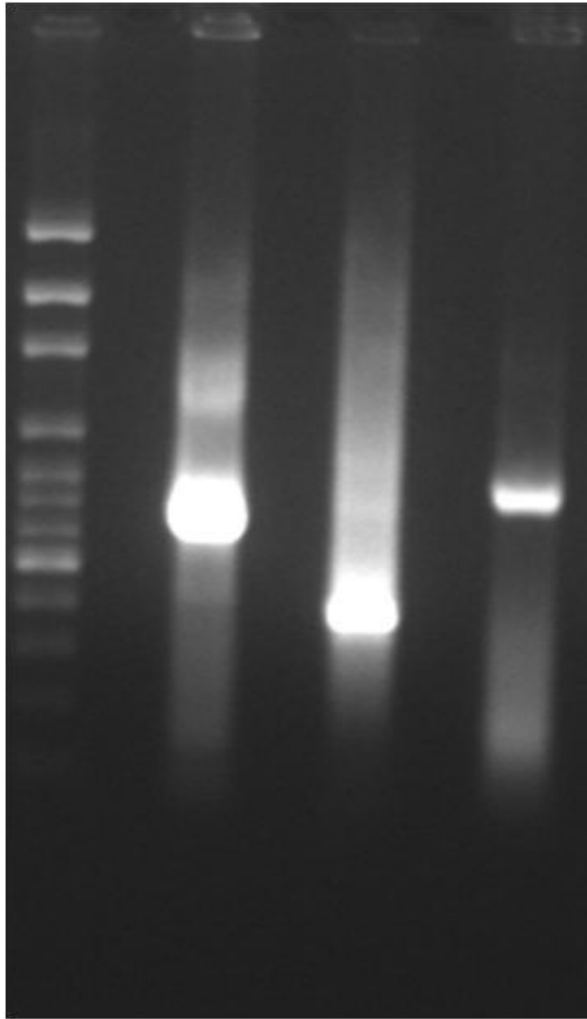


Fig. 30: Qualitative expression of B^(0,+), FR- α , and SMVT in ARPE-19 cells

Y-79



Lane-1: 100bp ladder
Lane-2: B⁰⁺ (698 bp)
Lane-3: FOLR (396 bp)
Lane-4: SMVT (774 bp)

Lane-1 Lane-2 Lane-3 Lane-4

Fig. 31: Qualitative expression of B^(0,+), FR- α , and SMVT in Y-79 cells

7.3.2. Quantitative real time PCR analysis

Quantitative real time PCR analysis was performed in order to compare the mRNA levels of B^(0,+), FR- α and SMVT in ARPE-19 and Y-79 cells. B^(0,+) expression at mRNA level was found to be 17 times higher in Y-79 than ARPE-19 cells. FR- α expression at mRNA level was found to be 3 times higher in Y-79 than ARPE-19 cells. SMVT mRNA expression level was 6 fold higher in Y-79 cells relative to ARPE-19 cells. These results clearly indicate the elevated expression of B^(0,+), FR- α and SMVT in Y-79 than ARPE-19 cells (Table 8, Fig.32).

7.3.3. Quantitative uptake of [³H] Biotin, [¹⁴C] Arginine and [³H] Folic acid, in ARPE-19 and Y-79 cells

Uptake of [³H] Biotin in ARPE-19 cells was also found to be significantly lower relative to Y-79 cells. This result indicates robust expression of SMVT in Y-79 retinoblastoma cells than normal ARPE-19 retinal cells. Uptake of [¹⁴C] Arginine in Y-79 cells was found to be significantly higher relative to ARPE-19 cells. This observation indicates high expression of B^(0,+) in Y-79 cancerous cells than normal ARPE-19 retinal cells. Similarly uptake of [³H] Folic acid in Y-79 cells was found to be significantly higher compared to ARPE-19 cells. This could be due to high expression of FR- α in Y-79 cells than ARPE-19 retinal cells (Fig. 33).

Table 8: Relative fold expression of SMVT, FR- α , B^(0,+) in ARPE-19 and Y-79 cells

	ARPE-19 cells	Y-79 cells
SMVT	1	6.31
FR-α	1	3.28
B^(0,+)	1	17.03

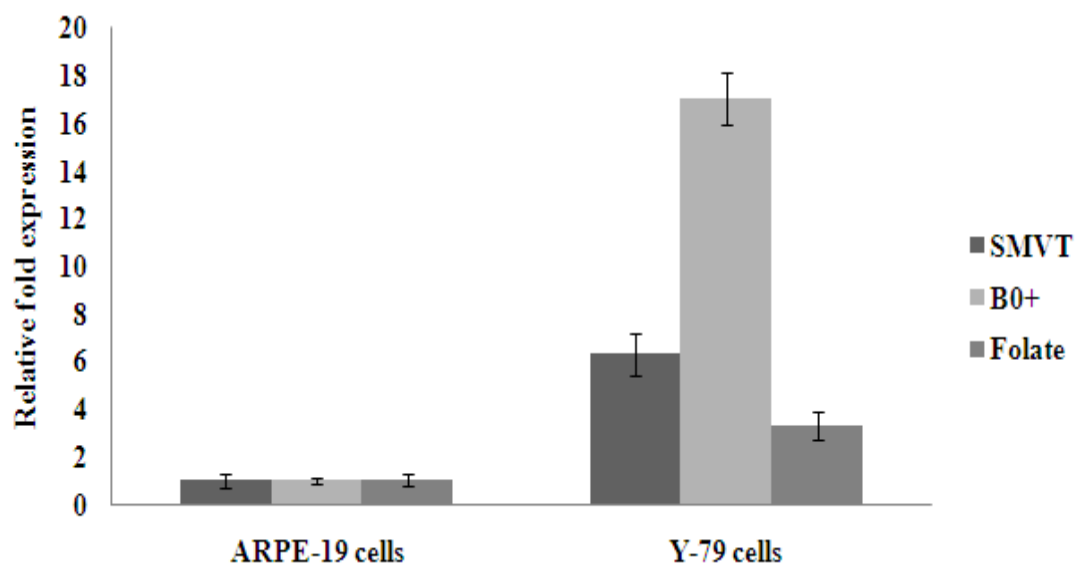


Fig. 32: Relative fold expression of SMVT, B^(0,+), FR- α , in ARPE-19 and Y-79 cells by quantitative real time PCR analysis

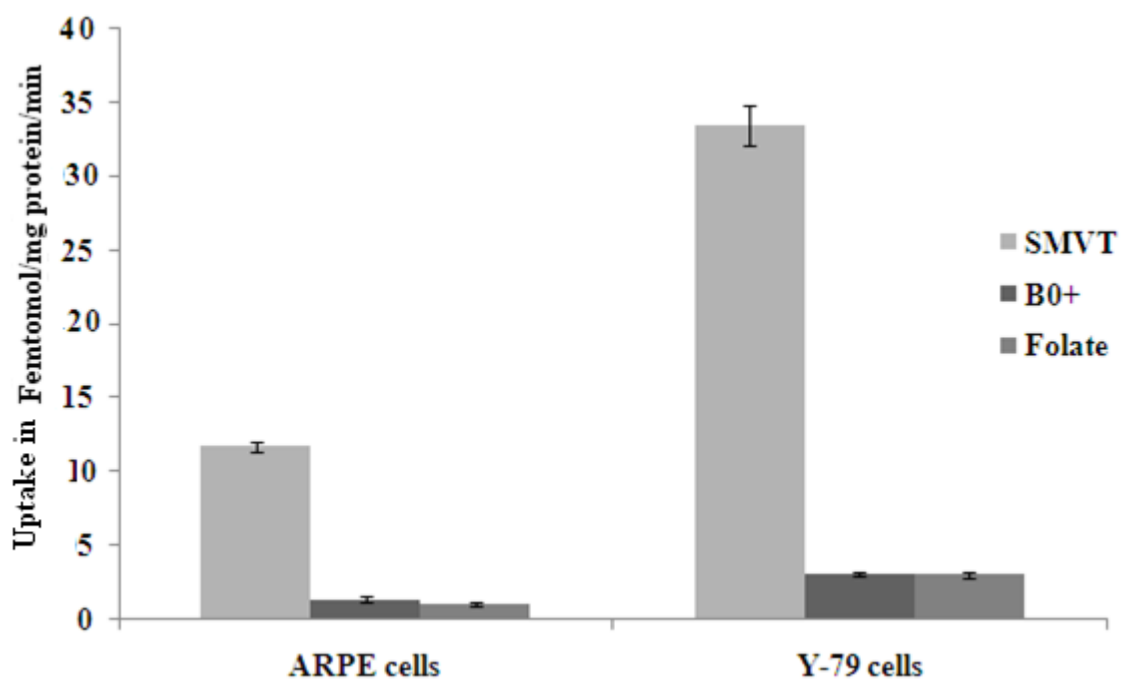


Fig. 33: Quantitative uptake of [³H] Folate, [³H] Biotin and [¹⁴C]Arginine in ARPE-19 and Y-79 cells

7.3.4. Concentration dependency of Folate in ARPE-19 cells

Uptake kinetics of a carrier-mediated system for folate in ARPE-19 cells was determined by evaluating the saturation kinetics of [³H] Folate in the presence of unlabeled folate. After fitting the data to modified Michaelis–Menten equation, an uptake process with apparent K_m of 0.08 μM and V_{max} of 0.49 pmol/min/mg protein was observed (Table 9, Fig. 34). Uptake kinetics of a carrier-mediated system for Folate in the Y-79 cell line was determined by Kansara et al, he evaluated the saturation kinetics of [³H] Folate in the presence of unlabeled folate. After fitting the data to modified Michaelis–Menten equation, an uptake process with apparent K_m of 0.0083 μM and V_{max} of 0.39 pmol/min/mg protein was obtained.

7.3.5. Concentration dependency of Biotin in ARPE-19 and Y-79 cells

Uptake kinetics of a carrier-mediated system for biotin in ARPE-19 cells was determined earlier from our lab (Janoria et al., 2009) by evaluating saturation kinetics of [³H] biotin in the presence of unlabeled biotin. After fitting the data to modified Michaelis–Menten equation, an uptake process with apparent K_m of 138.25 μM and V_{max} of 38.85 pmol/min/mg protein were obtained (Table 9). Uptake kinetics of a carrier-mediated system for biotin in Y-79 cells was determined by evaluating saturation kinetics of [³H] biotin in the presence of unlabeled biotin. After fitting the data to modified Michaelis–Menten equation, an uptake process with apparent K_m of 8.53 μM and V_{max} of 14.12 pmol/min/mg protein was obtained (Table 9).

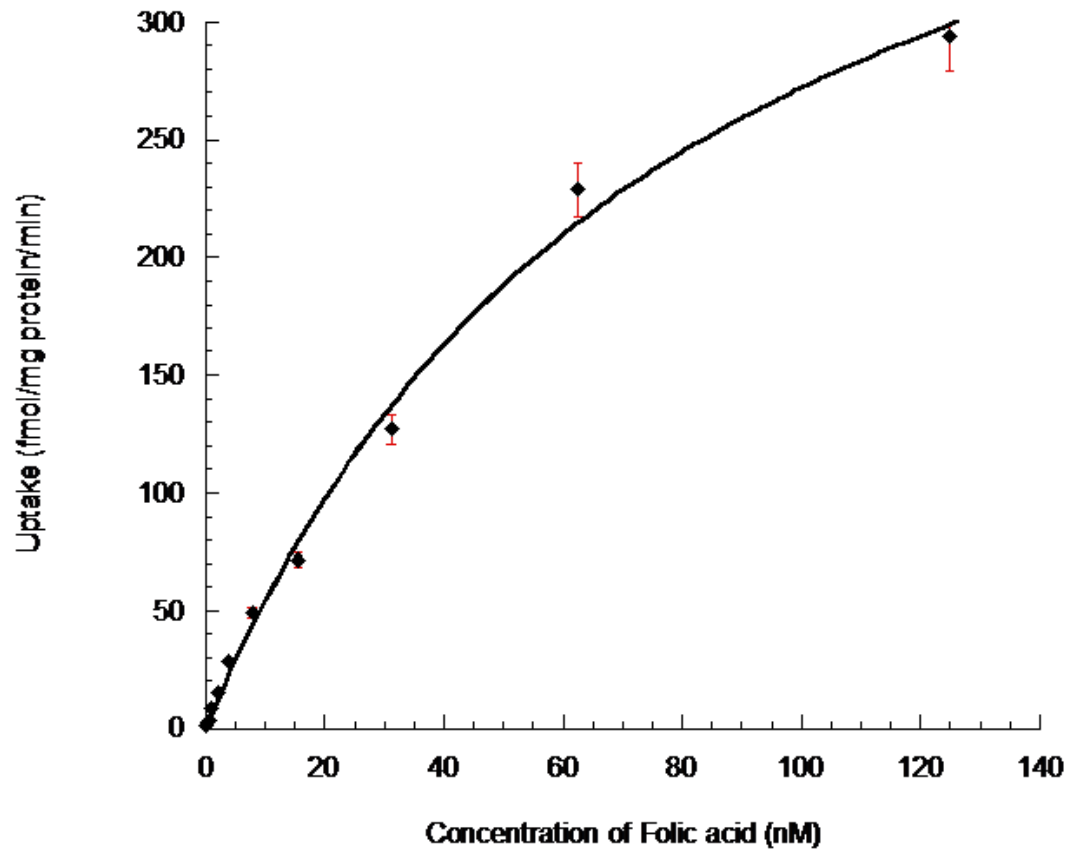


Fig. 34: Uptake of [³H] Folate by ARPE-19 cells as a function of substrate concentration at 37°C, pH 7.4. Each data point represents the mean ± S.D. of 4–6 separate uptake determinations.

7.3.6. Concentration dependency of Arginine in ARPE-19 and Y-79 cells

Uptake kinetics of a carrier-mediated system for Arginine in the ARPE-19 cells was determined by evaluating the saturation kinetics of [¹⁴C] Arginine in the presence of unlabeled arginine. After fitting the data to modified Michaelis–Menten equation, an uptake process with apparent K_m of 52.03 μM , V_{max} of 379.21 pmol/min/mg protein was observed (Table 9, Fig. 35). Uptake kinetics of a carrier-mediated system for Arginine in the Y-79 cells was determined by evaluating the uptake kinetics of [¹⁴C] Arginine in the presence of unlabeled arginine. After fitting the data to modified Michaelis–Menten equation, an uptake process with apparent K_m of 16.77 μM and V_{max} of 348.27 pmol/min/mg protein was obtained (Table 9, Fig. 36).

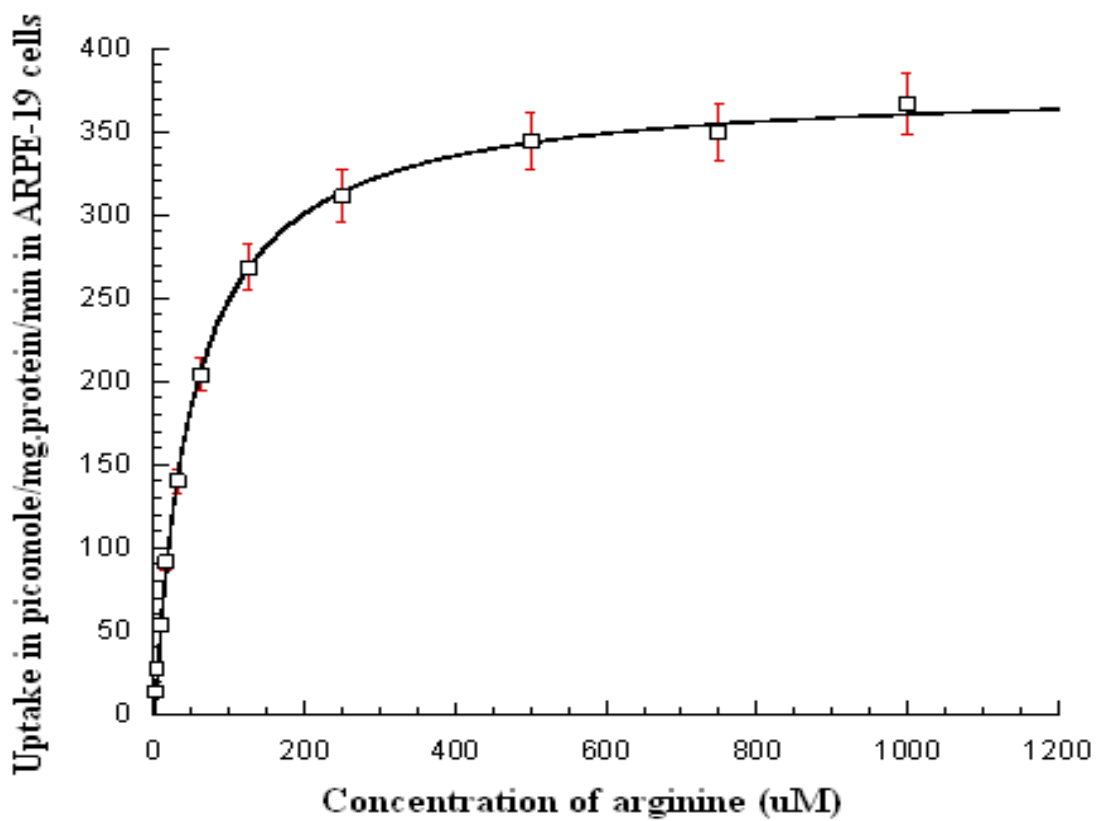


Fig. 35: Uptake of [^{14}C] Arginine by ARPE-19 cells as a function of substrate concentration at 37°C, pH 7.4. Each data point represents the mean \pm S.D. of 4–6 separate uptake determinations.

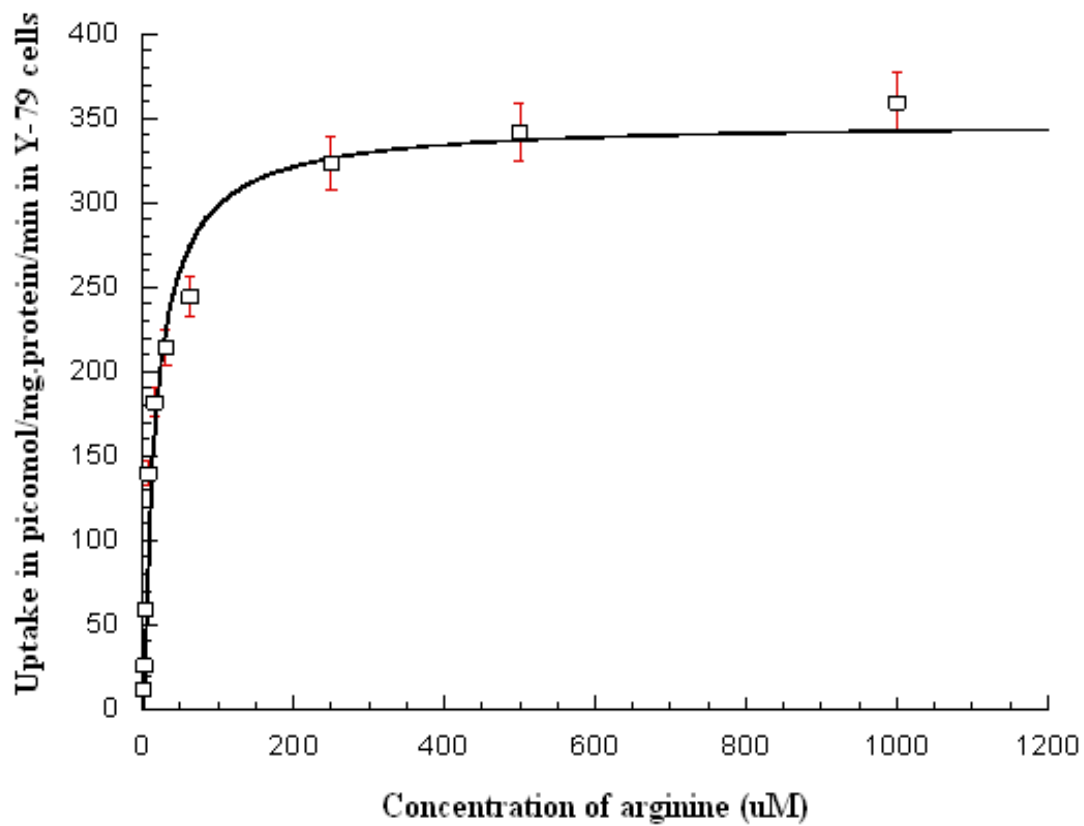


Fig. 36: Uptake of [^{14}C] Arginine by Y-79 cells as a function of substrate concentration at 37°C , pH 7.4. Each data point represents the mean \pm S.D. of 4–6 separate uptake determinations.

Table 9: K_m and V_{max} values of [3H] Biotin, [3H] Folate, and [^{14}C] Arginine in ARPE-19 and Y-79 cells

Carrier system	Cells	K_m (μM)	V_{max} (pmol/min/ mg protein)
SMVT	ARPE-19	138.25 \pm 2.5	38.85 \pm 1.9
	Y-79	8.53 \pm 1.2	14.12 \pm 1.2
FR-α	ARPE-19	0.080 \pm 0.002	0.49 \pm 0.03
	Y-79	0.0083 \pm 0.0007	0.39 \pm 0.009
B^(0,+)	ARPE-19	52.03 \pm 1.48	379.21 \pm 2.56
	Y-79	16.77 \pm 2.33	348.27 \pm 11.27

7.4. Discussion

Selective targeting reduces the minimum effective dose as well as associated toxicity and also enhances the therapeutic efficacy with equivalent plasma concentrations (Garcia-Bennett et al., 2011; Pan and Lee, 2004). Over expression of vitamin and amino acid transporters/receptors, by a variety of tumor cell lines may present an opportunity for targeted delivery of anticancer drugs for the treatment of various malignancies and diagnostic imaging. Most chemotherapeutic agents fail to enter tumor cells in therapeutic concentrations due to presence of efflux pumps (P-glycoprotein, multidrug resistance-associated protein, lung resistance-related protein, and breast cancer resistance protein) (Boddu et al., 2010a). Vitamins and amino acids as targeting moieties offer prospective advantages than macromolecules such as antibodies. These include: (a) small molecular size of the targeting moiety offers favorable pharmacokinetic properties and decreased probability of immunological reactions which allows chronic administration, (b) low cost and availability, (c) high affinity for receptors, (d) ligand can be internalized into tumor cells by endocytosis, which aids in cytosolic delivery of therapeutic agents, and (e) high frequency of expression among cancer cell lines with potential for future therapeutic and diagnostic applications (Sudimack and Lee, 2000).

Human retina is a delicate organization of neurons, glia and nourishing blood vessels. Biotin, an essential water soluble vitamin appears to play a critical role in cellular homeostasis and pathological conditions of retina including retinoblastoma. SMVT expressed on the retina, may be targeted following systemic and intravitreal administration to generate enhanced drug

availability in the retinal pigmented epithelium, choroid and Bruch's membrane. Amino acid transporters are widely expressed and contribute to uptake of neurotransmitters and nutrients (Uchiyama et al., 2008). B (0,+)⁻ is a sodium dependent neutral and cationic amino acid transporter. It transports over 20 proteinogenic amino acids. This transporter has the ability to translocate amino acids in their L-isomeric form and some in their D- isomeric form. The protein acts in an energy-dependent manner. This requires a combination of Na⁺ and Cl⁻ transmembrane gradient and membrane potential. The transporter can concentrate substrates 1000 fold more inside cells (Karunakaran et al., 2008). In addition to its amino acid transport, it can also transport carnitine, D-serine transporter, NOS (nitric oxide synthase) inhibitors, conjugated drugs and prodrugs. This property makes it unique among amino acid transporters (Ganapathy and Ganapathy, 2005). Furthermore, structural requirements for translocation are not very stringent. An absence of negative charge on the side chain of the amino acid is the only structural requirement. It is highly expressed in lung, colon and ocular tissues (Hatanaka et al., 2004; Jain-Vakkalagadda et al., 2004). These factors together offer a broad choice for the design of prodrugs.

The aim of this study was to evaluate the expression of B (0,+)⁻, FR- α and SMVT carrier systems in retinoblastoma Y-79 cells relative to normal retinal cells. Y-79 cell line was selected as a model system as it is derived from a tumor of the inner plexiform layer of the retina and has several membrane properties of the retina (Tombran-Tink et al., 1992). ARPE-19 cell line is yet another widely used human origin retinal cell line. ARPE-19 cells are similar to retinal pigment epithelium in terms of epithelial morphology, polarization and

expression of various ion channels, transporters, and RPE-specific markers (Janoria et al., 2009). RT-PCR analysis provided the preliminary evidence of the molecular expression of B^(0,+), FR- α and SMVT carrier systems in Y-79 and ARPE-19 cells. This was further confirmed by quantitative real time PCR which allows the quantification of gene expression. Quantitative uptake of [³H] Folic acid, [³H] Biotin and [¹⁴C] Arginine was significantly higher in Y-79 cells as compared to ARPE-19 cells. This could be attributed to the higher expression of B⁰⁺, FR- α and SMVT carrier systems in retinoblastoma cells than that of normal ARPE-19 cells. Tumor cells require a constant supply of nutrients for their uninterrupted growth and in order to facilitate the transport of nutrients, they express higher levels of nutrient transporters (Fuchs and Bode, 2005). Saturation kinetics of [³H] Folic acid, [³H] Biotin and [¹⁴C] Arginine was studied by performing the uptake in presence of various concentrations of unlabeled cold substrates. [³H]Folic acid uptake process followed saturation kinetics with apparent K_m of 80.55 nM and V_{max} of 491.86 fmol/min/ mg protein in ARPE-19 cells and K_m of 8.29 nM and V_{max} of 393.47 fmol/min/ mg protein in Y-79cells. [³H] Biotin uptake process also displayed saturation kinetics with K_m of 138.25 μ M and V_{max} of 38.85 pmol/min/mg protein in ARPE-19 cells and K_m of 8.53 μ M and V_{max} 14.12 pmol/min/mg protein in Y-79 cells. [¹⁴C] Arginine uptake process followed saturation kinetics with K_m of 52.03 μ M and V_{max} of 379.21 pmol/min/mg protein in ARPE-19 cells and K_m of 16.77 μ M and V_{max} of 348.27 pmol/min/mg protein in Y-79 cells. These results provide additional support for the presence and higher expression of B⁰⁺, folate and SMVT carrier systems in Y-79 cells. V_{max} and K_m are the two important parameters which define the

functional and kinetic behavior of a transporter protein as a function of substrate concentrations. K_m value represents the strength of binding and affinity of substrates. K_m value depends on several factors including substrate concentration, temperature and pH. K_m is a measure of apparent binding affinity of the respective substrate towards the transporter. Low K_m value indicates a tightly bound substrate, while loosely bound substrates have a high K_m values. V_{max} depends on the structure and concentration of the transporter protein and is a measure of the drug translocation capacity of the carrier system. Based on the saturation kinetics, the K_m values of [^3H] Folic acid, [^3H] Biotin and [^{14}C] Arginine were found to be relatively higher in Y-79 cells indicating the higher binding strength and affinity of substrates in cancerous cells. All of the results tend to suggest that FR- α , SMVT and B^(0,+) are over expressed in retinoblastoma Y-79 cells than normal retinal ARPE-19 cells. Enhanced expression of such transporters and receptors on retinoblastoma Y-79 cells may provide new opportunities for transporter-targeted prodrug design for enhanced drug delivery to treat retinoblastoma.

7.5. Conclusion

In conclusion, this is the first study showing the differential expression of specialized B^(0,+), FR- α and SMVT carrier systems in retinoblastoma Y-79 cells relative to ARPE-19 cells. Higher expression levels of B^(0,+), FR- α and SMVT carrier systems on retinoblastoma cells may be suitable for the design of surface modified nanoparticles and transporter-targeted prodrugs to achieve enhanced permeability for highly potent, but poorly bioavailable drugs.

A small increase in ocular bioavailability could significantly increase the therapeutic response of drugs.

CHAPTER 8

SUMMARY AND RECOMMENDATIONS

8.1. Summary

Drug delivery to the cornea is a clinically significant issue that challenges ophthalmologists and drug delivery scientists. The treatment of anterior segment diseases is challenging compared to other diseases because of various anatomical and physiological barriers. Anterior segment diseases are generally treated by topical eyedrops. Topical drug delivery is the most convenient method for drug administration to anterior segment of the eye. This method of administration provides numerous advantages such as ease of administration, non-invasive drug delivery, bypasses first-pass metabolism and provides local drug delivery (Davies, 2000). However, drugs in general fail to achieve required therapeutic concentrations in the eye following topical administration. It suffers from several disadvantages such as nasolachrymal drainage, loss in the conjunctival blood circulation, tear dilution, loss due to normal tear drainage, and reflux blinking (Fig. 2). Structural barriers like the corneal and conjunctival epithelia also limit drug concentrations in the anterior segment (Dey and Mitra, 2005).

There is an unmet need for the development of novel therapeutic strategies for the delivery of ophthalmic drugs without compromising patient comfort. Following topical administration drug molecules may exhibit varying corneal retention times depending on the molecular weight. Large linear (>40 kDa) and globular (> 70 kDa) molecules tend to have

longer retention times while small molecules exhibit shorter retention time requiring frequent administration.

In this dissertation project, I have provided proof of concept for a novel eye drop formulation controlled-release of LV-LV-ACV and LV-DV-ACV which can be indicated in the treatment of HSV corneal keratitis. LV-LV-ACV and LV-DV-ACV stereo isomeric peptide prodrug loaded nanoparticles suspended in thermosensitive gels can serve as an alternative to the current therapies like ointments, solution eye drops and implants. From the *in vitro* release studies I could observe a clear zero order release pattern of LV-LV-ACV and LV-DV-ACV from the formulations. With this formulation, ACV concentrations can be maintained well above the minimum effective concentrations for prolonged duration following single drop topical administration. Depending on the severity of inflammation various combinations of nanoparticles and thermosensitive gels (with varying molecular weights) loaded with LV-LV-ACV and LV-DV-ACV can be tailor made so as to match the dosing requirements of a patient.

8.2. Recommendations

During the last decade, drug loaded polymeric nanoparticles have gained significant of attention due to their improved properties such as: long shelf stability, high loading capacity, and ability to deliver both hydrophilic and hydrophobic molecules via peroral, transmucosal and inhalation routes. These nanoparticles have been successfully utilized for passive and active targeting of drugs. Active targeting aids in delivering therapeutic molecules to the site of action and hence minimizing its exposure to non-target regions. Active targeting can

potentially increase the efficacy and reduce the toxicity of therapeutic agents. This is achieved by prodrug derivatisation with cell specific ligands such as dipeptide which is a substrate for peptide transporter highly expressed on cornea. Transporter targeted delivery by a propeptide (peptide) appears to be a promising strategy for enhancing the ocular bioavailability since these peptide prodrugs have enhanced aqueous solubility as well as these compounds can serve as substrates for peptide transporters which are highly expressed on the cornea.

In this dissertation project I have successfully synthesized and characterized four peptide prodrugs of acyclovir (ACV) L-val-L-val-ACV, L-val-D-val-ACV, D-val-L-val-ACV and D-val-D-val-ACV. Transporter targeted delivery with a propeptide (peptide) was found to be a promising strategy for enhancing ocular bioavailability since these peptide prodrugs have enhanced aqueous solubility as well as serve as excellent substrates for peptide transporters which are highly expressed on the cornea. To sustain the release and protect these molecules against enzymatic degradation in the precorneal area we have encapsulated the prodrugs in various grades of PLGA polymeric nanoparticles. Prodrugs (L-val-L-val-ACV and L-val-D-val-ACV) loaded nanoparticles have been suspended in thermosensitive gelling polymers to prolong precorneal residence time of nanoparticles and also to minimize burst release of the prodrug from nanoparticles. These formulations will address the problems such as rapid precorneal elimination, tear turnover and drug loss through nasolacrimal drainage.

APPENDIX



RightsLink®

Home

Account
Info

Help



Title: Ocular Sustained Release Nanoparticles Containing Stereoisomeric Dipeptide Prodrugs of Acyclovir

Author: Jwala Jwala et al.

Publication: Journal of Ocular Pharmacology and Therapeutics

Publisher: Mary Ann Liebert, Inc. publishers

Date: Apr 1, 2011

Copyright © 2011, Mary Ann Liebert, Inc. publishers

Logged in as:
Jwala Jwals

LOGOUT

Author Reuse of Chart/Graph/Table or Text Excerpt

Please note Mary Ann Liebert, Inc. publishers does not require authors of the content being reused to obtain a license for their personal reuse of a figure, table, chart, or text excerpt.



Title: Novel Nanoparticulate Gel Formulations of Steroids for the Treatment of Macular Edema
Author: Sai H.S. Boddu et al.
Publication: Journal of Ocular Pharmacology and Therapeutics
Publisher: Mary Ann Liebert, Inc. publishers
Date: Feb 1, 2010
Copyright © 2010, Mary Ann Liebert, Inc. publishers

Logged in as:
Jwala Jwala
[LOGOUT](#)

Author Reuse of Chart/Graph/Table or Text Excerpt

Please note Mary Ann Liebert, Inc. publishers does not require authors of the content being reused to obtain a license for their personal reuse of a figure, table, chart, or text excerpt.

[BACK](#)

[CLOSE WINDOW](#)

Copyright © 2010 [Copyright Clearance Center, Inc.](#) All Rights Reserved. [Privacy statement.](#)
Comments? We would like to hear from you. E-mail us at customercare@copyright.com

REFERENCES

- Adibi, S.A. (1997). Renal assimilation of oligopeptides: physiological mechanisms and metabolic importance. *The American journal of physiology* 272, E723-736.
- Aerts, I., Lumbroso-Le Rouic, L., Gauthier-Villars, M., Brisse, H., Doz, F., and Desjardins, L. (2006). Retinoblastoma. *Orphanet J Rare Dis* 1, 31.
- Agarwal, S., Boddu, S.H., Jain, R., Samanta, S., Pal, D., and Mitra, A.K. (2008). Peptide prodrugs: improved oral absorption of lopinavir, a HIV protease inhibitor. *Int J Pharm* 359, 7-14.
- Ahmed, I., and Patton, T.F. (1985). Importance of the noncorneal absorption route in topical ophthalmic drug delivery. *Investigative ophthalmology & visual science* 26, 584-587.
- Al-Ghananeem, A.M., and Crooks, P.A. (2007). Phase I and phase II ocular metabolic activities and the role of metabolism in ophthalmic prodrug and codrug design and delivery. *Molecules (Basel, Switzerland)* 12, 373-388.
- Albert, D.M. (1987). Historic review of retinoblastoma. *Ophthalmology* 94, 654-662.
- Amaral, L., Engi, H., Viveiros, M., and Molnar, J. (2007). Review. Comparison of multidrug resistant efflux pumps of cancer and bacterial cells with respect to the same inhibitory agents. *In Vivo* 21, 237-244.
- Anand, B., Nashed, Y., and Mitra, A. (2003a). Novel dipeptide prodrugs of acyclovir for ocular herpes infections: Bioreversion, antiviral activity and transport across rabbit cornea. *Current eye research* 26, 151-163.
- Anand, B.S., Hill, J.M., Dey, S., Maruyama, K., Bhattacharjee, P.S., Myles, M.E., Nashed, Y.E., and Mitra, A.K. (2003b). In vivo antiviral efficacy of a dipeptide acyclovir prodrug, val-val-acyclovir, against HSV-1 epithelial and stromal keratitis in the rabbit eye model. *Investigative ophthalmology & visual science* 44, 2529-2534.
- Anand, B.S., Katragadda, S., Gunda, S., and Mitra, A.K. (2006). In vivo ocular pharmacokinetics of acyclovir dipeptide ester prodrugs by microdialysis in rabbits. *Molecular pharmaceutics* 3, 431-440.
- Anand, B.S., and Mitra, A.K. (2002). Mechanism of corneal permeation of L-valyl ester of acyclovir: targeting the oligopeptide transporter on the rabbit cornea. *Pharmaceutical research* 19, 1194-1202.
- Andersen, H., and Sander, B. (2003). The vitreous. In *Adler's physiology of the eye : clinical application*
- P.L. Kaufman, A. Alm, and F.H. Adler, eds. (St. Louis, Mosby), pp. 47-116.
- Anderson, R.G., Kamen, B.A., Rothberg, K.G., and Lacey, S.W. (1992). Potocytosis: sequestration and transport of small molecules by caveolae. *Science* 255, 410-411.
- Anumolu, S.S., Singh, Y., Gao, D., Stein, S., and Sinko, P.J. (2009). Design and evaluation of novel fast forming pilocarpine-loaded ocular hydrogels for sustained pharmacological response. *J Control Release* 137, 152-159.

Atluri, H., Anand, B.S., Patel, J., and Mitra, A.K. (2004). Mechanism of a model dipeptide transport across blood-ocular barriers following systemic administration. *Exp Eye Res* 78, 815-822.

Aukunuru, J.V., Sunkara, G., Bandi, N., Thoreson, W.B., and Kompella, U.B. (2001). Expression of multidrug resistance-associated protein (MRP) in human retinal pigment epithelial cells and its interaction with BAPSG, a novel aldose reductase inhibitor. *Pharmaceutical research* 18, 565-572.

Balakrishnan, A., Jain-Vakkalagadda, B., Yang, C., Pal, D., and Mitra, A.K. (2002). Carrier mediated uptake of L-tyrosine and its competitive inhibition by model tyrosine linked compounds in a rabbit corneal cell line (SIRC)--strategy for the design of transporter/receptor targeted prodrugs. *Int J Pharm* 247, 115-125.

Barratt, G.M. (2000). Therapeutic applications of colloidal drug carriers. *Pharm Sci Technol Today* 3, 163-171.

Bellamy, W.T. (1996). P-glycoproteins and multidrug resistance. *Annual review of pharmacology and toxicology* 36, 161-183.

Bishop, J.O., and Madson, E.C. (1975). Retinoblastoma. Review of the current status. *Surv Ophthalmol* 19, 342-366.

Boddu, S.H., Jwala, J., Chowdhury, M.R., and Mitra, A.K. (2010a). In vitro evaluation of a targeted and sustained release system for retinoblastoma cells using Doxorubicin as a model drug. *J Ocul Pharmacol Ther* 26, 459-468.

Boddu, S.H., Jwala, J., Vaishya, R., Earla, R., Karla, P.K., Pal, D., and Mitra, A.K. Novel nanoparticulate gel formulations of steroids for the treatment of macular edema. *J Ocul Pharmacol Ther* 26, 37-48.

Boddu, S.H., Jwala, J., Vaishya, R., Earla, R., Karla, P.K., Pal, D., and Mitra, A.K. (2010b). Novel nanoparticulate gel formulations of steroids for the treatment of macular edema. *J Ocul Pharmacol Ther* 26, 37-48.

Bourges, J.L., Gautier, S.E., Delie, F., Bejjani, R.A., Jeanny, J.C., Gurny, R., BenEzra, D., and Behar-Cohen, F.F. (2003). Ocular drug delivery targeting the retina and retinal pigment epithelium using polylactide nanoparticles. *Investigative ophthalmology & visual science* 44, 3562-3569.

Bozard, B.R., Ganapathy, P.S., Duplantier, J., Mysona, B., Ha, Y., Roon, P., Smith, R., Goldman, I.D., Prasad, P., Martin, P.M., *et al.* (2010). Molecular and biochemical characterization of folate transport proteins in retinal Muller cells. *Investigative ophthalmology & visual science* 51, 3226-3235.

Brandsch, M., Miyamoto, Y., Ganapathy, V., and Leibach, F.H. (1993). Regulation of taurine transport in human colon carcinoma cell lines (HT-29 and Caco-2) by protein kinase C. *The American journal of physiology* 264, G939-946.

Brubaker, R.F., Bourne, W.M., Bachman, L.A., and McLaren, J.W. (2000). Ascorbic acid content of human corneal epithelium. *Investigative ophthalmology & visual science* 41, 1681-1683.

- Brzezinska, A., Winska, P., and Balinska, M. (2000). Cellular aspects of folate and antifolate membrane transport. *Acta Biochim Pol* 47, 735-749.
- Chan, H.S., Gallie, B.L., Munier, F.L., and Beck Popovic, M. (2005). Chemotherapy for retinoblastoma. *Ophthalmol Clin North Am* 18, 55-63, viii.
- Chintagumpala, M., Chevez-Barrios, P., Paysse, E.A., Plon, S.E., and Hurwitz, R. (2007). Retinoblastoma: review of current management. *Oncologist* 12, 1237-1246.
- Christensen, M.T., Cohen, S., Rinehart, J., Akers, F., Pemberton, B., Bloomenstein, M., Leshner, M., Kaplan, D., Meadows, D., Meuse, P., *et al.* (2004). Clinical evaluation of an HP-guar gellable lubricant eye drop for the relief of dryness of the eye. *Current eye research* 28, 55-62.
- Civan, M.M., and Macknight, A.D. (2004). The ins and outs of aqueous humour secretion. *Exp Eye Res* 78, 625-631.
- Constable, P.A., Lawrenson, J.G., Dolman, D.E., Arden, G.B., and Abbott, N.J. (2006). P-Glycoprotein expression in human retinal pigment epithelium cell lines. *Exp Eye Res* 83, 24-30.
- Cortesi, R., and Esposito, E. (2008). Acyclovir delivery systems. *Expert opinion on drug delivery* 5, 1217-1230.
- Davies, N.M. (2000). Biopharmaceutical considerations in topical ocular drug delivery. *Clin Exp Pharmacol Physiol* 27, 558-562.
- de Campos, A.M., Diebold, Y., Carvalho, E.L., Sanchez, A., and Alonso, M.J. (2004). Chitosan nanoparticles as new ocular drug delivery systems: in vitro stability, in vivo fate, and cellular toxicity. *Pharmaceutical research* 21, 803-810.
- De Potter, P. (2002). Current treatment of retinoblastoma. *Curr Opin Ophthalmol* 13, 331-336.
- Dean, M., Fojo, T., and Bates, S. (2005). Tumour stem cells and drug resistance. *Nat Rev Cancer* 5, 275-284.
- Dean, M., Rzhetsky, A., and Allikmets, R. (2001). The human ATP-binding cassette (ABC) transporter superfamily. *Genome research* 11, 1156-1166.
- Dey, S., and Mitra, A.K. (2005). Transporters and receptors in ocular drug delivery: opportunities and challenges. *Expert opinion on drug delivery* 2, 201-204.
- Dey, S., Patel, J., Anand, B.S., Jain-Vakkalagadda, B., Kaliki, P., Pal, D., Ganapathy, V., and Mitra, A.K. (2003). Molecular evidence and functional expression of P-glycoprotein (MDR1) in human and rabbit cornea and corneal epithelial cell lines. *Investigative ophthalmology & visual science* 44, 2909-2918.
- Dias, C., Nashed, Y., Atluri, H., and Mitra, A. (2002). Ocular penetration of acyclovir and its peptide prodrugs valacyclovir and val-valacyclovir following systemic administration in rabbits: An evaluation using ocular microdialysis and LC-MS. *Current eye research* 25, 243-252.
- Dingeldein, S.A., and Klyce, S.D. (1988). Imaging of the cornea. *Cornea* 7, 170-182.
- Doukas, J., Mahesh, S., Umeda, N., Kachi, S., Akiyama, H., Yokoi, K., Cao, J., Chen, Z., Dellamary, L., Tam, B., *et al.* (2008). Topical administration of a multi-targeted kinase

inhibitor suppresses choroidal neovascularization and retinal edema. *Journal of cellular physiology*.

Duvvuri, S., Janoria, K.G., and Mitra, A.K. (2005). Development of a novel formulation containing poly(D,L-lactide-co-glycolide) microspheres dispersed in PLGA-PEG-PLGA gel for sustained delivery of ganciclovir. *J Control Release* 108, 282-293.

Eng, C., Li, F.P., Abramson, D.H., Ellsworth, R.M., Wong, F.L., Goldman, M.B., Seddon, J., Tarbell, N., and Boice, J.D., Jr. (1993). Mortality from second tumors among long-term survivors of retinoblastoma. *J Natl Cancer Inst* 85, 1121-1128.

Eytan, G.D., and Kuchel, P.W. (1999). Mechanism of action of P-glycoprotein in relation to passive membrane permeation. *International review of cytology* 190, 175-250.

Falcon, M.G. (1983). Herpes simplex virus infections of the eye and their management with acyclovir. *J Antimicrob Chemother* 12 Suppl B, 39-43.

Feschenko, M.S., Stevenson, E., and Sweadner, K.J. (2000). Interaction of protein kinase C and cAMP-dependent pathways in the phosphorylation of the Na,K-ATPase. *The Journal of biological chemistry* 275, 34693-34700.

File, R.R., and Patton, T.F. (1980). Topically applied pilocarpine. Human pupillary response as a function of drop size. *Arch Ophthalmol* 98, 112-115.

Fraunfelder, F.T., and Meyer, S.M. (1987). Systemic reactions to ophthalmic drug preparations. *Med Toxicol Adverse Drug Exp* 2, 287-293.

Friesner, R.A., Banks, J.L., Murphy, R.B., Halgren, T.A., Klicic, J.J., Mainz, D.T., Repasky, M.P., Knoll, E.H., Shelley, M., Perry, J.K., *et al.* (2004). Glide: a new approach for rapid, accurate docking and scoring. 1. Method and assessment of docking accuracy. *J Med Chem* 47, 1739-1749.

Frishman, W.H., Kowalski, M., Nagnur, S., Warshafsky, S., and Sica, D. (2001). Cardiovascular considerations in using topical, oral, and intravenous drugs for the treatment of glaucoma and ocular hypertension: focus on beta-adrenergic blockade. *Heart Dis* 3, 386-397.

Fuchs, B.C., and Bode, B.P. (2005). Amino acid transporters ASCT2 and LAT1 in cancer: partners in crime? *Semin Cancer Biol* 15, 254-266.

Fukasawa, Y., Segawa, H., Kim, J.Y., Chairoungdua, A., Kim, D.K., Matsuo, H., Cha, S.H., Endou, H., and Kanai, Y. (2000). Identification and characterization of a Na(+)-independent neutral amino acid transporter that associates with the 4F2 heavy chain and exhibits substrate selectivity for small neutral D- and L-amino acids. *The Journal of biological chemistry* 275, 9690-9698.

Ganapathy, M.E., and Ganapathy, V. (2005). Amino Acid Transporter ATB0,+ as a delivery system for drugs and prodrugs. *Current drug targets* 5, 357-364.

Ganapathy, V., and Leibach, F.H. (1982). Peptide transport in intestinal and renal brush border membrane vesicles. *Life Sci* 30, 2137-2146.

Gandhi, M.D., Pal, D., and Mitra, A.K. (2004). Identification and functional characterization of a Na(+)-independent large neutral amino acid transporter (LAT2) on ARPE-19 cells. *Int J Pharm* 275, 189-200.

Garcia-Bennett, A., Nees, M., and Fadeel, B. In search of the Holy Grail: Folate-targeted nanoparticles for cancer therapy. *Biochem Pharmacol* 81, 976-984.

Garcia-Bennett, A., Nees, M., and Fadeel, B. (2011). In search of the Holy Grail: Folate-targeted nanoparticles for cancer therapy. *Biochem Pharmacol* 81, 976-984.

Gaudana, R., Jwala, J., Boddu, S.H., and Mitra, A.K. (2009). Recent perspectives in ocular drug delivery. *Pharmaceutical research* 26, 1197-1216.

Ghate, D., and Edelhauser, H.F. (2006). Ocular drug delivery. *Expert opinion on drug delivery* 3, 275-287.

Giordano, G.G., Chevez-Barrios, P., Refojo, M.F., and Garcia, C.A. (1995). Biodegradation and tissue reaction to intravitreal biodegradable poly(D,L-lactic-co-glycolic)acid microspheres. *Current eye research* 14, 761-768.

Glide 5.5, User Manual, and Schrödinger, L., New York, NY, 2010.

Glide, version 5.5, and Schrödinger, L., New York, NY, 2010.

Golnik, K.C., and Schaible, E.R. (1994). Folate-responsive optic neuropathy. *J Neuroophthalmol* 14, 163-169.

Goskonda, V.R., Hill, R.A., Khan, M.A., and Reddy, I.K. (2000). Permeability of chemical delivery systems across rabbit corneal (SIRC) cell line and isolated corneas: a comparative study. *Pharm Dev Technol* 5, 409-416.

Gottesman, M.M., and Pastan, I. (1993). Biochemistry of multidrug resistance mediated by the multidrug transporter. *Annual review of biochemistry* 62, 385-427.

Gray, H., and Carter, H.V. (1991). *Anatomy, descriptive and surgical* (St. Louis, Mosby Year Book).

Gulsen, D., and Chauhan, A. (2004). Ophthalmic drug delivery through contact lenses. *Investigative ophthalmology & visual science* 45, 2342-2347.

Gunda, S., Hariharan, S., and Mitra, A.K. (2006). Corneal absorption and anterior chamber pharmacokinetics of dipeptide monoester prodrugs of ganciclovir (GCV): in vivo comparative evaluation of these prodrugs with Val-GCV and GCV in rabbits. *J Ocul Pharmacol Ther* 22, 465-476.

Gupta, H., Jain, S., Mathur, R., Mishra, P., Mishra, A.K., and Velpandian, T. (2007). Sustained ocular drug delivery from a temperature and pH triggered novel in situ gel system. *Drug Deliv* 14, 507-515.

Gupta, S., and Samanta, M.K. (2009). Design and evaluation of thermoreversible in situ gelling system of forskolin for the treatment of glaucoma. *Pharm Dev Technol*.

Gupta, S.K. (1986). Efficacy of miconazole in experimental keratomycosis. *Aust N Z J Ophthalmol* 14, 373-376.

Hamid, A., and Kaur, J. (2009). Role of signaling pathways in the regulation of folate transport in ethanol-fed rats. *J Nutr Biochem* 20, 291-297.

Hariharan, S., Janoria, K.G., Gunda, S., Zhu, X., Pal, D., and Mitra, A.K. (2006). Identification and functional expression of a carrier-mediated riboflavin transport system on rabbit corneal epithelium. *Current eye research* 31, 811-824.

Hassan, M.A. (2007). A long acting ophthalmic gel formulations of atenolol. *Drug Dev Ind Pharm* 33, 1192-1198.

Hatanaka, T., Haramura, M., Fei, Y.J., Miyauchi, S., Bridges, C.C., Ganapathy, P.S., Smith, S.B., Ganapathy, V., and Ganapathy, M.E. (2004). Transport of amino acid-based prodrugs by the Na⁺- and Cl⁻-coupled amino acid transporter ATB^{0,+} and expression of the transporter in tissues amenable for drug delivery. *J Pharmacol Exp Ther* 308, 1138-1147.

HF., E., and JL., U. (2003). The cornea and sclera. In *Adler's physiology of the eye : clinical application*, P.L. Kaufman, A. Alm, and F.H. Adler, eds. (St. Louis, Mosby), pp. 47-114.

Holash, J.A., and Stewart, P.A. (1993). The relationship of astrocyte-like cells to the vessels that contribute to the blood-ocular barriers. *Brain research* 629, 218-224.

Hsu, P.P., and Sabatini, D.M. (2008). Cancer cell metabolism: Warburg and beyond. *Cell* 134, 703-707.

<http://www.uniprot.org/uniprot/P36836>.

Hughes, P.M., and Mitra, A.K. (1993). Effect of acylation on the ocular disposition of acyclovir. II: Corneal permeability and anti-HSV 1 activity of 2'-esters in rabbit epithelial keratitis. *J Ocul Pharmacol* 9, 299-309.

Inoue, K., Nakai, Y., Ueda, S., Kamigaso, S., Ohta, K.Y., Hatakeyama, M., Hayashi, Y., Otagiri, M., and Yuasa, H. (2008). Functional characterization of PCFT/HCP1 as the molecular entity of the carrier-mediated intestinal folate transport system in the rat model. *Am J Physiol Gastrointest Liver Physiol* 294, G660-668.

Jabs, D.A. (1998). Acyclovir for recurrent herpes simplex virus ocular disease. *N Engl J Med* 339, 340-341.

Jain-Vakkalagadda, B., Dey, S., Pal, D., and Mitra, A.K. (2003). Identification and functional characterization of a Na⁺-independent large neutral amino acid transporter, LAT1, in human and rabbit cornea. *Investigative ophthalmology & visual science* 44, 2919-2927.

Jain-Vakkalagadda, B., Pal, D., Gunda, S., Nashed, Y., Ganapathy, V., and Mitra, A.K. (2004). Identification of a Na⁺-dependent cationic and neutral amino acid transporter, B^{0,+}, in human and rabbit cornea. *Molecular pharmaceuticals* 1, 338-346.

Janoria, K.G., Boddu, S.H., Wang, Z., Paturi, D.K., Samanta, S., Pal, D., and Mitra, A.K. (2009). Vitreal pharmacokinetics of biotinylated ganciclovir: role of sodium-dependent multivitamin transporter expressed on retina. *J Ocul Pharmacol Ther* 25, 39-49.

Janoria, K.G., Gunda, S., Boddu, S.H., and Mitra, A.K. (2007). Novel approaches to retinal drug delivery. *Expert opinion on drug delivery* 4, 371-388.

Janoria, K.G., Hariharan, S., Paturi, D., Pal, D., and Mitra, A.K. (2006). Biotin uptake by rabbit corneal epithelial cells: role of sodium-dependent multivitamin transporter (SMVT). *Current eye research* 31, 797-809.

Janoria, K.G., and Mitra, A.K. (2007). Effect of lactide/glycolide ratio on the in vitro release of ganciclovir and its lipophilic prodrug (GCV-monobutyrate) from PLGA microspheres. *Int J Pharm* 338, 133-141.

Jorgensen, W., and Tirado-Rives, J. (1988). The OPLS Force Field for Proteins. Energy Minimizations for Crystals of Cyclic Peptides and Crambin. *J Am Chem Soc* *110*, 1657-1666.

Juntunen, J., Jarvinen, T., and Niemi, R. (2005). In-vitro corneal permeation of cannabinoids and their water-soluble phosphate ester prodrugs. *J Pharm Pharmacol* *57*, 1153-1157.

Jwala, J., Boddu, S.H., Paturi, D.K., Shah, S., Smith, S.B., Pal, D., and Mitra, A.K. (2011). Functional characterization of folate transport proteins in Staten's Seruminstitut rabbit corneal epithelial cell line. *Current eye research* *36*, 404-416.

Kamen, B.A., Wang, M.T., Streckfuss, A.J., Peryea, X., and Anderson, R.G. (1988). Delivery of folates to the cytoplasm of MA104 cells is mediated by a surface membrane receptor that recycles. *The Journal of biological chemistry* *263*, 13602-13609.

Kanai, Y., and Hediger, M.A. (2004). The glutamate/neutral amino acid transporter family SLC1: molecular, physiological and pharmacological aspects. *Pflugers Arch* *447*, 469-479.

Kansara, V., Hao, Y., and Mitra, A.K. (2007). Dipeptide monoester ganciclovir prodrugs for transscleral drug delivery: targeting the oligopeptide transporter on rabbit retina. *J Ocul Pharmacol Ther* *23*, 321-334.

Kansara, V., Luo, S., Balasubrahmanyam, B., Pal, D., and Mitra, A.K. (2006). Biotin uptake and cellular translocation in human derived retinoblastoma cell line (Y-79): a role of hSMVT system. *Int J Pharm* *312*, 43-52.

Kansara, V., Pal, D., Jain, R., and Mitra, A.K. (2005). Identification and functional characterization of riboflavin transporter in human-derived retinoblastoma cell line (Y-79): mechanisms of cellular uptake and translocation. *J Ocul Pharmacol Ther* *21*, 275-287.

Kansara, V., Paturi, D., Luo, S., Gaudana, R., and Mitra, A.K. (2008). Folic acid transport via high affinity carrier-mediated system in human retinoblastoma cells. *Int J Pharm* *355*, 210-219.

Karla, P.K., Earla, R., Boddu, S.H., Johnston, T.P., Pal, D., and Mitra, A. (2009). Molecular expression and functional evidence of a drug efflux pump (BCRP) in human corneal epithelial cells. *Current eye research* *34*, 1-9.

Karla, P.K., Pal, D., and Mitra, A.K. (2007a). Molecular evidence and functional expression of multidrug resistance associated protein (MRP) in rabbit corneal epithelial cells. *Exp Eye Res* *84*, 53-60.

Karla, P.K., Pal, D., Quinn, T., and Mitra, A.K. (2007b). Molecular evidence and functional expression of a novel drug efflux pump (ABCC2) in human corneal epithelium and rabbit cornea and its role in ocular drug efflux. *Int J Pharm* *336*, 12-21.

Kartner, N., Evernden-Porelle, D., Bradley, G., and Ling, V. (1985). Detection of P-glycoprotein in multidrug-resistant cell lines by monoclonal antibodies. *Nature* *316*, 820-823.

Karunakaran, S., Umopathy, N.S., Thangaraju, M., Hatanaka, T., Itagaki, S., Munn, D.H., Prasad, P.D., and Ganapathy, V. (2008). Interaction of tryptophan derivatives with SLC6A14 (ATB0,+) reveals the potential of the transporter as a drug target for cancer chemotherapy. *Biochem J* *414*, 343-355.

Katragadda, S., Gunda, S., Hariharan, S., and Mitra, A.K. (2008). Ocular pharmacokinetics of acyclovir amino acid ester prodrugs in the anterior chamber: evaluation of their utility in treating ocular HSV infections. *Int J Pharm* 359, 15-24.

Katragadda, S., Talluri, R.S., and Mitra, A.K. (2006). Modulation of P-glycoprotein-mediated efflux by prodrug derivatization: an approach involving peptide transporter-mediated influx across rabbit cornea. *J Ocul Pharmacol Ther* 22, 110-120.

Katragadda, S., Talluri, R.S., Pal, D., and Mitra, A.K. (2005). Identification and characterization of a Na⁺-dependent neutral amino acid transporter, ASCT1, in rabbit corneal epithelial cell culture and rabbit cornea. *Current eye research* 30, 989-1002.

Kaur, I.P., and Kanwar, M. (2002). Ocular preparations: the formulation approach. *Drug Dev Ind Pharm* 28, 473-493.

Kitagawa, K., Fukuda, M., and Sasaki, K. (1989). Intraocular penetration of topically administered acyclovir. *Lens Eye Toxic Res* 6, 365-373.

Kruh, G.D., Guo, Y., Hopper-Borge, E., Belinsky, M.G., and Chen, Z.S. (2007). ABCC10, ABCC11, and ABCC12. *Pflugers Arch* 453, 675-684.

Kumar, C.K., Moyer, M.P., Dudeja, P.K., and Said, H.M. (1997). A protein-tyrosine kinase-regulated, pH-dependent, carrier-mediated uptake system for folate in human normal colonic epithelial cell line NCM460. *The Journal of biological chemistry* 272, 6226-6231.

Kyritsis, A.P., Tsokos, M., Triche, T.J., and Chader, G.J. (1984). Retinoblastoma--origin from a primitive neuroectodermal cell? *Nature* 307, 471-473.

Lallemant, F., Varesio, E., Felt-Baeyens, O., Bossy, L., Hopfgartner, G., and Gurny, R. (2007). Biological conversion of a water-soluble prodrug of cyclosporine A. *Eur J Pharm Biopharm* 67, 555-561.

Lentz, K.A., Hayashi, J., Lucisano, L.J., and Polli, J.E. (2000). Development of a more rapid, reduced serum culture system for Caco-2 monolayers and application to the biopharmaceutics classification system. *Int J Pharm* 200, 41-51.

Li, B., Gao, R., Zhang, H., Li, L.Q., Gao, F., and Ren, R.J. (2009). [Studies on multidrug resistance associated protein in retinoblastoma]. *Zhonghua Yan Ke Za Zhi* 45, 314-317.

Li, V.H., Wood, R.W., Kreuter, J., Harmia, T., and Robinson, J.R. (1986). Ocular drug delivery of progesterone using nanoparticles. *J Microencapsul* 3, 213-218.

Liang, W.J., Johnson, D., and Jarvis, S.M. (2001). Vitamin C transport systems of mammalian cells. *Molecular membrane biology* 18, 87-95.

Liesegang, T.J. (1988). Ocular herpes simplex infection: pathogenesis and current therapy. *Mayo Clin Proc* 63, 1092-1105.

Ligprep, version 2.3, and Schrödinger, L., New York, NY, 2010.

Liu, Z., Li, J., Nie, S., Liu, H., Ding, P., and Pan, W. (2006). Study of an alginate/HPMC-based in situ gelling ophthalmic delivery system for gatifloxacin. *Int J Pharm* 315, 12-17.

Lofors, K.T., Hovding, G., Viksmoen, L., Aasved, H., Bergaust, B., and Bulie, T. (1990). Twelve-hour IOP control obtained by a single dose of timolol/pilocarpine combination eye drops. *Acta Ophthalmol (Copenh)* 68, 323-326.

Luo, S., Kansara, V.S., Zhu, X., Mandava, N.K., Pal, D., and Mitra, A.K. (2006). Functional characterization of sodium-dependent multivitamin transporter in MDCK-MDR1 cells and its utilization as a target for drug delivery. *Molecular pharmaceutics* 3, 329-339.

Maestro, version 9.0, and Schrödinger, L., New York, NY, 2010.

Majumdar, S., Nashed, Y.E., Patel, K., Jain, R., Itahashi, M., Neumann, D.M., Hill, J.M., and Mitra, A.K. (2005). Dipeptide monoester ganciclovir prodrugs for treating HSV-1-induced corneal epithelial and stromal keratitis: in vitro and in vivo evaluations. *J Ocul Pharmacol Ther* 21, 463-474.

Mantyč, G.J., Hageman, G.S., and Devaskar, S.U. (1993). Characterization of glucose transporter isoforms in the adult and developing human eye. *Endocrinology* 133, 600-607.

Matherly, L.H., and Goldman, D.I. (2003). Membrane transport of folates. *Vitam Horm* 66, 403-456.

Meredith, D., and Price, R.A. (2006). Molecular modeling of PepT1--towards a structure. *J Membr Biol* 213, 79-88.

Merriman-Smith, R., Donaldson, P., and Kistler, J. (1999). Differential expression of facilitative glucose transporters GLUT1 and GLUT3 in the lens. *Investigative ophthalmology & visual science* 40, 3224-3230.

Mishima, S., Gasset, A., Klyce, S.D., Jr., and Baum, J.L. (1966). Determination of tear volume and tear flow. *Invest Ophthalmol* 5, 264-276.

Muller, U., Brandsch, M., Prasad, P.D., Fei, Y.J., Ganapathy, V., and Leibach, F.H. (1996). Inhibition of the H⁺/peptide cotransporter in the human intestinal cell line Caco-2 by cyclic AMP. *Biochem Biophys Res Commun* 218, 461-465.

Nambu, H., Nambu, R., Melia, M., and Campochiaro, P.A. (2003). Combretastatin A-4 phosphate suppresses development and induces regression of choroidal neovascularization. *Investigative ophthalmology & visual science* 44, 3650-3655.

Nanjawade, B.K., Manvi, F.V., and Manjappa, A.S. (2007). In situ-forming hydrogels for sustained ophthalmic drug delivery. *J Control Release* 122, 119-134.

Nashed, Y.E., and Mitra, A.K. (2003). Synthesis and characterization of novel dipeptide ester prodrugs of acyclovir. *Spectrochim Acta A Mol Biomol Spectrosc* 59, 2033-2039.

Nguyen, T.T., Dyer, D.L., Dunning, D.D., Rubin, S.A., Grant, K.E., and Said, H.M. (1997). Human intestinal folate transport: cloning, expression, and distribution of complementary RNA. *Gastroenterology* 112, 783-791.

Ocheltree, S.M., Keep, R.F., Shen, H., Yang, D., Hughes, B.A., and Smith, D.E. (2003). Preliminary investigation into the expression of proton-coupled oligopeptide transporters in neural retina and retinal pigment epithelium (RPE): lack of functional activity in RPE plasma membranes. *Pharmaceutical research* 20, 1364-1372.

Pan, X., and Lee, R.J. (2004). Tumour-selective drug delivery via folate receptor-targeted liposomes. *Expert opinion on drug delivery* 1, 7-17.

Parkin, D.M., Stiller, C.A., Draper, G.J., and Bieber, C.A. (1988). The international incidence of childhood cancer. *Int J Cancer* 42, 511-520.

- Pesin, S.R., and Shields, J.A. (1989). Seven cases of trilateral retinoblastoma. *Am J Ophthalmol* 107, 121-126.
- Prasad, P.D., Ramamoorthy, S., Leibach, F.H., and Ganapathy, V. (1995). Molecular cloning of the human placental folate transporter. *Biochem Biophys Res Commun* 206, 681-687.
- Prausnitz, M.R., and Noonan, J.S. (1998). Permeability of cornea, sclera, and conjunctiva: a literature analysis for drug delivery to the eye. *Journal of pharmaceutical sciences* 87, 1479-1488.
- Prime, 2.1, v., and Schrödinger, L., New York, NY, 2010.
- Rada, J.A., Shelton, S., and Norton, T.T. (2006). The sclera and myopia. *Exp Eye Res* 82, 185-200.
- Ragab, A.H., Sutow, W.W., Komp, D.M., Starling, K.A., Lyon, G.M., Jr., and George, S. (1975). Adriamycin in the treatment of childhood solid tumors. A Southwest Oncology Group study. *Cancer* 36, 1567-1576.
- Roelofsen, H., Hooiveld, G.J., Koning, H., Havinga, R., Jansen, P.L., and Muller, M. (1999). Glutathione S-conjugate transport in hepatocytes entering the cell cycle is preserved by a switch in expression from the apical MRP2 to the basolateral MRP1 transporting protein. *Journal of cell science* 112 (Pt 9), 1395-1404.
- Romanelli, L., Valeri, P., Morrone, L.A., Pimpinella, G., Graziani, G., and Tita, B. (1994). Ocular absorption and distribution of bendazac after topical administration to rabbits with different vehicles. *Life Sci* 54, 877-885.
- Roy, A., Kucukural, A., and Zhang, Y. I-TASSER: a unified platform for automated protein structure and function prediction. *Nat Protoc* 5, 725-738.
- Saettone, M.F., Giannaccini, B., and Monti, D. (2001). Ophthalmic emulsions and suspensions. *Cutaneous and Ocular Toxicology* 20, 183 - 201
- Saha, P., Yang, J.J., and Lee, V.H. (1998). Existence of a p-glycoprotein drug efflux pump in cultured rabbit conjunctival epithelial cells. *Investigative ophthalmology & visual science* 39, 1221-1226.
- Said, H.M., Nguyen, T.T., Dyer, D.L., Cowan, K.H., and Rubin, S.A. (1996). Intestinal folate transport: identification of a cDNA involved in folate transport and the functional expression and distribution of its mRNA. *Biochim Biophys Acta* 1281, 164-172.
- Said, H.M., Wang, S., and Ma, T.Y. (2005). Mechanism of riboflavin uptake by cultured human retinal pigment epithelial ARPE-19 cells: possible regulation by an intracellular Ca²⁺-calmodulin-mediated pathway. *The Journal of physiology* 566, 369-377.
- Sarkadi, B., Homolya, L., Szakacs, G., and Varadi, A. (2006). Human multidrug resistance ABCB and ABCG transporters: participation in a chemoimmunity defense system. *Physiological reviews* 86, 1179-1236.
- Schoenwald, R.D., and Ward, R.L. (1978). Relationship between steroid permeability across excised rabbit cornea and octanol-water partition coefficients. *Journal of pharmaceutical sciences* 67, 786-788.
- Sharma, R., and Ehinger, B. (2003). Development and Structure of the Retina. In Adler's physiology of the eye : clinical application

P.L. Kaufman, A. Alm, and F.H. Adler, eds. (St. Louis, Mosby), pp. 319–347.

Sharom, F.J. (2008). ABC multidrug transporters: structure, function and role in chemoresistance. *Pharmacogenomics* 9, 105-127.

Shell, J.W. (1982). Pharmacokinetics of topically applied ophthalmic drugs. *Surv Ophthalmol* 26, 207-218.

Shimomura, Y. (2008). [Herpes simplex virus latency, reactivation, and a new antiviral therapy for herpetic keratitis]. *Nippon Ganka Gakkai Zasshi* 112, 247-264; discussion 265.

Shirasaki, Y. (2007). Molecular design for enhancement of ocular penetration. *Journal of pharmaceutical sciences*.

Sieg, J.W., and Robinson, J.R. (1975). Vehicle effects on ocular drug bioavailability i: evaluation of fluorometholone. *Journal of pharmaceutical sciences* 64, 931-936.

Sierra, E.E., and Goldman, I.D. (1999). Recent advances in the understanding of the mechanism of membrane transport of folates and antifolates. *Semin Oncol* 26, 11-23.

Snell, R.S., and Lemp, M.A. (1989). *Clinical anatomy of the eye* (Cambridge, MA, Blackwell Scientific Publications).

Soppimath, K.S., Aminabhavi, T.M., Kulkarni, A.R., and Rudzinski, W.E. (2001). Biodegradable polymeric nanoparticles as drug delivery devices. *J Control Release* 70, 1-20.

Spiegelstein, O., Eudy, J.D., and Finnell, R.H. (2000). Identification of two putative novel folate receptor genes in humans and mouse. *Gene* 258, 117-125.

Steuer, H., Jaworski, A., Elger, B., Kausmann, M., Keldenich, J., Schneider, H., Stoll, D., and Schlosshauer, B. (2005). Functional characterization and comparison of the outer blood-retina barrier and the blood-brain barrier. *Investigative ophthalmology & visual science* 46, 1047-1053.

Sudimack, J., and Lee, R.J. (2000). Targeted drug delivery via the folate receptor. *Adv Drug Deliv Rev* 41, 147-162.

Tak, R.V., Pal, D., Gao, H., Dey, S., and Mitra, A.K. (2001). Transport of acyclovir ester prodrugs through rabbit cornea and SIRC-rabbit corneal epithelial cell line. *Journal of pharmaceutical sciences* 90, 1505-1515.

Takahashi, K., Saishin, Y., Saishin, Y., Mori, K., Ando, A., Yamamoto, S., Oshima, Y., Nambu, H., Melia, M.B., Bingaman, D.P., *et al.* (2003). Topical nepafenac inhibits ocular neovascularization. *Investigative ophthalmology & visual science* 44, 409-415.

Talluri, R.S., Katragadda, S., Pal, D., and Mitra, A.K. (2006). Mechanism of L-ascorbic acid uptake by rabbit corneal epithelial cells: evidence for the involvement of sodium-dependent vitamin C transporter 2. *Current eye research* 31, 481-489.

Talluri, R.S., Samanta, S.K., Gaudana, R., and Mitra, A.K. (2008). Synthesis, metabolism and cellular permeability of enzymatically stable dipeptide prodrugs of acyclovir. *Int J Pharm* 361, 118-124.

Toma, H.S., Murina, A.T., Areaux, R.G., Jr., Neumann, D.M., Bhattacharjee, P.S., Foster, T.P., Kaufman, H.E., and Hill, J.M. (2008). Ocular HSV-1 latency, reactivation and recurrent disease. *Semin Ophthalmol* 23, 249-273.

- Tombran-Tink, J., Li, A., Johnson, M.A., Johnson, L.V., and Chader, G.J. (1992). Neurotrophic activity of interphotoreceptor matrix on human Y79 retinoblastoma cells. *J Comp Neurol* 317, 175-186.
- Turner, J., Turner, O.C., Baird, N., Orme, I.M., Wilcox, C.L., and Baldwin, S.L. (2003). Influence of increased age on the development of herpes stromal keratitis. *Exp Gerontol* 38, 1205-1212.
- Uchiyama, T., Fujita, T., Gukasyan, H.J., Kim, K.J., Borok, Z., Crandall, E.D., and Lee, V.H. (2008). Functional characterization and cloning of amino acid transporter B(0,+)⁺ (ATB(0,+)) in primary cultured rat pneumocytes. *Journal of cellular physiology* 214, 645-654.
- Vander Heiden, M.G., Cantley, L.C., and Thompson, C.B. (2009). Understanding the Warburg effect: the metabolic requirements of cell proliferation. *Science* 324, 1029-1033.
- Vandervoort, J., and Ludwig, A. (2002). Biocompatible stabilizers in the preparation of PLGA nanoparticles: a factorial design study. *Int J Pharm* 238, 77-92.
- Vega, E., Gamisans, F., Garcia, M.L., Chauvet, A., Lacoulonche, F., and Egea, M.A. (2008). PLGA nanospheres for the ocular delivery of flurbiprofen: drug release and interactions. *Journal of pharmaceutical sciences* 97, 5306-5317.
- Verrey, F., Meier, C., Rossier, G., and Kuhn, L.C. (2000). Glycoprotein-associated amino acid exchangers: broadening the range of transport specificity. *Pflugers Arch* 440, 503-512.
- Wagstaff, A.J., Faulds, D., and Goa, K.L. (1994). Aciclovir. A reappraisal of its antiviral activity, pharmacokinetic properties and therapeutic efficacy. *Drugs* 47, 153-205.
- Wander, A.H. (1984). Herpes simplex and recurrent corneal disease. *Int Ophthalmol Clin* 24, 27-38.
- White, L. (1991). Chemotherapy in retinoblastoma: current status and future directions. *Am J Pediatr Hematol Oncol* 13, 189-201.
- Winkler, B.S. (1981). Glycolytic and oxidative metabolism in relation to retinal function. *The Journal of general physiology* 77, 667-692.
- Wu, J., Zhang, J.J., Koppel, H., and Jacob, T.J. (1996). P-glycoprotein regulates a volume-activated chloride current in bovine non-pigmented ciliary epithelial cells. *The Journal of physiology* 491 (Pt 3), 743-755.
- Xiang, C.D., Batugo, M., Gale, D.C., Zhang, T., Ye, J., Li, C., Zhou, S., Wu, E.Y., and Zhang, E.Y. (2009). Characterization of human corneal epithelial cell model as a surrogate for corneal permeability assessment: metabolism and transport. *Drug metabolism and disposition: the biological fate of chemicals* 37, 992-998.
- Yamamoto, Y., Shimizu, E., Masuda, N., Takada, M., and Sone, S. (1998). RB protein status and chemosensitivity in non-small cell lung cancers. *Oncol Rep* 5, 447-451.
- Yang, C., Tirucherai, G.S., and Mitra, A.K. (2001). Prodrug based optimal drug delivery via membrane transporter/receptor. *Expert Opin Biol Ther* 1, 159-175.
- Yang, J.J., Ann, D.K., Kannan, R., and Lee, V.H. (2007). Multidrug resistance protein 1 (MRP1) in rabbit conjunctival epithelial cells: its effect on drug efflux and its regulation by adenoviral infection. *Pharmaceutical research* 24, 1490-1500.

- Zhang, L., Li, Y., Zhang, C., Wang, Y., and Song, C. (2009). Pharmacokinetics and tolerance study of intravitreal injection of dexamethasone-loaded nanoparticles in rabbits. *Int J Nanomedicine* 4, 175-183.
- Zhang, T., Xiang, C.D., Gale, D., Carreiro, S., Wu, E.Y., and Zhang, E.Y. (2008). Drug transporter and cytochrome P450 mRNA expression in human ocular barriers: implications for ocular drug disposition. *Drug metabolism and disposition: the biological fate of chemicals* 36, 1300-1307.
- Zhang, Y. (2008). I-TASSER server for protein 3D structure prediction. *BMC Bioinformatics* 9, 40.
- Zhang, Y. (2009). I-TASSER: fully automated protein structure prediction in CASP8. *Proteins* 77 *Suppl* 9, 100-113.
- Zhao, R., and Goldman, I.D. (2007). The molecular identity and characterization of a Proton-coupled Folate Transporter--PCFT; biological ramifications and impact on the activity of pemetrexed. *Cancer Metastasis Rev* 26, 129-139.
- Zhu, H., and Chauhan, A. (2008). Effect of viscosity on tear drainage and ocular residence time. *Optom Vis Sci* 85, 715-725.

VITA

Jwala Jwala was born on May 14th 1982, in Mahabubnagar, Andhra Pradesh, India. She completed her education from Chaitanya Central School, Yenugonda, located at Mahabubnagar District, Andhra Pradesh, India. Later she obtained her Bachelor of Pharmacy degree from JSS College of Pharmacy, Ooty, which is affiliated to Dr. M.G.R. Medical University, in August 2005. She has received gold medal from JSS college of Pharmacy in 2003 and best outgoing student award for year 2005. Jwala has joined University of Missouri-Kansas City, Department of Pharmaceutical Sciences in January 2007 in pursuit of a doctorate degree. She has received Chancellor's Non-residential Award for year 2007-2011. She has also received Amgen Travel Award for attending AAPS, 2010 at Los Angeles and UMKC women's award for year 2010.

Mrs. Jwala is a member of American Association of Pharmaceutical Scientists (AAPS) and Association of Research in Vision and Ophthalmology (ARVO). She has authored/co-authored 7 peer reviewed research and review articles in reputed international journals.